ESL-TR-87-76

TECHNICAL FEASIBILITY OF CENTRIFUGAL TECHNIQUES FOR EVALUATING HAZARDOUS WASTE MIGRATION

G.F. GOFORTH, R. VICEVICH, F.C. TOWNSEND, D. BLOOMQUIST

UNIVERSITY OF FLORIDA
300 WELL HALL
GAINESVILLE FL 32611

DECEMBER 1987

FINAL REPORT

MAY 1985 - MARCH 1987

AFESC

ENGINEERING & SERVICES LABORATORY
AIR FORCE ENGINEERING & SERVICES CENTER
TYNDALL AIR FORCE BASE, FLORIDA 32403

NOTICE

PLEASE DO NOT REQUEST COPIES OF THIS REPORT FROM HQ AFESC/RD (ENGINEERING AND SERVICES LABORATORY). ADDITIONAL COPIES MAY BE PURCHASED FROM:

NATIONAL TECHNICAL INFORMATION SERVICE
5285 PORT ROYAL ROAD
SPRINGFIELD, VIRGINIA 22161

FEDERAL GOVERNMENT AGENCIES AND THEIR CONTRACTORS REGISTERED WITH DEFENSE TECHNICAL INFORMATION CENTER SHOULD DIRECT REQUESTS FOR COPIES OF THIS REPORT TO:

DEFENSE TECHNICAL INFORMATION CENTER
CAMERON STATION
ALEXANDRIA, VIRGINIA 22314

UNCLASSIFIED

SECURITY CLASSIFICATION OF THIS PAGE

REPORT DOCUMENTATION PAGE

Form Approved OMB No. 0704-0188

1a. REPORT SECURITY CLASSIFICATION UNCLASSIFIED	1b. RESTRICTIVE MARKINGS N/A
2a. SECURITY CLASSIFICATION AUTHORITY N/A	3. DISTRIBUTION/AVAILABILITY OF REPORT Approved for public release. Distribution Unlimited
2b. DECLASSIFICATION/DOWNGRADING SCHEDULE N/A	
4. PERFORMING ORGANIZATION REPORT NUMBER(S)	5. MONITORING ORGANIZATION REPORT NUMBER(S) ESL-TR-87-76
6a. NAME OF PERFORMING ORGANIZATION University of Florida 6b. OFFICE SYMBOL (If applicable)	7a. NAME OF MONITORING ORGANIZATION HQ AFESC/RDVW
6c. ADDRESS (City, State, and ZIP Code) Department of Civil Engineering 300 Well Hall Gainesville FL 32611	7b. ADDRESS (City, State, and ZIP Code) Tyndall AFB FL 32403-6001
8a. NAME OF FUNDING/SPONSORING ORGANIZATION Same as Block 7 8b. OFFICE SYMBOL (If applicable)	9. PROCUREMENT INSTRUMENT IDENTIFICATION NUMBER F08635-83-C-0136 T.O. 85-9
8c. ADDRESS (City, State, and ZIP Code)	10. SOURCE OF FUNDING NUMBERS PROGRAM ELEMENT NO. 62601F; PROJECT NO. 1900; TASK NO. 7033; WORK UNIT ACCESSION NO.

11. TITLE (Include Security Classification)
Technical Feasibility of Centrifugal Techniques for Evaluating Hazardous Waste Migration

12. PERSONAL AUTHOR(S)
G.F. GoForth, R. Vicevich, F.C. Townsend, D. Bloomquist

13a. TYPE OF REPORT	13b. TIME COVERED	14. DATE OF REPORT (Year, Month, Day)	15. PAGE COUNT
Final	FROM May 85 TO Mar 87	December 1987	170

16. SUPPLEMENTARY NOTATION
Availability of this report is specified on reverse of front cover.

17. COSATI CODES			18. SUBJECT TERMS (Continue on reverse if necessary and identify by block number)
FIELD	GROUP	SUB-GROUP	Groundwater transport, centrifugal modeling, hydraulic conductivity, Darcy's law, instantaneous profile method, contaminant migration.
07	01		
07	04		

19. ABSTRACT (Continue on reverse if necessary and identify by block number)

This study was designed and executed to assess the technical feasibility of using centrifugal techniques to predict the transport characteristics of hazardous waste through soil. Advection is generally the major mechanism of contaminant migration from a waste source. For soluble contaminants, advection occurs within the aqueous phase. For immiscible fluid contaminants, such as the jet fuel JP-4, migration rates are often independent of the rates of water movement. Advection in saturated and unsaturated soils can be predicted from physical models or from measurements of the hydraulic conductivity in conjunction with knowledge of existing hydraulic gradients. A flexible wall permeameter was designed and utilized for determining saturated hydraulic conductivity of soil samples in the centrifuge and on the laboratory bench. Fundamental relationships of hydrodynamic pressure distribution and fluid kinematics within a soil volume undergoing radial acceleration were derived and verified during the study. Reagent grade decane was utilized as a surrogate for JP-4 jet fuel. Estimates of the hydraulic conductivity for water and decane were obtained in sand/clay
(Cont'd.)

20. DISTRIBUTION/AVAILABILITY OF ABSTRACT	21. ABSTRACT SECURITY CLASSIFICATION
☒ UNCLASSIFIED/UNLIMITED ☐ SAME AS RPT. ☐ DTIC USERS	UNCLASSIFIED
22a. NAME OF RESPONSIBLE INDIVIDUAL RICHARD A. ASHWORTH, Capt, USAF, BSC	22b. TELEPHONE (Include Area Code) (904) 283-4628 22c. OFFICE SYMBOL HQ AFESC/RDVW

DD Form 1473, JUN 86 *Previous editions are obsolete.*

SECURITY CLASSIFICATION OF THIS PAGE
UNCLASSIFIED

AQM03-06-1181

19. ABSTRACT (Cont'd.)

and 100 percent kaolinite samples. Testing conducted in the centrifuge reproduced bench test results, including the deviation from Darcy's law observed in the sand samples above a gradient of ten. A possible benefit of centrifugal techniques for saturated soils was the more accurate reproduction of soil stresses within the sample. Several laboratory techniques to determine the unsaturated hydraulic conductivity as a function of soil moisture content were evaluated. The instantaneous profile method (IPM) was selected as a technique which would be most conducive to adaptation for use in the centrifuge. An apparatus was designed and fabricated for conducting the IPM tests on the laboratory bench and in the centrifuge. Computer results indicated that a significant decrease in the testing time and a greater range of moisture contents can be realized by conducting the IPM test in the centrifuge. However, the use of the centrifuge for physical modeling of unsaturated phenomena, such as leachate from a waste pit, offers no advantage over laboratory bench models because of the dominance of soil moisture suction gradients over gravity gradients in unsaturated soils.

PREFACE

This report was prepared by the Department of Civil Engineering, University of Florida, Gainesville, Florida, 32611, under Contract No. F08635-83-C-0136, Task Order 85-9, "The Feasibility of Centrifugal Modeling to Aid in Prediction of Contaminant Migration Through Soils," for the Air Force Engineering and Services Center, Environics Division, Tyndall Air Force Base, Florida, 32403-6001, under Job Order No. 124504050.

This report is published as submitted to the University of Florida by Mr. Gary F.E. Goforth as his Ph.D. dissertation, with the exception of Chapter VI, which was prepared by Mr. Robert Vicevich as part of his Master of Engineering thesis. This report is being published because of its interest to the worldwide scientific and engineering community. Dr. Goforth was directly supervised by Professors F.C. Townsend and D. Bloomquist, with valuable contributions from Professors Jim Heaney, Wayne Huber, Dinesh Shah, Jim Davidson, and Siresh Rao. Capt. Richard Ashworth, Ph.D., was the HQ AFESC/RDVW Project Officer. This report summarizes work performed between May 1985 and March 1987.

The report discusses the feasibility of using centrifugal modeling to predict contaminant migration through saturated and partially saturated soils. The results show that centrifugal modeling offers no advantage over bench tests at comparable effective stresses for predicting 1-D flow through saturated soils, but could be used to develop rapidly hydraulic conductivity versus water content relationships for partially saturated soils.

Mention of trademarks and trade names of material and equipment does not constitute endorsement or recommendation for use by the Air Force.

This report has been reviewed by the Public Affairs Office (PA) and is releasable to the National Technical Information Service (NTIS). At NTIS, it will be available to the general public, including foreign nationals.

This technical report has been reviewed and is approved for publication.

Richard A. Ashworth
RICHARD A. ASHWORTH, Capt, USAF, BSC
Environmental Research Engineer

Thomas J. Walker
THOMAS J. WALKER, Lt Col, USAF, BSC
Chief, Environics Division

F. Thomas Lubozynski
F. THOMAS LUBOZYNSKI, Maj, USAF, BSC
Chief, Environmental Engineering Branch

Lawrence D. Hokanson
LAWRENCE D. HOKANSON, Colonel, USAF
Director, Engineering and Services Laboratory

(The reverse of this page is blank.)

TABLE OF CONTENTS

LIST OF TABLES

LIST OF FIGURES

KEY TO SYMBOLS USED IN TEXT

a_r	acceleration acting on control mass	(L/T^2)
A,a	cross-sectional area	(L^2)
b	contact angle	(rad)
C	solute concentration	(M/L^2)
c	minor energy loss coefficient	(dimensionless)
D	hydrodynamic dispersion coefficient	(L^2/T)
d	representative length	(L)
f	friction factor	(dimensionless)
g	acceleration due to gravity	(L/T^2)
H	total hydraulic energy	(varies)
H_L	energy loss between two points	(varies)
h_a	air entry pressure	(L)
J	convective-dispersive solute flux	(M/L^2T)
K	hydraulic conductivity	(varies)
k	intrinsic permeability	(L^2)
L	representative length	(L)
M	representative mass	(M)
N	ratio of model to prototype acceleration	(dimensionless)
n	nominal porosity of soil	(dimensionless)
Θ	volumetric water content	(L^3/L^3)
P	pressure	(M/LT^2)
p	mass density	(M/L^3)
P_e	Peclet number	(dimensionless)
q	specific discharge	(L/T)
R_e	Reynolds number	(dimensionless)
r	representative radius	(L)
S	sum of source/sink components	(M/L^2T)
s	surface tension	(M/T^2)
t	representative time	(T)
u	dynamic (absolute) viscosity	(M/TL)
V	average fluid velocity	(L/T)
v	kinematic viscosity	(L^2/T)
w	angular velocity	(rad/T)
X	ratio of prototype to model length	(dimensionless)
z	representative elevation	(L)

(The reverse of this page is blank)

CHAPTER I
INTRODUCTION

Scope

The assessment of local and regional impacts on groundwater resources due to leachate of hazardous wastes from confined disposal areas and accidental spills necessitates the prediction of contaminant migration. In general, either a physical or numerical model can be applied to depict the mass transport phenomena.

Tyndall Air Force Base was considering the construction of a large-scale centrifuge for structural, geotechnical and environmental research applications. The U.S. Department of Defense Installation and Restoration Program has identified over 200 high priority hazardous waste sites at Air Force facilities which require mitigative measures (Heaney, 1984). Categories of waste sources are presented in Table 1. Of significant concern is the transport characteristics of jet fuel JP-4 through soil. A laboratory research study was designed and executed to evaluate the feasibility of using centrifugal techniques to determine hazardous waste migration characteristics. The utilization of a centrifuge may offer several advantages over traditional physical modeling apparatus as well as provide the dual capability of performing as a laboratory instrument capable of testing material properties. The centrifugal techniques were evaluated on the following criteria:

1. Can they significantly shorten the testing period?
2. Can they reduce the uncertainty associated with estimates of hydraulic conductivity of soil samples?

Table 1. Classification of the Top 216 Installation Restoration Program Sites by Type of Waste Area

Type of Waste Area	Number in Top 216	Percent in Top 216
Landfills	61	28.2
Surface impoundments, lagoons, beds and waste pits	57	26.4
Leaks and spills	43	19.9
Fire training areas	28	13.0
Drainage areas	16	7.4
Other	11	5.1
TOTAL	216	100.0

Source: Heaney, 1984

3. How do the costs compare with conventional techniques?

Objectives

The objective of this study was to assess the technical feasibility of using a large-scale centrifuge for determining migration rates and characteristics of hazardous wastes. Centrifugal techniques for evaluating hazardous waste migration include physical modeling and material properties testing. While physical modeling has been successfully conducted under 1-g conditions on the laboratory bench, gravity-dominated phenomena can be accelerated within a centrifuge, thereby providing an additional scaling factor and attendant reduction in testing time. Several geotechnical applications have demonstrated the feasibility of centrifugal modeling for such gravity-dominated phenomena as sedimentation and consolidation (Bloomquist and Townsend,

1984; Mikasa and Takada, 1984). An additional advantage of centrifugal modeling is the accurate reproduction of effective stresses in the scaled down soil profile as a result of the greater acceleration force acting on the soil particles. To fully utilize the potential of physical modeling in the centrifuge, the fundamental relationships of radial acceleration, hydraulic pressures and pore fluid kinematics within the centrifuge soil sample needed to be developed and verified. The execution of concurrent bench and centrifuge hydraulic conductivity testing provided the opportunity to investigate these fundamental fluid flow properties as well as allowed the direct assessment of the feasibility of material properties testing within the centrifuge. The objective of the laboratory research program was to develop centrifugal testing methods for determining saturated and unsaturated hydraulic conductivity of soil samples. The testing program encompassed

1. design, fabrication and analysis of permeameters for use in the centrifuge;
2. execution of hydraulic conductivity tests in a 1-g environment to provide a benchmark to compare centrifuge results;
3. derivation of the appropriate equations of motion for fluid flow in a centrifuge;
4. execution of hydraulic conductivity tests in the centrifuge at various accelerations;
5. comparison of centrifuge results with 1-g test result; and
6. (if necessary) modification of the centrifuge device, testing procedures and/or data analysis based on results of the comparison.

A secondary goal of the project was to establish the theoretical and practical operating limits of centrifugal techniques. The flow and

storage characteristics of commercially available n-decane were evaluated during the course of this study as a surrogate for JP-4. Results of the testing program will serve as the foundation for subsequent research in the area of centrifugal modeling of hazardous waste migration.

CHAPTER II
BACKGROUND

Contaminant Migration

Predicting the migration of jet fuel and its derivatives from storage areas is a challenging problem. Fluid flow will occur in both partially saturated and fully saturated soil. Material storage and transport can be dominated by either the lateral movement of vapors (Reichmuth, 1984), the advection and dispersion of soluble fractions within percolating water (Schwille, 1984), interfacial phenomena occurring between the fuel and the soil matrix, e.g., adsorption and biodegradation (Borden et al., 1984) or a variety of rheological phenomena associated with multiple phase (e.g, air-water-oil) flow systems, including the pure advection of the water insoluble fractions.

The cumulative mass transport from the waste source to the water table and/or a downstream water resource is sensitive to site-specific advective, dispersive and reactive properties of the soil-fluid system. In lieu of collecting extensive site-specific data to describe the transport phenomena, a conservative estimate is often initially presented which considers only advective transport. The efforts of the current study are hence directed at techniques for estimating the advective properties of jet fuel in unsaturated and saturated soil.

Contaminant migration within the soil profile is a complex phenomenon, reflecting the chemical diversity of contaminants as well as the variety and heterogeneity of the geohydrologic regimes and soil

matrices encountered. Nonetheless, predictions of the travel rates and directions of contaminant movement can be formalized based on generalized transport phenomena. The movement of a soluble contaminant will in general be governed by the flux of water through the soil profile. Below a disposal area, this fluid movement may resemble the pattern depicted in Figure 1. Figure 2 presents a schematic of a porous soil volume through which a solute is passing. Basically, four fundamental transport phenomena account for all significant movement of a solute within a soil profile:

1. Advection refers to the movement of a solute by virtue of its entrainment within the bulk fluid.
2. Mechanical dispersion is the flux of a solute which results from nonuniform pore fluid velocities, i.e., due to flow path tortuosity and dead-end channels, the velocities within typical soil volumes are not uniformly distributed.
3. Molecular diffusion is the movement of a solute solely on the basis of concentration gradients. Because of their similar influence on solute movement, mechanical dispersion and molecular diffusion are often represented by a single term referred to as hydrodynamic dispersion.
4. Source/sink phenomena, including adsorption. Adsorption phenomena encompass a variety of interactions of the solute with the surfaces of the soil matrix. Source/sink phenomena are influenced by many factors, including soil and bulk fluid pH, the ionic nature of the soil and solute, and the surface characteristics of the soil.

These phenomena are significant to varying degrees, entirely specific to the site characteristics. For example, in the transport of a low

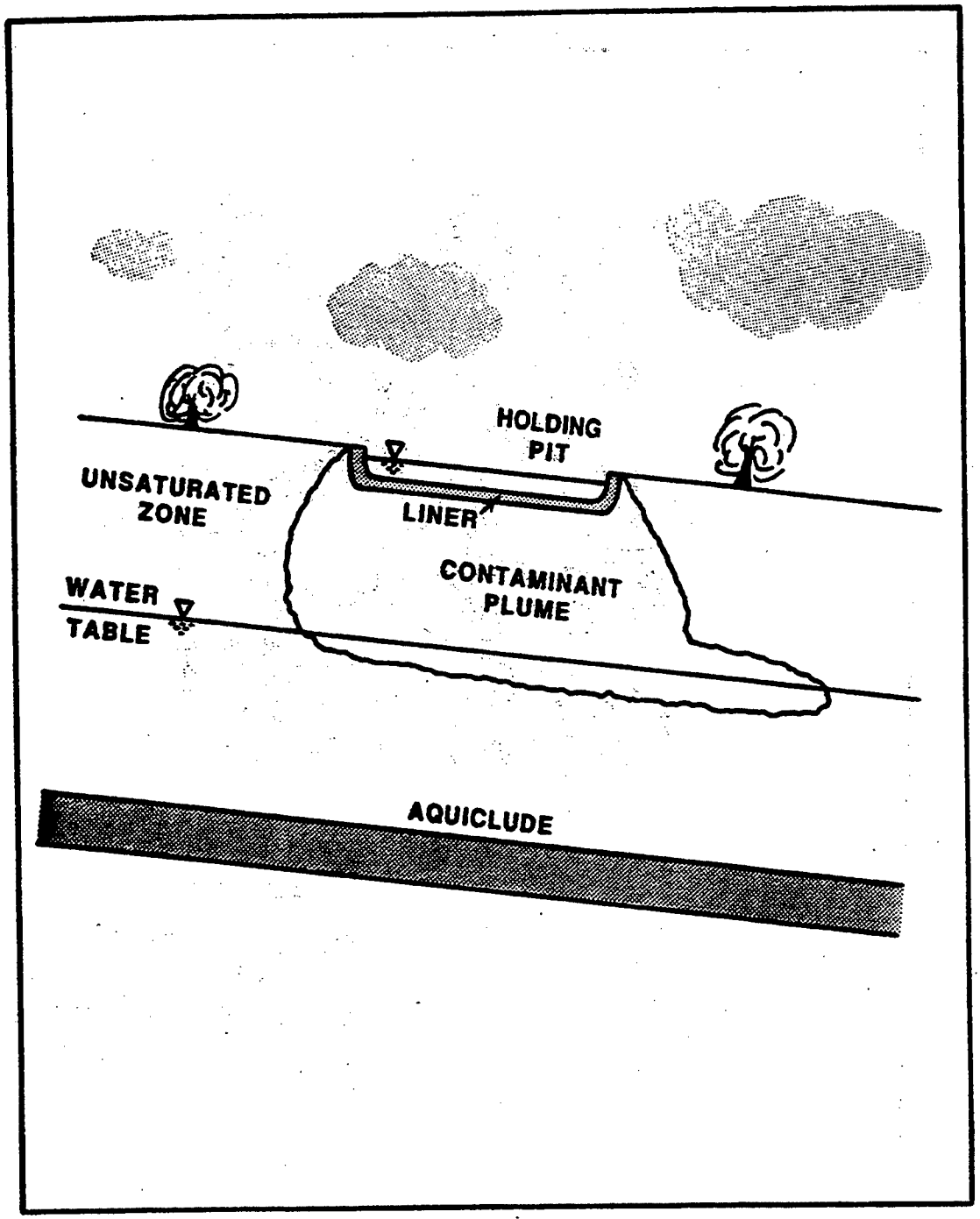

Figure 1. Flow Pattern of a Soluble Contaminant Beneath a Waste Source

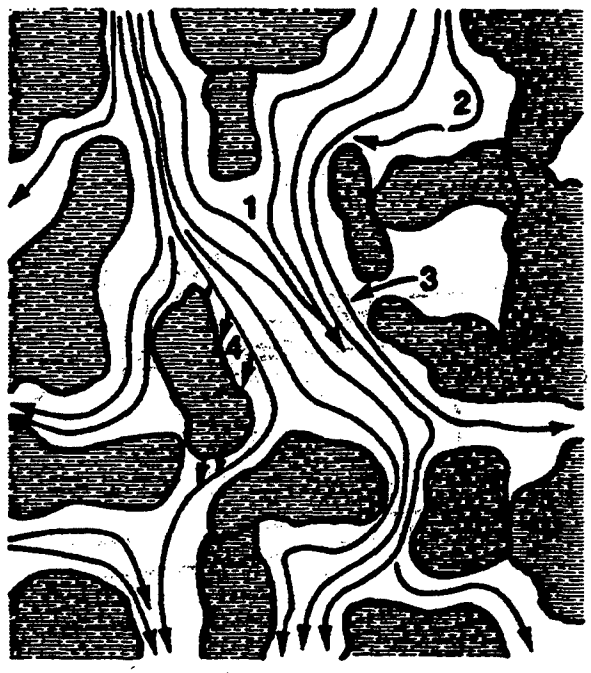

LEGEND

1. ADVECTION
2. MECHANICAL DISPERSION
3. MOLECULAR DIFFUSION
4. ADSORPTION PHENOMENA

Figure 2. Transport Processes of a Soluble Contaminant Within a Soil Volume

concentration of a nonionic compound through uniformly graded coarse sand, the advection term would dominate the material transport; molecular diffusion would be insignificant due to relatively large pore fluid velocities and the small concentration gradients of the solute; adsorption phenomena may also be insignificant due to the relatively large advection component, nonionic nature of the solute and small specific surface area of the soil. At the other extreme, the movement of a high concentration of a cationic solute through a thick clay landfill liner would be governed less by advection and more by adsorption and diffusion phenomena. The mass transport of a contaminant can be expressed quantitatively as a composite of these elements (Davidson et al., 1983)

$$J = -D\,\theta\,\frac{dC}{dz} + qC + S \qquad (1)$$

where J = convective-dispersive solute flux per unit cross-sectional area (M/L^2T);

D = hydrodynamic dispersion coefficient (L^2/T);

θ = volumetric soil water content (L^3/L^3);

$\frac{dC}{dz}$ = solute concentration gradient in the z direction (M/L^4);

q = specific discharge, i.e., the volumetric discharge of bulk fluid per unit cross-sectional area (L/T);

C = solute concentration (M/L^3); and

S = sum of the source/sink components (M/L^2T).

The advective component, qC, can be further expanded as

$$qC = C\left[-K(\theta)\,\frac{dH}{dz}\right] \qquad (2)$$

where $K(\theta)$ = hydraulic conductivity, which is dependent on the water content; and

$\frac{dH}{dz}$ = hydraulic potential gradient in the z direction

which explicitly relates the mass transport of a solute to the hydraulic conductivity and the gradient. In addition, the magnitude of the hydraulic conductivity is important not only for the advection of a solute but also for the kinetics of the other components as well. The hydrodynamic dispersion coefficient in most natural soils with uniform porosities is dependent on the pore fluid velocity, as is the reaction time for adsorption and other source/sink phenomena (Rao and Jessup, 1983). The relative magnitudes of the transport phenomena can be expressed by the Peclet number, P_e, a dimensionless quantity defined as (Bear, 1972)

$$P_e = qL/\theta D \qquad (3)$$

where L = representative length. During flow conditions at low Peclet numbers, the dispersion and diffusion phenomena dominate the transport process, while advection dominates solute migration under flow conditions with high Peclet numbers. However, to assess the relative significance of each term, the influential parameters of the solute, soil matrix and extant geohydrologic regimes must be evaluated. The geohydrologic regime of a particular site may be saturated, unsaturated or some heterogeneous combination. In turn, the character and significance of each component of the material transport phenomena is highly influenced by this regime.

Advection

In many cases of pollutant transport, consideration of downstream risks requires that conservative estimates of travel time through the medium in question be obtained. In a soil matrix, this conservative value of contaminant migration is generally the advection term and is estimated from the saturated hydraulic conductivity of the soil, which

may be three to five orders of magnitude greater than the hydraulic conductivity of the unsaturated soil at its average moisture content. However, for engineering design purposes, the average value of the hydraulic conductivity may be desired, as there may be tremendous differences in control technologies and economics compared to solutions using the saturated values.

The rate of bulk fluid movement through the soil profile is the most fundamental process affecting the migration of soluble or immiscible contaminants. A fluid moves through the soil matrix in response to hydraulic energy (potential) gradients. The hydraulic potential of fluid in the pores of a soil volume has been defined as the amount of work necessary to transport, reversibly and isothermally, a volume of pure water from an external reservoir at a known elevation to the soil volume at a known location and pressure. While the validity of this definition has been debated, it does convey the fundamental concepts of hydraulic energy of pore fluid. The flux of fluid through a soil volume, whether saturated or unsaturated, is proportional to the existing potential gradient, as stated by Darcy's law, written in one dimension as

$$q = -K \, (dH/dz) \qquad (4)$$

where q = specific discharge, defined as the volume of fluid passing through a unit area of soil in a unit time (L/T).

The terms hydraulic conductivity and permeability are often used interchangeably, reflecting the broad range of disciplines which employ the parameter. The term hydraulic conductivity will be used throughout this text when referring to the constant of proportionality between the total hydraulic potential gradient and the specific discharge.

The gradient of the total hydraulic potential provides the driving force for water movement in soils. The total potential energy can be expressed on the basis of energy per unit weight, defined as the hydraulic potential, or head, which has the dimension of length. The potential energy can also be expressed as energy per unit volume, defined as the pressure potential, with the dimensions M/LT^2; or as energy per unit mass, defined as the specific energy potential, with the dimensions L^2/T^2. The units of hydraulic conductivity must be dimensionally consistent with the potential energy term; Table 2 summarizes these relationships, such that the product of K dh/dz has units of L/T.

Table 2. Fundamental Relationships Between the Potential Gradient and Hydraulic Conductivity

Potential Gradient	Dimensions of K	Example of K
Hydraulic Potential	L/T	cm/s
Pressure Potential	TL^3/M	cm^3s/g
Specific Energy Potential	T	sec

Darcy's original work employed the dimension of length for the hydraulic potential (Darcy, 1856). As a consequence, the dimensions of the potential gradient were length per unit length and the dimensions of the hydraulic conductivity were length per time, later expressed as a function of both the bulk fluid and the soil media (Bear, 1979)

$$K = k\, g\, /\, v \qquad (5)$$

where k = intrinsic permeability of the medium (L^2);

g = acceleration due to gravity acting on the fluid (L/T^2); and

v = kinematic viscosity of the fluid (L^2/T).

The influence of acceleration due to gravity can be separated by employing the dimensions of the specific energy potential. The resulting coefficient of proportionality has the dimension of time, and still preserves the direct relation between the properties of the medium and fluid. Accordingly, equation 5 can be modified as

$$K = k / v \qquad (6)$$

Based on this relationship, the hydraulic conductivity, and hence flow rates, of various bulk fluids in a similar medium theoretically can be determined from the fluid's kinematic viscosity. This principle is relevant in predicting the bulk transport of nonaqueous fluids as well as the advection of solutes in aqueous flow. However, this extrapolation is based on the implicit condition that chemical interactions between the bulk fluid and the soil matrix would not alter the intrinsic permeability. In fact, in investigations of contaminant migration the solution properties and surface chemistry of the solute and soil need to be examined. Numerous studies have documented increases or decreases in the hydraulic conductivity beyond that suggested by equation 5 (Gordon and Forrest, 1981; Brown et al., 1984). For example, one study reported an increase in conductivity of three orders of magnitude with the addition of gasoline to water in a clay soil (Brown et al., 1984). The viscosity of gasoline is approximately one half that of water, so a two-fold increase in the conductivity was expected from equation 5. The tremendous increase was attributed to the surface chemistry properties of the water/gasoline/clay system. The gasoline apparently displaced the water molecules separating the clay sheets which in turn created numerous cracks through which the fluid passed more readily.

Darcy's law is generally regarded as valid in laminar flow ranges, that is, where viscous forces predominate over inertial forces acting on the fluid. By analogy to open channel hydraulics, a Reynolds number, R_e, has been defined for flow through porous media as (Bear, 1979)

$$R_e = q\, d / v \qquad (7)$$

where d = representative length of the porous matrix (L). Often d is taken as either the mean grain diameter or the diameter such that 10 percent by weight are smaller. Experimental evidence suggests that Darcy's law becomes invalid at some point in the range of R_e between 1 and 10 (Bear, 1979).

Flow in Unsaturated Media

The infiltration of leachate from a waste storage pond, an accidental spill or other source will generally encounter unsaturated soil directly below the site. As is the case in saturated media, hydraulic potential gradients determine the flow conditions in unsaturated soils. The unsaturated hydraulic gradient is composed of similar components such as pressure potential and gravitational potential; also, thermal gradients can exist which influence fluid movement. However, unlike the positive pressures acting on pore fluid in saturated media, pressures which are less than atmospheric are exerted on fluid volumes within unsaturated soil. By convention these pressures are considered negative, and the positive (in sign) terms soil moisture suction and matric potential are widely used. Soil suction increases rapidly as the pore water content decreases. The relationship between soil suction and water content is referred to as a moisture retention curve and exhibits a hysteretic effect between the wetting (imbibition) and desorption (drainage) paths. In association with the

wide range of moisture contents and cycles of imbibition and drainage, the hydraulic gradient in the unsaturated zone can be dominated by any one of the components during specific flow conditions.

As the soil dries, the influence of gravity on the movement of pore fluid decreases. The majority of the time fluid flux in natural soils is dominated by suction gradients, which can typically be 1000 to 10,000 times greater than the gradient due to gravity (Hillel, 1982). In a uniformly dry soil, water movement below an influent source will occur in a radial pattern, as in Figure 3, demonstrating the negligible influence of gravity. Thus, in the scenario of percolation of leachate from a hazardous waste site overlaying an unsaturated soil profile, the movement of fluid will be dominated by the soil suction gradients.

Another consequence of decreasing soil moisture content as the soil dries out is the attendant decrease in the hydraulic conductivity. Reductions of up to five orders of magnitude from the saturated hydraulic conductivity value have been documented (Hillel, 1982). This reduction may be attributed to several phenomena: (1) the first pores to empty are the larger ones which offer the least flow resistance; (2) as the center of the pores lose water first, the adsorption influence of the soil particles on the water film further increases the resistance to flow; (3) the tortuosity of the flow paths increases as the pores drain; and (4) the total cross-sectional area of flow decreases, thereby requiring a larger gradient to maintain a given specific discharge.

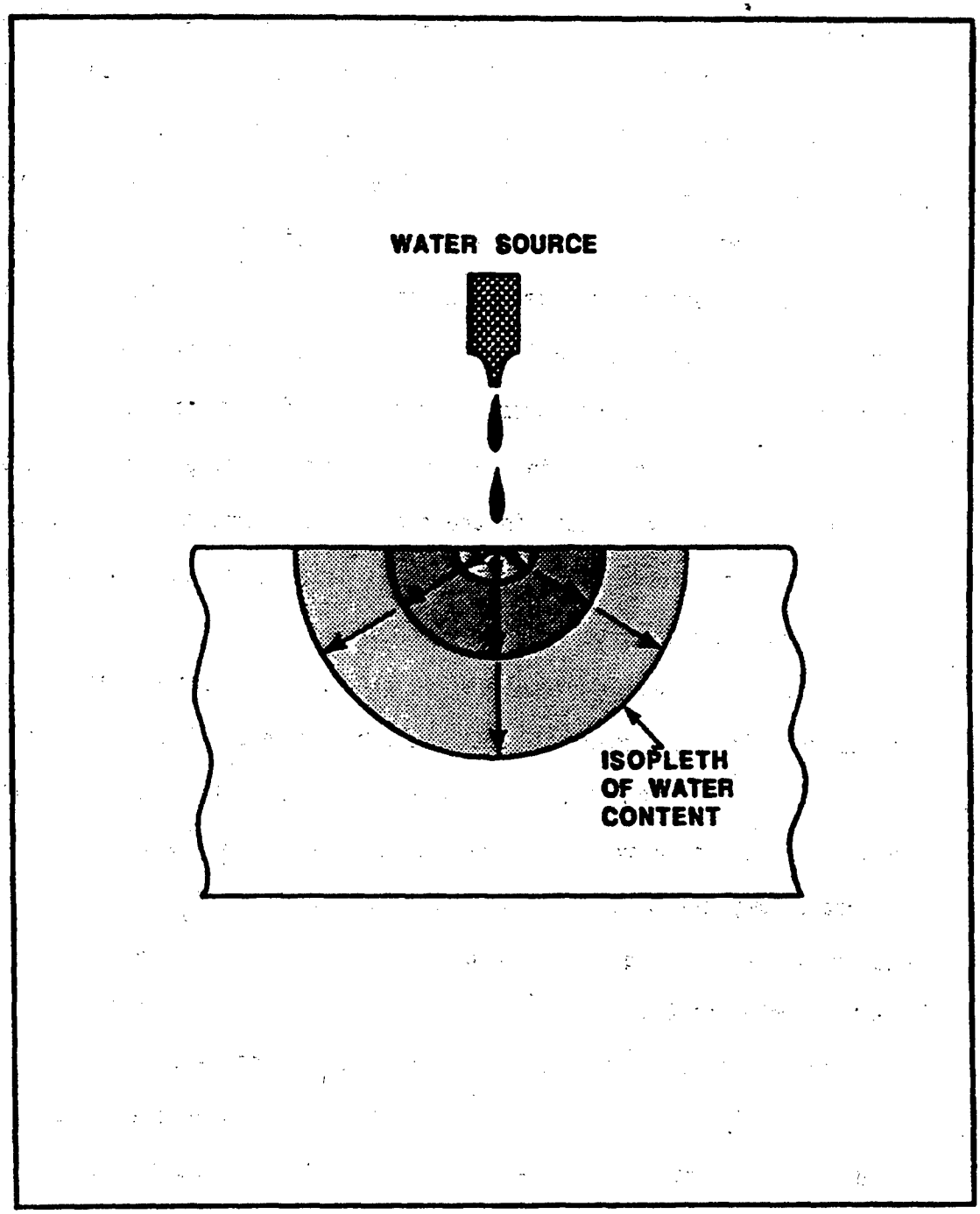

Figure 3. Radial Movement of Moisture in a Uniformly Dry Soil

Immiscible Fluid Flow

Two fluids are mutually immiscible if their solubility in the other is very low. Decane and JP-4 jet fuel are immiscible in water; decane has a solubility of 0.009 mg/l at 20°C. The movement of these fluids through soil, as depicted in Figure 4, is vastly different than the transport of a soluble contaminant. The advection and hydrodynamic dispersion within the water phase are negligible due to their limited solubility. In soils that are initially water-saturated, insoluble wastes must displace extant water from soil pores in order to migrate through the voids. The energy required to displace the existing liquid from the pores is termed the interfacial energy (Adamson, 1982). An analogous situation occurs when saturating a porous media (e.g., a porous stone) originally filled with air. In that case, the interfacial energy is commonly expressed as the air entry pressure or bubble pressure (Brooks and Corey, 1964). The magnitude of the interfacial energy is inversely proportional to the diameters of the pore, or (Adamson, 1982)

$$h_a = 2\ s\ \cos(b)\ /(dp\ r\ g) \qquad (8)$$

where h_a = air entry pressure (L);

s = surface tension (M/T^2);

b = contact angle (rad);

dp = difference in fluid densities (M/L^3); and

r = radius of the pores (L).

For flow to occur, the hydraulic energy gradient across a sample must be sufficient to satisfy the interfacial energy requirements. The smaller the soil pores, the greater the driving force required to displace the water.

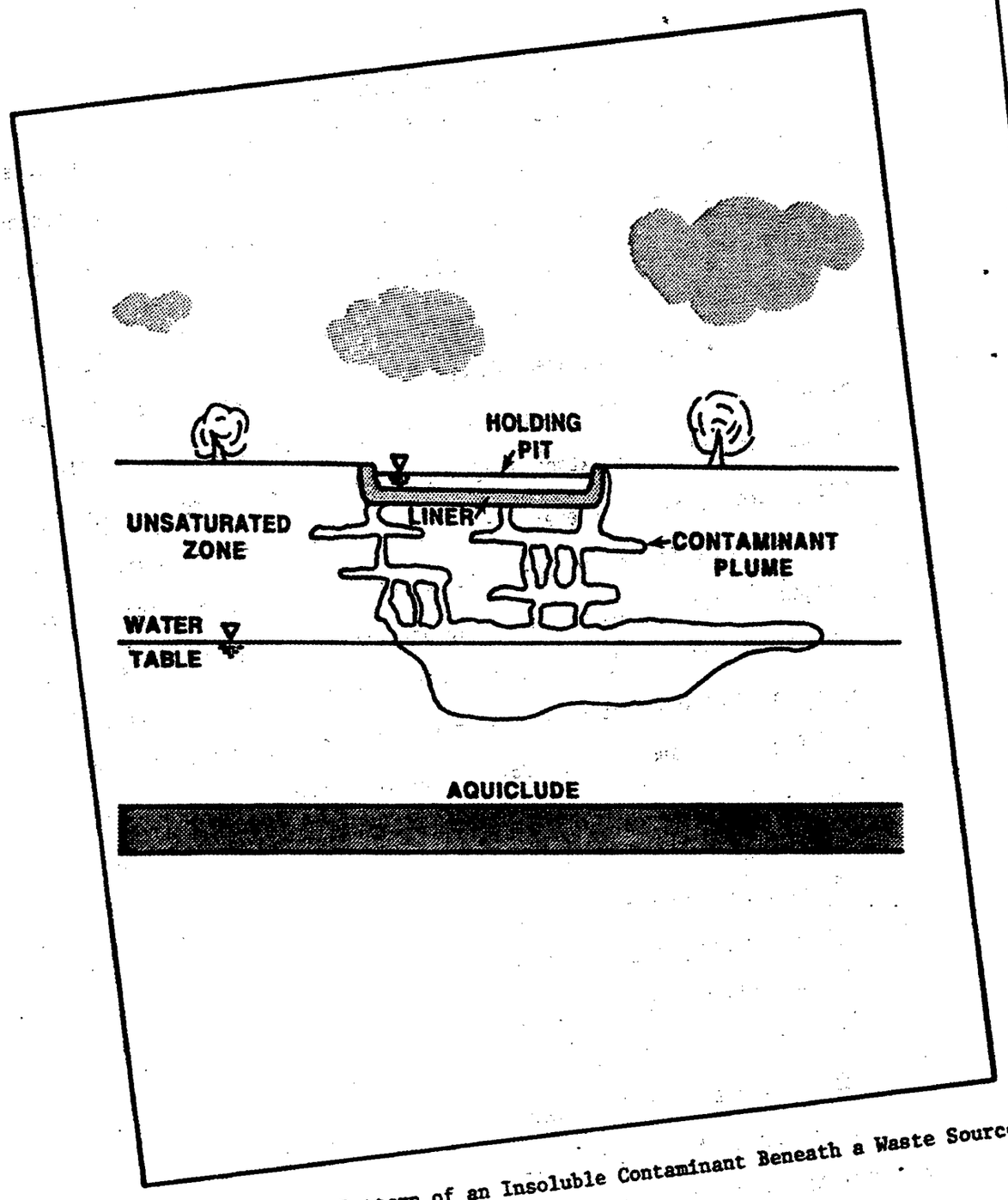

Figure 4. Flow Pattern of an Insoluble Contaminant Beneath a Waste Source

In unsaturated soil, a three-phase flow system exists, composed of air, water and the immiscible fluid. The movement of each fluid occurs only after the volume of that fluid attains a minimum value, referred to as the residual saturation. The residual saturation is specific to the fluid and soil type. Most components of JP-4 are less dense than water; hence, any of these lighter fluids which reaches the water table will spread on the surface. The travel distance is limited by the residual saturation flow requirement. Migration into and along with the surficial aquifer fluid will be limited by the solubility of the various fractional components of JP-4.

Methods of Prediction

A wide variety of analytical, numerical and physical techniques have been developed to predict hazardous waste transport (Anderson-Nichols, 1984). In all cases, an estimate of the hydraulic conductivity is paramount to estimating the migration rate of a material through the soil. Literature from soil physics, groundwater hydraulics, geohydrology and geotechnical engineering publications was reviewed to provide a comprehensive information base of field and laboratory methods used to estimate hydraulic conductivity. In general, all the lab tests provide an estimate of hydraulic conductivity for one-dimensional flow, whereas field conditions are often two- or three-dimensional.

Field Tests

Field tests are often preferred over laboratory tests for saturated soils because they generally utilize a larger volume of soil, which includes the effects of the soil macrostructure, e.g., worm holes, roots and fissures, which contribute to the overall anisotropy of the flow

region. Field tests also are generally designed to account for three-dimensional flow. Discrepancies of three orders of magnitude have been observed between field and laboratory tests (Day and Daniel, 1985). A summary of field methods for measuring hydraulic conductivity is presented in Table 3.

Laboratory Tests

Laboratory tests can be conducted to determine the physical and chemical properties of the soil medium and the contaminant. These data can be used in subsequent analysis of migration rates and/or evaluation of appropriate mitigative measures. In the classical treatment of a soil volume as a physical continuum, the concept of a representative elementary volume (REV) emerges when conducting laboratory tests. The REV is defined as the smallest volume of soil which accurately characterizes the extrinsic and intrinsic variability of the parameter in question. A summary of laboratory techniques for determining the hydraulic conductivity of a soil specimen is presented in Table 4.

Saturated hydraulic conductivity tests

Laboratory procedures for determining saturated hydraulic conductivity of soil specimens have been standardized by several organizations. The American Society for Testing Materials (ASTM), the U. S. Geological Survey (USGS), the U. S. Army Corps of Engineers (USCOE) and others have documented techniques for specific soil types. The principle of the test has remained essentially unchanged from the famous Dijon, France sand filter experiments conducted by Henri Darcy in 1855. However, the apparatus used to conduct the test has been modified

Table 3. Field Methods of Estimating Hydraulic Conductivity

Method	Physical Scale	Moisture Content Range	Reference(s)
Unsteady Flow Tests			
1. Instantaneous Profile	Point	Moist to saturated	Green et al., 1983 Dane and Hruska, 1983 Chong et al., 1981
2. Theta method	Point	Moist to saturated	Libardi et al., 1980 Jones and Wagenet, 1984
3. Flux method	Point	Moist to saturated	Libardi et al., 1980 Jones and Wagenet, 1984
4. Pump test nonsteady flow	Regional	Unconfined aquifer	Bear, 1979
5. Double tube method	Point	Saturated	Bouma et al., 1982 USGS, 1982
6. Auger hole	Point	Saturated	Bouma et al., 1982 USGS, 1982
7. Piezometer method	Point	Saturated	Boersma, 1965b USGS, 1982
Steady Flux Tests			
8. Crust-imposed flux	Point	Moist to saturated	Green et al., 1983
9. Sprinkler-imposed flux	Point	Moist to saturated	Green et al., 1983
10. Tracer transport	Field	Saturated	Bear, 1979
11. Double-ring infiltrometer	Point	Saturated	Chong et al., 1981
12. Pump test - steady flow	Regional	Unconfined aquifer	Bear, 1979
13. Dry auger hole method	Point	Saturated	Boersma, 1965a Bouma et al., 1982
14. Carved column	Point	Saturated	Bouma et al., 1982
15. Permeameter method	Point	Saturated	Boersma, 1965a

Table 4. Laboratory Methods of Estimating Hydraulic Conductivity

	Method	Flow Condition	Moisture Content Range	Reference(s)
1.	Constant head permeameter	Steady	Saturated	ASTM, 1974 Olson and Daniel, 1981
2.	Falling head permeameter	Unsteady	Saturated	Bear, 1972 Olson and Daniel, 1981
3.	Triaxial cell test	Unsteady	Saturated	Edil and Erickon, 1985 USAEWES, 1970
4.	Low-gradient constant flux	Steady	Saturated	Olsen, 1966
5.	Constant pressure	Steady	Moist to saturated	Olson and Daniel, 1981
6.	Method of van Genuchten	Unsteady	Moist to saturated	Dane, 1980
7.	Outflow method	Unsteady	Moist to saturated	Kirkham and Powers, 1972
8.	Centrifuge balance	Unsteady	Moist to saturated	Alemi et al., 1976
9.	Steady flux	Steady	Moist to saturated	Klute, 1965a
10.	Pressurized steady flux	Steady	Moist to saturated	Klute, 1965a
11.	Consolidation testing	Unsteady	Saturated	Cargill, 1985 Znidarcic, 1982
12.	Instantaneous profile	Unsteady	Moist to saturated	Olson and Daniel, 1981
13.	Crust-imposed flux	Steady	Moist to saturated	Green et al., 1983 Dunn, 1983
14.	Sprinkler-imposed flux	Steady	Moist to saturated	Dunn, 1983 Green et al., 1983
15.	Centrifuge flow through	Unsteady	Moist to saturated	This study

as appropriate to test a wide range of soil specimens under a variety of soil stress conditions.

Permeameters in general consist of a sample cell, a fluid conduit system and may or may not incorporate a pressurized air system. The sample cell can be a rigid wall container; however, to prevent short circuiting of permeant along the wall of the sample container, some sample cells utilize a flexible membrane in association with an applied external pressure.

Unsaturated hydraulic conductivity tests

In contrast to the numerous techniques and apparatus available to conduct a saturated hydraulic conductivity test, only a few methods exist for determining the relationship between hydraulic conductivity and water contents below saturation. However, this is commensurate with the commercial demand for such methodology. For many engineering purposes, including many aspects of contaminant migration, the highest rate of flux is of concern; for these applications the saturated hydraulic conductivity tests are appropriate.

A variety of techniques have been developed for estimating unsaturated hydraulic conductivity. Along with steady flow tests, transient flow methods have been developed which yield estimates of unsaturated hydraulic conductivity over a range of moisture contents. Estimates can be obtained during the imbibition (wetting) and/or desorption (drainage) cycle. As in the tests for saturated hydraulic conductivity, these methods generally yield an estimate of hydraulic conductivity for one-dimensional flow.

Laboratory techniques for determining unsaturated hydraulic conductivity are preferred over field tests for several reasons (Hillel, 1982, Christiansen, 1985):

1. the flow during unsaturated conditions is dominated by the film of water along soil particles, hence the influence of macrostructures is much less than during saturated conditions;
2. better control of initial and boundary conditions is provided in the lab and more sensitive measurements can be obtained, yielding more accurate interpretation of data; and
3. lab tests are generally less expensive.

Physical Modeling

Another approach to predicting contaminant migration and evaluating treatment alternatives is to construct a prototype of the field site and conduct appropriate dynamic tests. The results can subsequently be extrapolated to field conditions by use of appropriate scaling relationships. The choices of materials and testing conditions are governed by geometric, mechanical and dynamic similitude between the model and field prototype.

CHAPTER III
CENTRIFUGE THEORY

Historical Use of Centrifugation

Centrifuges have been used as laboratory apparatus by soil physicists and geotechnical engineers since the turn of the century. Centrifugal techniques have been developed for performing physical models of field-scale prototypes and for testing the physical properties of materials. A brief history of centrifugal applications is presented below; specific areas of interest include soil moisture retention, soil moisture movement and solute transport. An overview of past and current centrifuge projects is presented below to emphasize the wide range of practical and research applications.

Soil Moisture Capacity

Centrifugal techniques have been developed to quantify the moisture retention capacity of soils. Briggs and McLane (1907) presented the development of experimental procedures and test results of a centrifugal method for determining a soil parameter they designated as moisture equivalent. They were after a way to quantitatively compare disturbed soil samples and elected to compare samples on the basis of capillary equilibrium in a sample undergoing a constant rotational velocity. The centrifuge they designed was driven by a steam turbine and was capable of rotating eight 0.5 cm soil samples up to 5500 rpm (approximately 3550

times the force of gravity, or 3550 g's). Their experimental assessment included the influence of test duration, angular velocity and initial water content on the moisture content after centrifugation. They presented moisture equivalent values for 104 soil types.

In 1935 the American Society of Testing and Materials (ASTM) adopted a standard test method for determining the moisture equivalent of soils (ASTM, 1981). The moisture content of an air-dried and reconstituted sample after centrifugation at 1000 g's for one hour was suggested as an approximation for the air-void ratio, also referred to as the water holding capacity or the specific retention. Additional testing development was conducted by Johnson et al. of the U. S. Geological Survey (1963).

Bear (1972) presented a simple method to rapidly obtain the moisture retention curves of thin soil samples by repeated centrifugation periods at different rotational speeds. Corey (1977) discussed the use of gamma radiation attenuation during centrifugation to obtain an entire segment of the moisture retention curve during the course of a single test.

Soil Moisture Movement

Alemi et al. (1976) presented the theoretical development and experimental design of two methods for determining the unsaturated hydraulic conductivity of undisturbed soil cores by centrifugation. The potential savings in time was a major advantage of the proposed method. A closed system method was based on describing the redistribution of moisture within a sample after centrifugation by means of the mass shift, as detected by a pair of analytical balances. Relevant assumptions included constant hydraulic conductivity along the sample

during redistribution and a linear relation between moisture content and soil-water pressure head. Acceleration levels between seven and 285 g's were imposed on a 5-cm long sample for durations of 60, 70 and 100 minutes. Estimates of conductivities from two cores of Yolo loam compared well to field and other lab results.

Alemi et al. (1976) proposed a pressure outflow method for determining the unsaturated hydraulic conductivity from a centrifuged sample. Estimates of conductivity could be obtained from the record of total outflow resulting from a specific increase in rotational velocity. No experimental results were available to assess the method.

Cargill and Ko (1983) presented details of a centrifugal modeling study of transient water flow in earthen embankments. The total hydraulic head was monitored with miniature pressure transducers fitted with porous tips. Their results suggested the movement of fines (clay to silt grain sizes) caused anomalous increases in conductivity via development of channelized flow paths. Comparison of centrifuge model results with a finite element program indicated very similar heights of the phreatic surface at the headwater end with a gradual discrepancy toward the tailwater side of the embankment.

Solute Transport

Arulanandan et al. (1984) presented cursory details of a study utilizing a centrifuge to execute a simple physical model of infiltration below a ponded water surface. Breakthrough curves of electrical resistivity in saturated sand samples were obtained under steady water flux conditions. Acceleration levels between 1 g and 53 g's were imposed on sand samples with a saturated hydraulic conductivity

in a 1-g environment of 0.01 cm/sec. A constant head was maintained throughout the tests. The authors suggested that centrifugal modeling "may have significant application" in determining the advective and dispersive components of contaminant transport (1984, p. 1). However, careful review of their testing procedure and results indicated that only a single aspect of centrifugal techniques offers a possible advantage over laboratory bench (i.e., 1-g) physical models.

The paper described a prototype scenario of fresh water infiltrating into a saltwater stratum of soil under a constant ponded depth, although the conditions actually constructed were appropriate for the much simpler one-dimensional model of a constant head saturated hydraulic conductivity test. The breakthrough curve of fresh water was determined at multiple acceleration levels by means of an electrical resistivity probe located within the soil specimen. A comparison of modeled breakthrough curves at 1 g and 53 g's indicated a reduced pore fluid velocity at the higher acceleration. While this lag may be an artifact of the delayed response of the resistivity probe, the results possibly reflected lower flow rates due to an increase in effective stress on the soil particles, caused by the increasing acceleration level with sample depth. The accurate reproduction of the prototype effective stress profile would be a definite advantage of centrifugal models over laboratory bench models.

The assumption of a reduction in model length by a factor of N (the ratio of accelerations between model and prototype) to maintain dynamic similitude resulted in a proportionate increase in the hydraulic gradient across the sample. This led to a major pronouncement of the paper, i.e., that test durations will decrease proportionately by the

square of the acceleration ratios. While this result is valid in the reference frame of the conceptually simple tests conducted, the suggestion that the results are generally valid and uniquely a characteristic of centrifugal modelling is misleading. The reduction in testing time realized by centrifugal modeling can be readily duplicated on a bench model. The equivalence in terms of hydraulic potential of fluid pressure forces and gravity-induced body forces allows reproduction of centrifuge acceleration potential in bench models by merely increasing the pressure on the fluid delivery systems. Thus, the centrifuge does not offer a unique capability for decreasing the testing time of physical models.

The authors' suggestion that dispersive characteristics of soil media can be modelled at accelerated velocities was apparently disputed by the study results. Hydrodynamic dispersion coefficients reflect the nonuniform pore fluid velocity distribution within a soil volume. Accordingly, the dispersion coefficient has been observed to vary significantly with the velocity of the bulk fluid, demonstrating greater variation in soils with a wide distribution of pore sizes. While the breakthrough curve results presented clearly demonstrated the dependence between the dispersion coefficient and pore fluid velocity, the authors failed to recognize this and optimistically suggested that estimates of this parameter can indeed be determined at accelerated velocities. Extrapolation of dispersion coefficients determined by centrifuge tests to field conditions and pore velocities would be severely restricted to laboratory media with an extremely uniform pore size distribution such that hydrodynamic dispersion would be independent of pore fluid velocity.

In summary, the study highlighted a principal feature of physical modeling in a centrifuge, that of increasing the body forces imposed on fluid and soil particles. However, the testing conditions were too narrow in range to warrant the authors' general conclusion that centrifugal modeling is superior to bench models in determining advective characteristics of contaminant transport. In addition, the breakthrough curve results disputed their suggestion that dispersive characteristics of soils under field conditions can be determined in a centrifuge model. Because the prototype condition was never executed, there was no independent base with which to compare the model results.

Geotechnical Engineering Applications

The use of centrifuges in geotechnical engineering research has increased at an accelerated rate in the last decade. From the earliest reference in American literature (a study of mine roof design) centrifuges have been utilized to investigate a wide spectrum of problems, including landfill cover subsidence, soil liquefaction, slope stability, cellular coffer dam performance, bearing capacity of footings in sand, tectonic modeling, explosive and planetary impact cratering, sinkhole collapse and evaluation of sedimentation and consolidation of fine-grained materials.

Research centers specializing in centrifuge projects have developed in many nations, notably England (Cambridge University), the United States (University of California - Davis, University of Florida, University of Colorado, University of Kentucky, NASA Ames Research Center, and others), Japan (four research centers) and France. A recent review of the state of the art ambitiously projected "the day will come when every well-equipped geotechnical research laboratory will include a

centrifuge for model testing . . ." (University of California, 1984, p. 36). The growth curve presented in Figure 5 demonstrates the increase in interest in centrifugal applications. A summary of advantages and limitations of centrifugal techniques compiled from several articles is presented in Tables 5 and 6.

University of Florida Centrifuge Equipment

The University of Florida geotechnical centrifuge has a 1-m radius and can accelerate 25 kg to 85 g's (2125 g-kg capacity). Figure 6 presents a schematic drawing of the centrifuge and photographic equipment. A photograph of the centrifuge is presented in Figure 7. A window on the centrifuge housing allows visual observations of the model in flight. A photo-electric pick-off and flash delay augment the system for visual observation and photographic recording. Two hydraulic slip rings supply fluid to the apparatus, while 32 slip rings are available for transmission of electrical current.

Fluid Mechanics and Hydraulics in a Centrifuge

All laboratory systems utilized as a permeameter or physical model inherently entail fluid flow through conduits and through porous media. The design and analysis of such an apparatus necessitated an understanding of fluid flow in both regimes as well as any modifications of their behavior under the influence of radial acceleration. In this context, fluid flow is discussed below.

Flow Through Conduits

During the execution of a laboratory hydraulic conductivity test, the hydraulic energy at the sample boundaries is determined by the

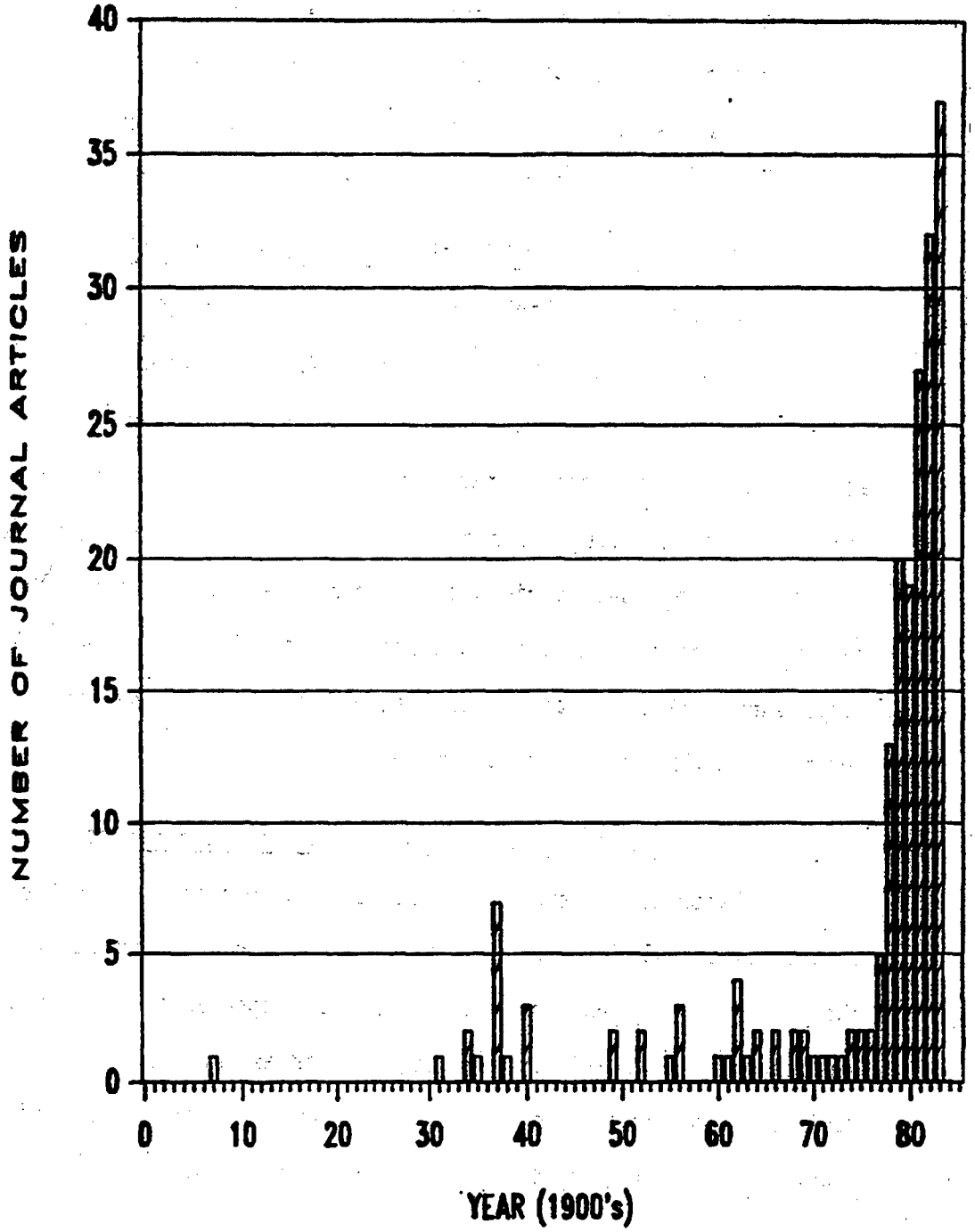

Figure 5. Number of Journal Articles on Centrifuge Applications

Table 5. Advantages of Centrifugal Modeling

1. It is the only means for subjecting laboratory models to gravity-induced self-weight stresses comparable to those in the full-scale field prototypes.
2. Many gravity-dominated phenomena take place at dramatically increased rates.
3. It allows for verification of model to prototype scaling relationships by repeating the tests at various acceleration levels, a technique referred to as modeling of models.
4. A single model configuration can be used to evaluate many different prototype configurations by varying the acceleration levels.
5. It is the only realistic way to model large-scale phenomena such as nuclear explosive effects and planetary impacts.

Table 6. Limitations of Centrifugal Model Testing

1. The acceleration level in the centrifuge varies with the radius of rotation, in contrast to the essentially constant gravitational force field at the earth's surface.
2. Coriolis effects may have an influence if movements occur within the model during rotation.
3. The start-up period, when model acceleration is increased, has no counterpart in the prototype.
4. Tangential acceleration effects may be significant if centrifuge speeds are changed too rapidly.
5. Grain size similarity is difficult to achieve.
6. There is a risk of injury and/or property damage during operation of a large centrifuge due to the large forces that are developed.
7. They can be more expensive than conventional apparatus.

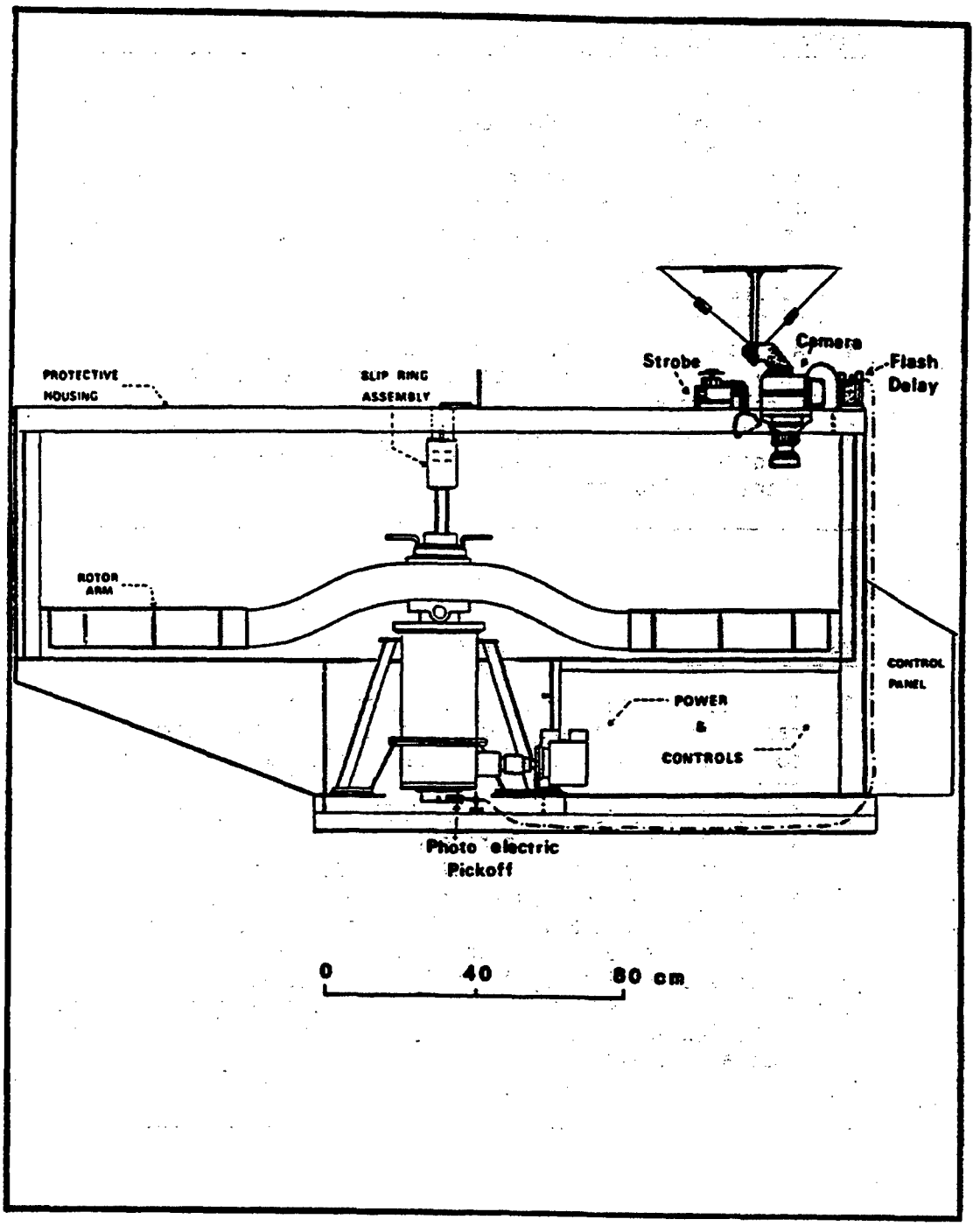

Figure 6. Schematic of the U. F. Geotechnical Centrifuge

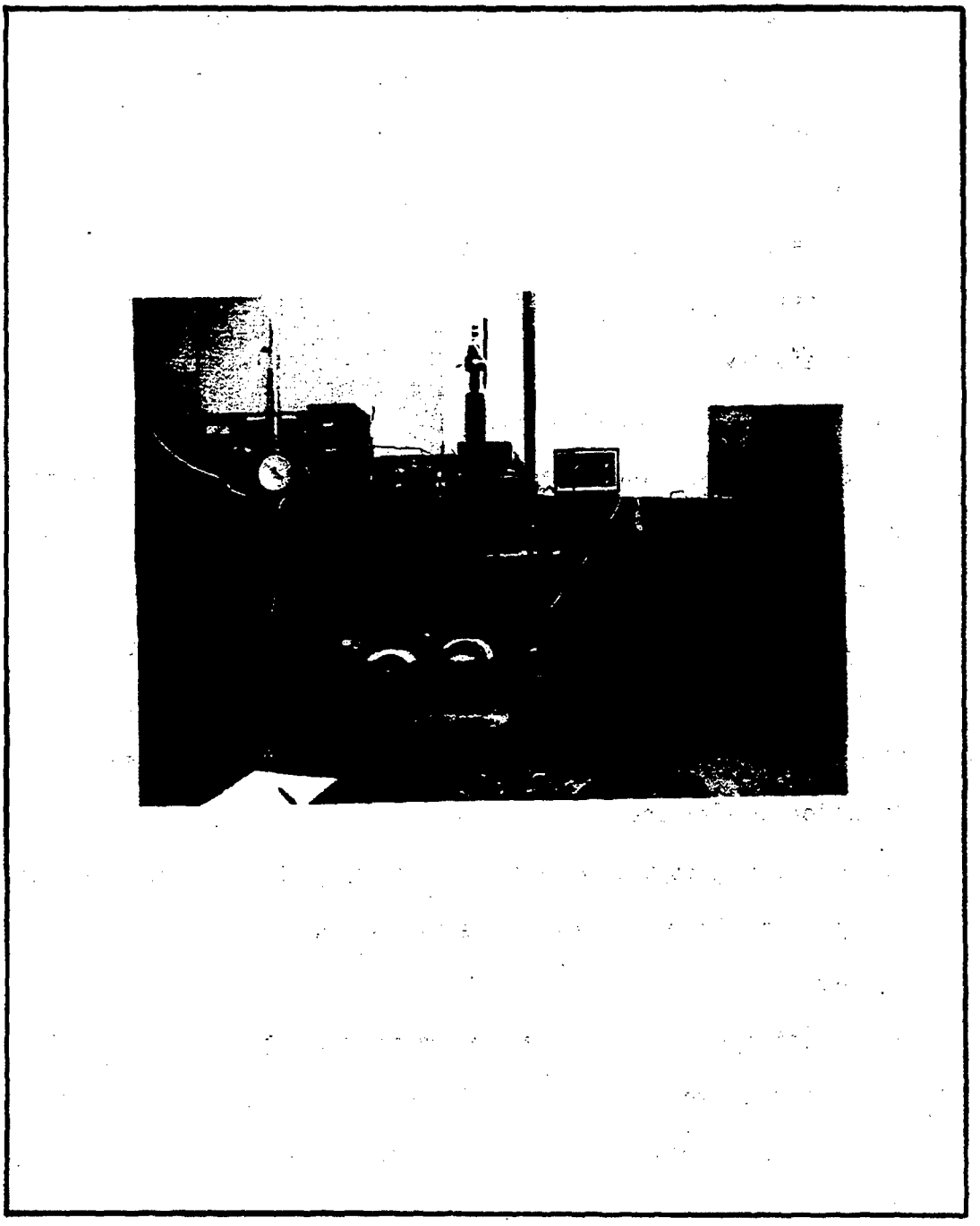

Figure 7. Photograph of the U. F. Geotechnical Centrifuge

influent and effluent reservoir conditions and the flow characteristics of the conduit system. Under the influence of the earth's gravitational acceleration, the one-dimensional relationship between the pressure distribution and fluid kinematics in a conduit flowing full between two points is the Bernoulli equation (Fox and McDonald, 1978)

$$(P/\rho + V^2/2 + gz)_1 = (P/\rho + V^2/2 + gz)_2 \quad (9)$$

where P = pressure acting on the fluid (M/LT^2);

ρ = mass density of the fluid (M/L^3);

V = velocity of the fluid (L/T); and

z = elevation of the point (L).

The Bernoulli equation is an integrated form of the Euler equations of motion. An analogous equation was derived to describe the same relationship within a centrifuge. The equations of fluid motion were evaluated in the reference frame of a centrifugal permeameter. For the elementary mass of fluid in a tube (see Figure 8), motion is parallel to the radial acceleration. The forces acting on the element in the direction of flow are

1. hydraulic pressures acting on the surfaces of the control element;
2. shearing forces of adjacent elements and/or the walls of the tube; and
3. centrifugal body forces acting on the element.

For a control volume in a centrifuge, the acceleration, a_r, acting on the mass is a function of the radius, r, expressed as

$$a_r = rw^2 \quad (10)$$

where w = angular velocity (rad/T), which is constant at all distances from the axis of rotation. Newton's second law of motion in one

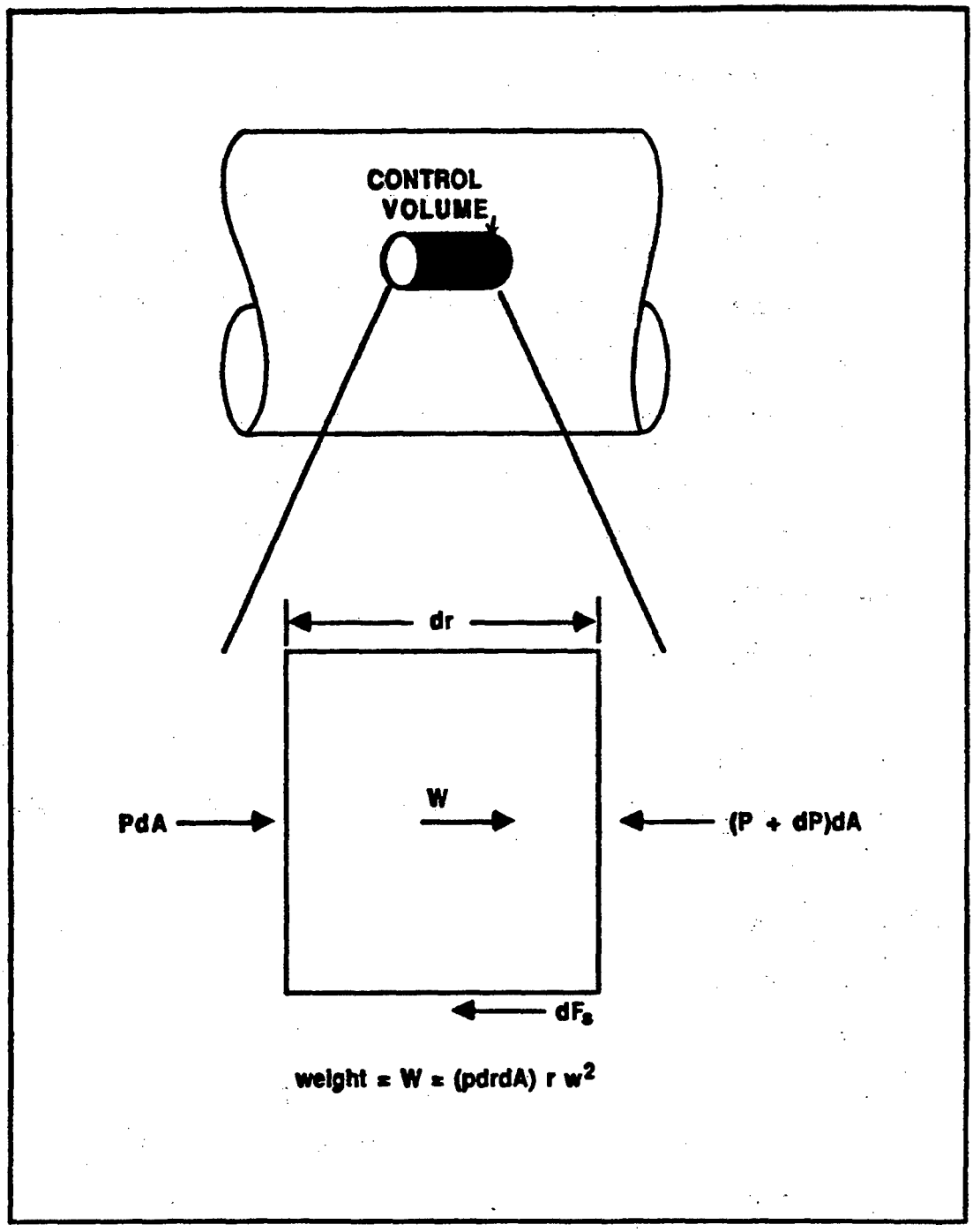

Figure 8. Definition Sketch for Analysis of Forces Acting on a Fluid Volume in a Centrifuge

dimension can be expressed as

$$F = Ma_r = M(dV/dt) = p\ dr\ dA\ dV/dt \quad (11)$$

where F = sum of the forces acting on the control volume (ML/T^2);

M = mass of the element (M); and

A = cross-sectional area of the element (L^2)

Substituting in the forces acting on the element, equation 11 becomes

$$PdA - (P+dP)dA - dF_s + p\ a_r d\ A\ dr = p\ dr\ dA\ dV/dt \quad (12)$$

where P = pressure acting on the control surface of the element; and

dFs = total shear forces.

Dividing equation 12 by (pdA) and simplifying yields

$$(-dP/p) - (dF_s/pdA) + a_r dr = dr\ dV/dt \quad (13)$$

Replacing dr/dt with the fluid velocity, V, (dF_s/pdA) with dH_L and incorporating equation 10 yields

$$(-dP/p) - dH_L + w^2\ rdr = VdV \quad (14)$$

Collecting terms,

$$-w^2\ rdr + dP/p + dH_L + VdV = 0 \quad (15)$$

For an incompressible fluid equation 15 is integrated across the element to yield

$$-w^2(r_2^2 - r_1^2)/2 + (P_2 - P_1)/p + H_L + (V_2^2 - V_1^2)/2 = 0 \quad (16)$$

Separating terms yields the centrifugal equivalent of the Bernoulli equation:

$$(V^2/2 + P/p - w^2r^2/2)_1 = (V^2/2 + P/p - w^2r^2/2)_2 + H_L \quad (17)$$

Defining the specific energy hydraulic potential as

$$H = V^2/2 + P/p - w^2r^2/2 \quad (18)$$

Equation 17 can be written as

$$H_1 = H_2 + H_L \quad (19)$$

The dimensions of the specific energy potential are energy per unit mass. For a system in hydrostatic equilibrium, the velocity and hence the frictional losses are zero. The relationship between the pressure distribution and the radial location is thus

$$P_2 = P_1 + \rho w^2(r_2^2 - r_1^2)/2 \qquad (20)$$

This relationship is demonstrated in Figure 9 for $P_1 = 0$ and $r_1 = 50$ cm.

Flow Through Porous Media

For flow through porous media, the velocity component of the hydraulic potential is negligible compared to the pressure and elevation terms. In reference to the control volume in Figure 10, Darcy's law within a centrifuge sample can be expressed using the specific energy potential gradient by introducing equation 18 into equation 4 as

$$q = -K \frac{d}{dr}(P/\rho - w^2 r^2/2) \qquad (21)$$

Consistent with the units of the hydraulic potential, the hydraulic conductivity, K, has the units of time. This dimensional definition retains the basic relationship of flow conductivity to the soil matrix and fluid properties, i.e.,

$$K = k / \nu \qquad (22)$$

This definition of K is not a function of the gravity induced acceleration acting on the fluid mass. Expanding equation 21 yields.

$$q = -K \left(\frac{d(P/\rho)}{dr} - \frac{w^2\{(r + dr)^2 - r^2\}}{2\,dr}\right) \qquad (23)$$

expanding the quadratic term yields

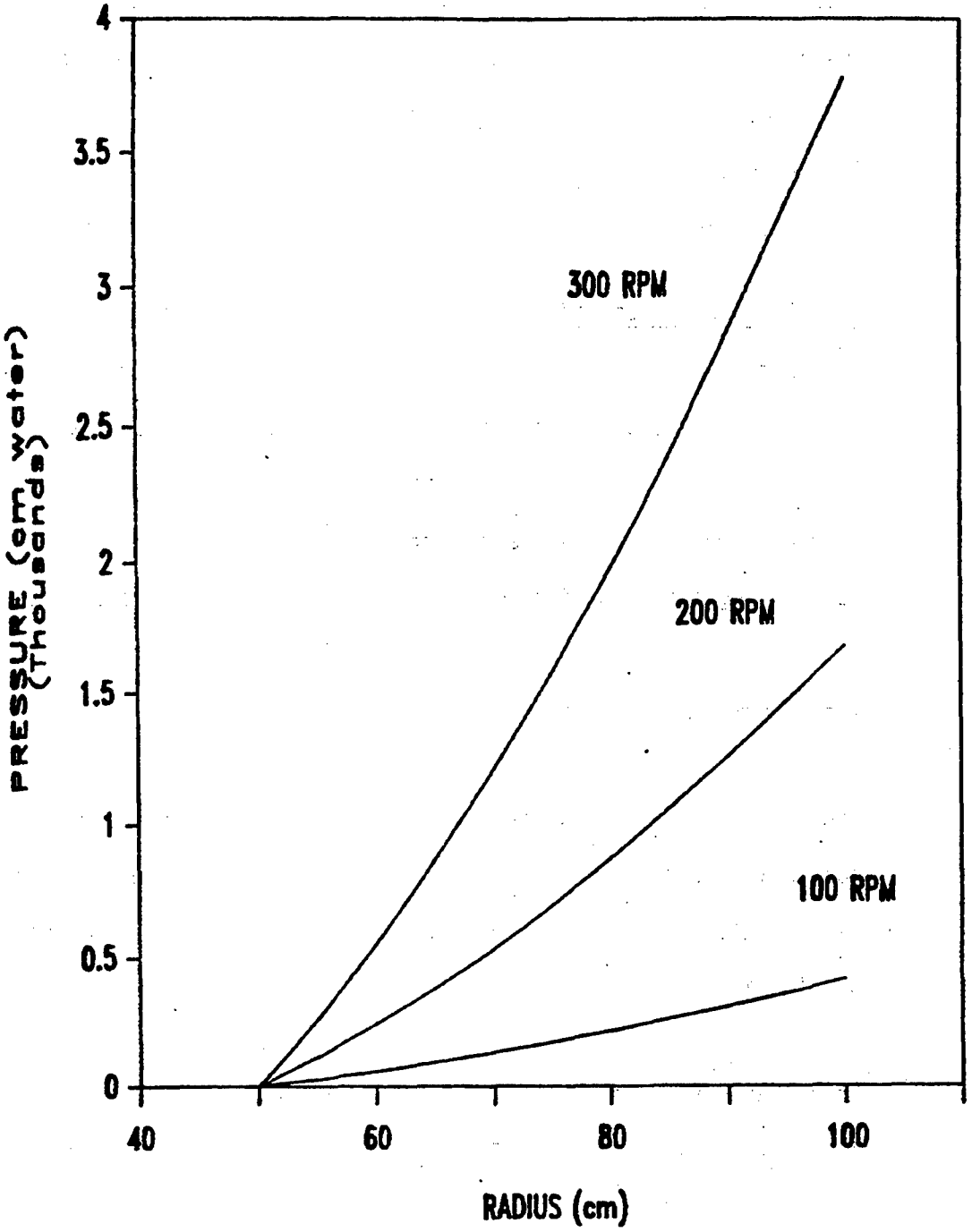

Figure 9. Hydrostatic Equilibrium in a Fluid Sample in a Centrifuge

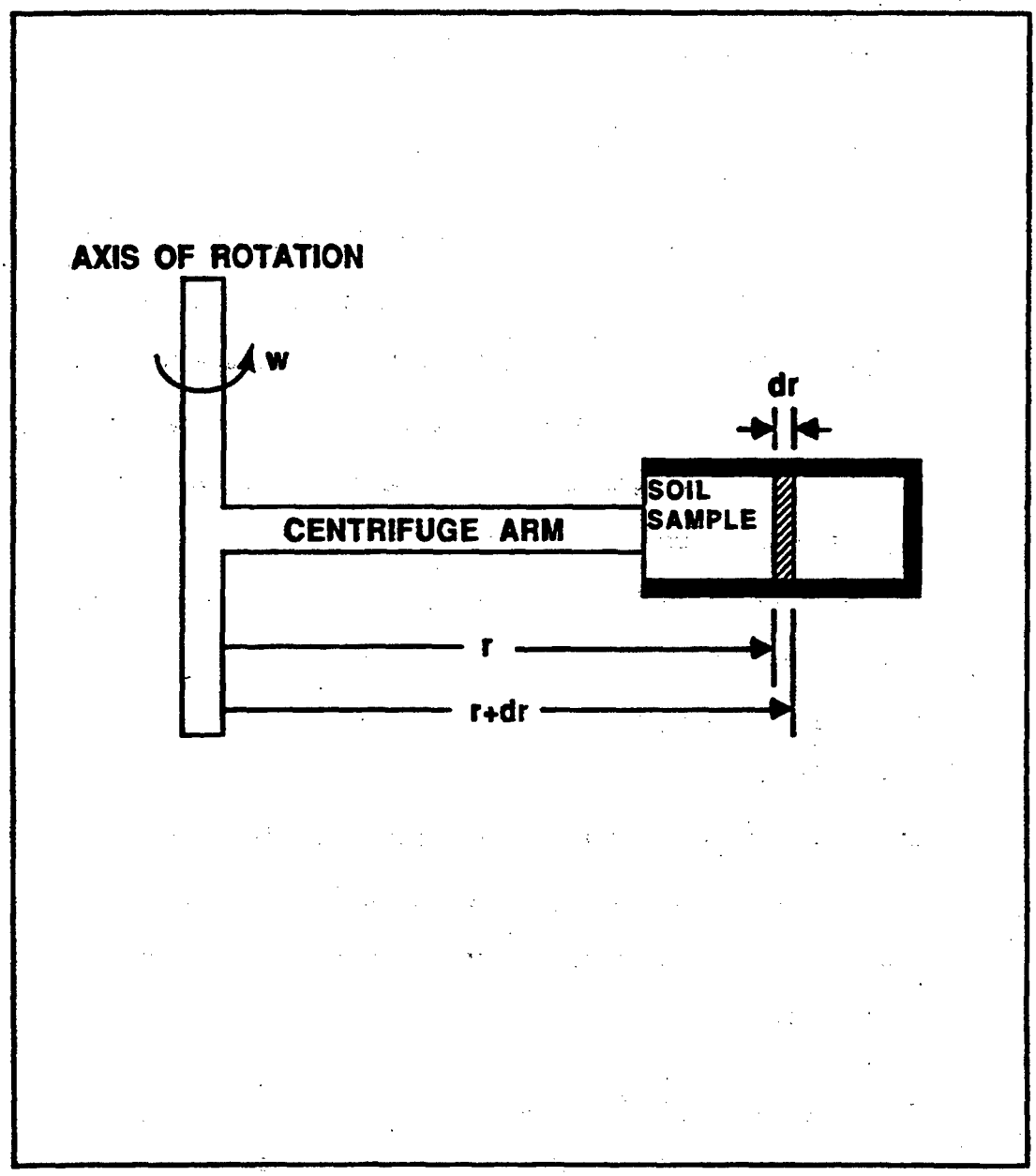

Figure 10. Definition Sketch of a Soil Volume in a Centrifuge

$$q = -K \left(\frac{d(P/p)}{dr} - \frac{w^2\{r^2 + 2rdr + dr^2 - r^2\}}{2\,dr}\right) \tag{24}$$

$$q = -K \left(\frac{d(P/p)}{dr} - \frac{w^2(2rdr + dr^2)}{2\,dr}\right) \tag{25}$$

Evaluating equation 25 at a point and neglecting the second order differential yields.

$$q = -K \left(\frac{d(P/p)}{dr} - rw^2\right) = -K \left(\frac{d(P/p)}{dr} - a_r\right) \tag{26}$$

In a 1-g environment, the second term in brackets is equal to unity, while in a multiple-g environment, it is equal to the acceleration acting on the fluid mass. Assuming that the pressure gradient component is not influenced by the acceleration induced by the centrifuge, the hydraulic potential gradient within the centrifuge will increase over a 1-g sample by an amount equal to (a_r-1).

This additional gradient will result in a proportionate increase in the fluid flux through the soil, i.e., the flux at a radius, r, will increase by an amount equal to

$$q = -K\,(a_r - 1) \tag{27}$$

where a_r is given by equation 10. However, it is important to note from equation 26 that the increase in specific discharge is directly proportional to the acceleration level only if the pressure gradient equals zero.

Energy Losses in The Permeameter

Along with the energy loss induced across the soil sample, mechanical energy is lost in the permeameter due to friction along the tubing walls, and, of minor importance, due to flow contractions, expansions and bends. These losses are generally expressed in the form of the Darcy-Weisbach equation

$$H_L = (f + C)\, LV^2/2D \qquad (28)$$

where H_L = lost mechanical energy per unit mass (L^2/T^2);

f = friction factor (dimensionless);

C = coefficient for minor energy losses (dimensionless);

L = length of the conduit (L); and

D = inside diameter of the conduit (L).

Dimensional Analysis

When used to conduct physical modeling of prototype behavior, appropriate relationships between the forces acting on the control volume must be preserved in the centrifuge model. Scaling relationships between the fundamental dimensions, mass, length and time, of the prototype and centrifuge model are determined by dimensional analysis. Historically, three methods of determining scaling factors have been utilized. Croce et al. (1984) employed an approach based on Newton's original definition of mechanical similarity requiring proportionality of all the forces acting on similar systems. Cargill and Ko (1983) derived scaling relationships from a method of dimensional analysis incorporating the Buckingham Pi Theorem. Others have based scaling relations on the differential equations governing the phenomena. Each of these methods, when properly applied, yields identical scaling factors for the same phenomena and assumptions. Verification of the scaling factors is accomplished by comparing results of tests with various geometrical and/or acceleration ratios; this latter process is referred to as modeling of models and can be readily executed by spinning the same sample at various speeds and comparing results. An apparent discrepancy concerning the scaling of hydraulic conductivity was based

on an inconsistent definition of the total potential gradient. When the potential is defined as the hydraulic potential, with the dimension of length, K scales as 1/N, where N is the ratio of acceleration in the model to that in the prototype. When the potential is defined as the pressure potential or the specific energy potential, K scales as unity. The reason for the difference in scaling is that the definition of K in the latter cases is independent of the acceleration acting on the fluid. A general set of scaling factors is presented in Table 7; however, individual analysis of the hydraulic conditions specific to the model under consideration should be conducted.

Table 7. Summary of Scaling Relationships for Centrifugal Modeling

Property	Scaling Factor
Potential gradient (specific energy potential)	1/N
Potential gradient (hydraulic potential)	1
Potential gradient (pressure potential)	1/N
Hydraulic conductivity (specific energy potential)	1
Hydraulic conductivity (hydraulic potential)	1/N
Hydraulic conductivity (pressure potential)	1
Time	XN
Pressure	X/N
Darcian flux in saturated soil	1/N
Darcian flux in unsaturated soil	1
Volumetric flow rate	X^2/N
Capillary rise	N

Note: N = (acceleration of model)/(acceleration of prototype)
X = (unit length of prototype)/(unit length of model)

CHAPTER IV
TESTING PROGRAM

Centrifugal techniques for evaluating hazardous waste migration include physical modeling and material properties testing. To fully utilize the potential of physical modeling in the centrifuge, the fundamental relationships of radial acceleration, hydraulic pressures and pore fluid kinematics within the centrifuge soil sample needed to be developed and verified. The execution of concurrent bench and centrifuge hydraulic conductivity testing provided the opportunity to investigate these fundamental fluid flow properties as well as allowed the direct assessment of the feasibility of material properties testing within the centrifuge. A secondary objective of the project was to establish the theoretical and practical operating limits of centrifugal techniques. The design and execution of the laboratory testing program is discussed below.

Objectives

The laboratory research program was designed and implemented to develop centrifugal testing methods for determining saturated and unsaturated hydraulic conductivity of soil samples. The testing program encompassed:

1. the analysis, design and fabrication of permeameters for use in the centrifuge;
2. execution of hydraulic conductivity tests in a 1-g environment to provide a benchmark for comparing centrifuge test results;

3. derivation of the appropriate equations of motion for fluid flow in a centrifuge;
4. execution of hydraulic conductivity tests in the centrifuge at various accelerations;
5. comparison of centrifuge results with 1-g test results; and
6. if necessary, modification of the centrifuge device, testing procedures and/or data analysis based on results of the comparison.

The technical feasibility of centrifugal techniques for evaluating hazardous waste migration was assessed based on the results obtained. Results of the testing program will also serve as the foundation for subsequent research in the area of centrifugal modeling of hazardous waste migration. A summary of the testing program is presented in Table 8.

Table 8. Summary of Permeability Testing Matrix

Soil Type	Soil Moisture Condition: Saturated Water	Saturated Decane	Unsaturated Water	Unsaturated Decane
Bench tests				
Sand	L[a]	L	C	
Sand/clay[b]	L	L		
Kaolinite[c]	L	L		
Kaolinite[d]	L	L		
Centrifuge tests				
Sand	L	L	C	
Sand/clay[b]	L			

Notes: a L indicates a laboratory test; C indicates analysis by computer model
b 80 percent sand, 20 percent kaolinite, by weight
c initial moisture content was 29 percent by weight
d initial moisture content was 32 percent by weight

Materials

Permeants

Saturated and unsaturated hydraulic conductivity tests were performed using distilled water and decane as the permeants. A survey of current hydraulic conductivity studies and published testing procedures indicated that distilled water was the most common permeant, although most agree that so-called native water should be used. Several studies have documented reductions in the estimates of hydraulic conductivity through clays using distilled water of up to two orders of magnitude lower than estimates from tests using native water or a weak electrolyte solution (Uppot, 1984; Olson and Daniel, 1981). The discrepancy has been attributed to electric double layer interaction of the clay particles with the fluid (Dunn, 1983; Uppot, 1984; Olson and Daniel, 1981). When distilled water flows past clay particles with high surface potentials, the electric double layer of diffuse ions expands as the number of counter ions (anions in this case) in solution decreases, increasing the surface viscosity and resulting in reduced estimates of hydraulic conductivity (Adamson, 1982). The use of distilled water did not present a problem in this study because the initially dry kaolinite was prepared to an initial moisture content with distilled water. In essence, distilled water was the "native" water for these clays.

Reagent grade, i.e. at least 99 percent pure, decane was used as the nonaqueous permeant. Decane is a straight chain hydrocarbon with similar properties to the U. S. Air Force jet-fuel JP-4. A comparison of physical and chemical properties of water, JP-4 and decane is presented in Table 9. Like jet fuel, decane is flammable in specific mixtures with air. The lower and upper explosive limits for decane in

Table 9. Comparison Between Properties of JP-4, Decane and Water (at 25°C)

Property	JP-4 Jet Fuel[a]	n-Decane[b]	Water[c]
Fluid density (g/cc)	0.774	0.686	0.997
Kinematic viscosity (cm^2/s)	0.01184	0.01195	0.00900
Surface tension (dyne/cm)	24.18	18.59	72.14
Freezing point (C)	-60.000	-29.661	0.000
Boiling point (C)	not available	174.123	100.00
Vapor pressure (cm water)	not available	3.240	32.69
Solubility in water (mg/l)	not available	0.009	-
Polarity	Nonpolar	Nonpolar	Polar

Sources: a Ashworth, 1985
b Chemical Rubber Company, 1981
c Giles, 1962

air are 0.67 and 2.60 percent by volume, respectively. The auto-ignition temperature of decane is greater than 260°C, while the closed cup open flame flash point is 46°C. However, decane is not susceptible to spontaneous heating (Strauss and Kaufman, 1976). Suitable extinguishing agents include foam, carbon dioxide and dry chemicals. Because of the explosive potential and otherwise hazardous nature of decane, safety procedures in handling and disposal were implemented. Recommended precautions for safe handling of decane include the use of rubber gloves, lab coats, face shields, good ventilation and a respirator. Recommended disposal procedures consist of absorbing in

vermiculite, collection in combustible boxes, transferal to open pit and burning (Strauss and Kaufman, 1976). During the course of the testing program waste decane and water were separated by density differences; the waste decane was decanted into the original shipping containers and picked up by a University of Florida hazardous waste removal group.

The potential existed for atomizing substantial volumes of decane during centrifugation, which could have resulted in a potentially explosive atmosphere. The presence of elevated hydraulic pressure under high acceleration could cause a rapid efflux of decane from the permeameter should a seal in the apparatus fail. Depending on the location of the seal failure, the amount of decane released could result in a concentration in the centrifuge atmosphere between the lower and upper explosive limits, and hence present a combustion hazard if an ignition source was present. The decane could be sprayed and subsequently condensed on the walls of the centrifuge housing. The relatively cool temperature (25°C) of the housing is well below the auto-ignition point (260°C) and below the open flame flash point of 46°C. In summary, the actual combustion behavior of decane released during centrifugation is not definitively predictable. However, general calculations of explosive potential coupled with a concerted exercise of caution suggest that there is little potential of combustion during centrifuge testing.

Soils

Four soil preparations were utilized in the testing program. The soils were chosen to span the wide range of pore fluid velocities of natural soils as well as for their low degree of reactivity:

1. fine-grained silica sand;

2. 80% sand - 20% kaolinite (by weight);

3. 100% kaolinite - prepared to an initial water content of 29%; and

4. 100% kaolinite - prepared to an initial water content of 32%.

The uniform fine-grained silica sand used in the laboratory tests was obtained from the Edgar Mine Company of Edgar, Florida. A summary of the physical and chemical characteristics of the sand is presented in Table 10.

Table 10. Characteristics of the Sand Used in the Testing Program

Parameter	Value
Chemical Composition	
SiO2	99.3 percent by weight
Other minerals	< 1 percent by weight
Particle Size Distribution	Cumulative percent undersize
1.00 mm	100.0
0.25 mm	93.0
0.20 mm	50.0
0.125 mm	10.0
0.07 mm	0.6
Specific surface area (based on spherical grain)	0.01 m^2/g
Specific Gravity	2.64

The kaolinite employed for the laboratory tests was also obtained from the Edgar Mine of Edgar, Florida. A summary of the physical and chemical characteristics of the clay is presented in Table 11. Kaolinite was selected as a representative fine-grained soil with extremely low values of hydraulic conductivity, with the advantage that its shrink/swell and reactivity tendencies are small compared to other clays such as illite. The hydrogen bonding and Van der Waal forces which hold the silica and alumina sheets together are sufficiently

Table 11. Characteristics of the Clay Used in the Testing Program

Parameter	Value
Chemical Composition	Weight percent, dry basis
SiO2	46.5
Al2	37.6
Other minerals	< 2
Loss on ignition	13.77
Mineral Content (x-ray diffraction)	
Kaolinite (Al_2O_3 $2SiO_2$ $2H_2O$)	97 percent
Particle Size Distribution	Cumulative percent undersize
40 micron	100
10 micron	90
5 micron	78
3 micron	68
1 micron	49
0.5 micron	40
0.2 micron	20
Specific Surface Area	11.36 m^2/g
Specific Resistivity	35,000 ohms/cm
Oil Absorption	47.3 g oil/100 g clay
pH	
5% solids	6.05
10% solids	6.07
20% solids	5.85
30% solids	5.89
Cation Exchange Capacity	5.8 Meq/100 g
Specific gravity	2.50

strong to restrict interlayer expansion (Mitchell, 1976). A net negative charge is present on the edges of kaolinite particles resulting in a relatively low cation exchange capacity of 3-13 milliequivalents per 100 grams. Relative to other clay, e.g., montmorillonite and illite, kaolinite has a small specific surface area of 5-12 square meters per gram. The particular kaolinite employed in the laboratory tests had an average specific surface area of 11.36 m^2/g as determined

by the BET method using nitrogen. The clay samples were prepared at two initial water contents, one below the optimum water content of 30 percent by weight and one above the optimum water content. Theory and practical experience indicated that the resulting pore structures would differ enough to produce discernible differences in hydraulic conductivity values (Mitchell, 1976).

A mixture of sand and clay was prepared to create a soil with intermediate values of hydraulic conductivity. The mixture was prepared to the ratio of 4 parts sand to one part kaolinite by weight.

The relationship between the moisture content and the soil moisture suction of a soil volume is referred to as a soil moisture retention curve, or moisture characteristic curve. The curves are specific to each soil type and generally exhibit a hysteretic response during the absorption and drainage cycles. Moisture retention curves were prepared for each soil during a drainage cycle using water covering the range from saturation to 15 bars suction. The results, presented in Figure 11, were used in the unsaturated hydraulic conductivity analysis.

Testing Equipment

Evaluation of Current Technology

A preliminary task was the design of the permeameter for the testing program. A review of current research revealed that two major types of permeameters are utilized for determining the hydraulic conductivity of water and nonaqueous fluids in saturated samples. Historically, sample containers had rigid walls. Mechanical simplicity, ease of sample preparation and ability to facilitate field cores were among the reasons for their popularity. However, sidewall leakage,

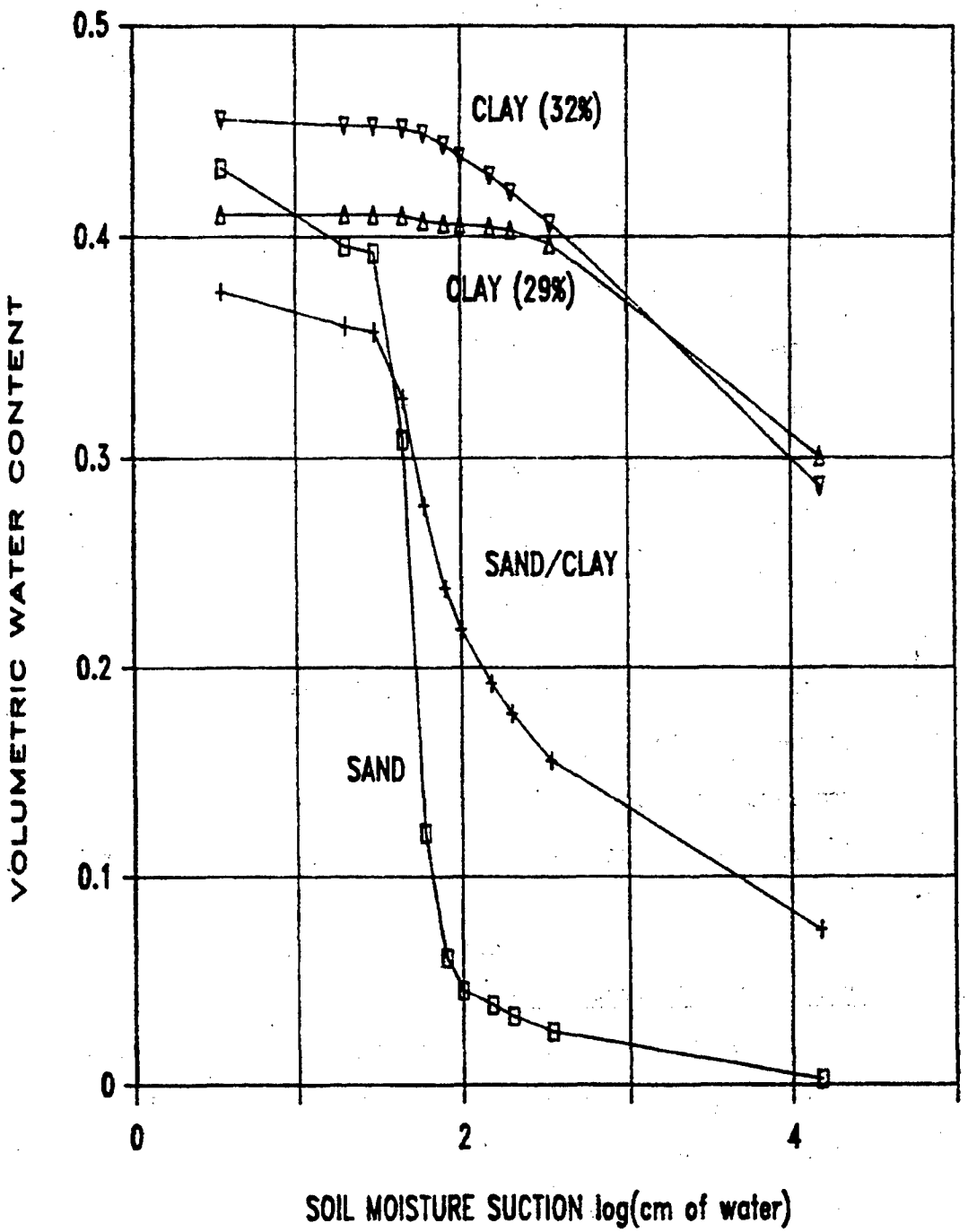

Figure 11. Moisture Retention Curves for the Sand, Sand/Clay and Clay Samples

i.e., flow along the wall rather than through the sample, has been documented, raising the question of validity of results for a rigid wall apparatus (Daniel et al., 1985). Prevention of sidewall leakage was addressed by various remedial measures, as exemplified by the practice of sealing the top of the sample adjacent to the wall with sodium bentonite. Another practical problem encountered in rigid wall apparatus has been volumetric change of reactive soils when exposed to nonaqueous permeants. Reports of tremendous increases in the hydraulic conductivity of soils to organic solvents have been criticized because the rigid wall apparatus utilized were conducive to unrestrained shrinking resulting from chemical reaction between the fluid and the soil matrix (Brown et al., 1984). With the advent of triaxial apparatus (see Figure 12), used for measurements of soil strength, an alternative to the rigid wall container developed. The triaxial apparatus confines the soil sample in a flexible membrane which allows transmittal of confining pressures to the soil specimen. Flow along the wall outside the specimen is prevented by the continuous contact between the sample and the flexible wall. Review of current research indicated that flexible wall permeameters are the preferred laboratory apparatus for saturated hydraulic conductivity measurements of nonaqueous permeants (Dunn, 1983; Uppot, 1984; Daniel et. al., 1985).

The flexible wall apparatus also has the advantage over rigid wall permeameters in that complete saturation of the soil sample can be ensured by applying high pressure from both ends of the sample. In the process of introducing water into the sample, air is entrapped in the interior voids, preventing complete saturation of the sample. These air pockets effectively block the flow of water through the sample, reducing

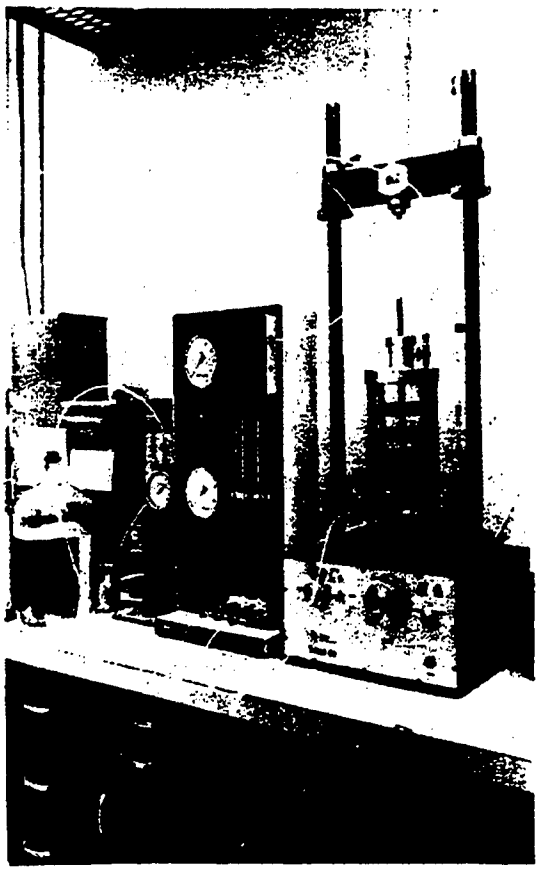

Figure 12. Photograph of a Commercial Triaxial Apparatus

the observed value of the hydraulic conductivity. By applying high back pressures, the trapped air dissolves into the pore fluid. Attempts to utilize back pressure saturation in rigid wall permeameters have exacerbated the sidewall leakage problem (Edil and Erickson, 1985). A related advantage of flexible wall apparatus over rigid wall permeameters is the ability to verify complete saturation of the sample before testing begins. Application of an incremental increase in the confining pressure, transmitted to the sample by the flexible membrane, will cause an equal incremental increase in pore fluid pressure when the sample is fully saturated. The ratio of the observed pore pressure increase to the applied increment of confining pressure is referred to as the "B" value, and is equal to unity for complete saturation. It is not possible to check for "B" values in a rigid wall device (Christiansen, 1985).

Another benefit of the flexible wall apparatus is the ability to control the effective stresses acting on the sample particles. During back pressure saturation, the external applied pressure is proportionately increased to maintain specified effective stresses on the soil particles. Neglecting the weight of the overlaying sample, the effective stress of a sample in a flexible membrane is the net pressure difference between the pore fluid pressure and the external chamber pressure. This unique capability allows the sample to be tested under similar effective stress conditions as exist in the field, e.g., fifty feet below the surface. A comparison between the confining stress distribution in a flexible wall and a rigid wall container is presented in Figure 13. Flexible wall permeameters also allow direct measurement of sample volume change during testing.

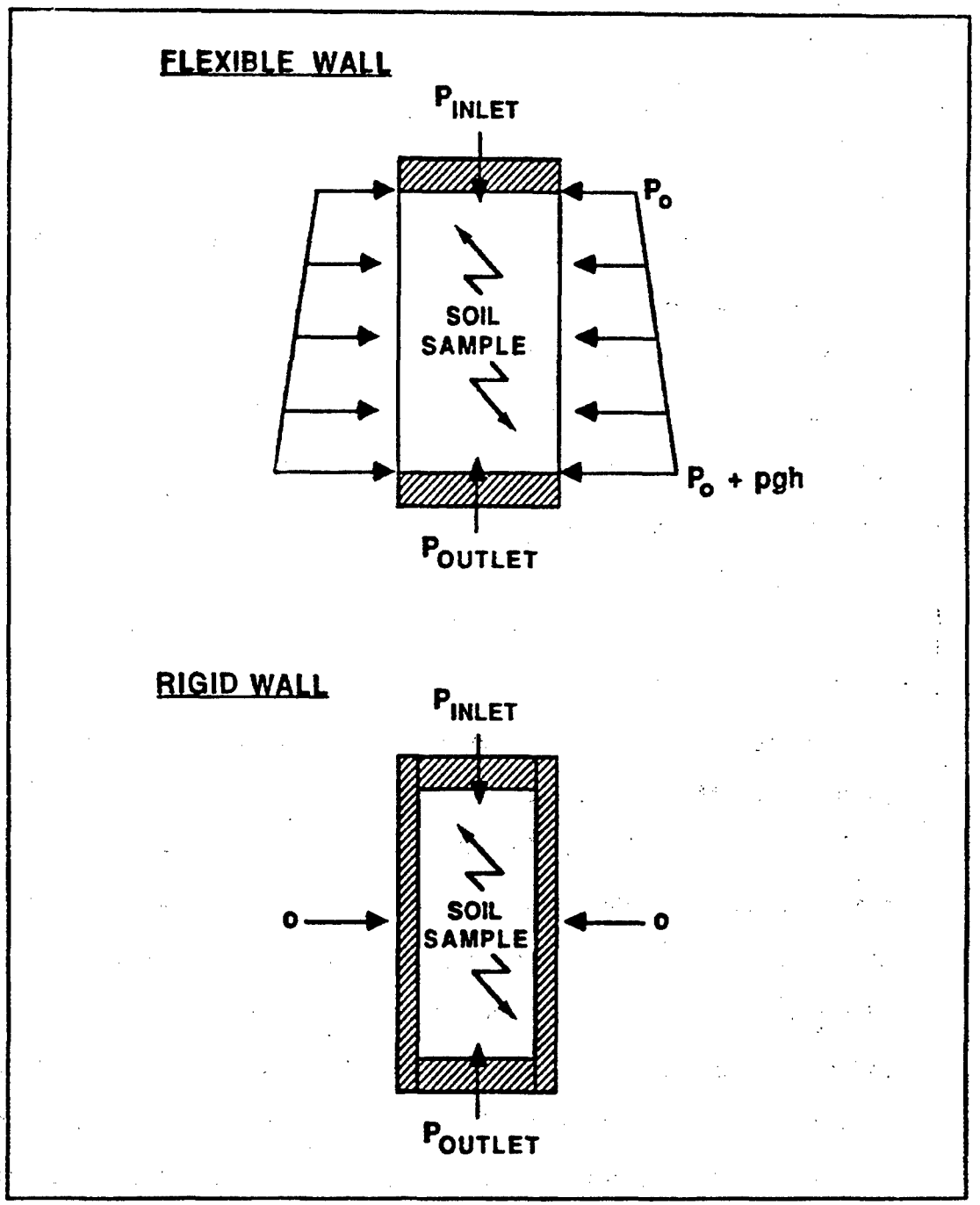

Figure 13. Comparison of Confining Stress Profiles

Disadvantages of a flexible wall apparatus include higher equipment costs, possible reactivity of the flexible membrane with nonaqueous permeants, and the inability to reproduce zero effective stress at the top of the sample, a condition which exists at the soil surface. When exposed to the atmosphere, desiccation cracks open up in clay soil and liners due to shrinkage. The resulting fissures significantly increase the rate of liquid movement through the layer. Currently, there is no way to reproduce this condition of zero effective stress at the surface in the flexible wall permeameter. A study comparing field seepage rates of a carefully compacted clay liner with rates determined in a flexible wall apparatus documented a difference of three orders of magnitude (Day and Daniel, 1985). Rigid wall field apparatus (double-ring infiltrometers) recorded values within an order of magnitude of observed field rates.

A carefully controlled investigation of the effects of permeameter type concluded that there was no significant difference in saturated hydraulic conductivity measurements for water in clay (Boynton and Daniel, 1985). However, estimates of hydraulic conductivity of concentrated organics were an order of magnitude higher for tests conducted in rigid wall containers than in a flexible wall permeameter. In that study results from a flexible wall apparatus were compared to estimates from a standard consolidation cell and compaction mold.

Design of the Hydraulic Conductivity Apparatus

Separate permeameters were designed for use in the saturated and unsaturated hydraulic conductivity tests. After a review of current technology, the saturated hydraulic conductivity permeameter was designed as a modular apparatus to facilitate uncomplicated sample

preparation and for the convenience of incorporating possible future design revisions. The device incorporated the current best technology in permeameters, including

1. incorporation of a flexible membrane;
2. capability for de-airing the permeant and sample via vacuum;
3. capability for back pressure saturation; and,
4. capability to check for complete saturation by means of the "B" value test.

The design also included constraints brought about by its intended use in the centrifuge. These included

1. size constraint - the device must fit on the 75-cm long lower flat portion of the centrifuge arm, while at the same time, be narrow enough so that the radial acceleration forces act in nearly parallel directions;
2. the weight must remain balanced in flight - hence the apparatus must have a self-contained permeant system;
3. the permeameter is limited to two hydraulic slip rings on the centrifuge assembly; and
4. the permeant tubing system should be as large as possible to minimize flow velocities and hence minimize the energy losses due to friction.

A schematic of the completed device is presented in Figure 14. A photograph of the apparatus attached to the centrifuge arm is presented in Figure 15. The unit consisted of 1.25-cm thick, 11.43-cm inside diameter acrylic cylinders separated by 2.54-cm thick acrylic plates. Conduits were drilled in the plates to conduct the test permeant. O-rings between the individual elements provided high pressure seals, and

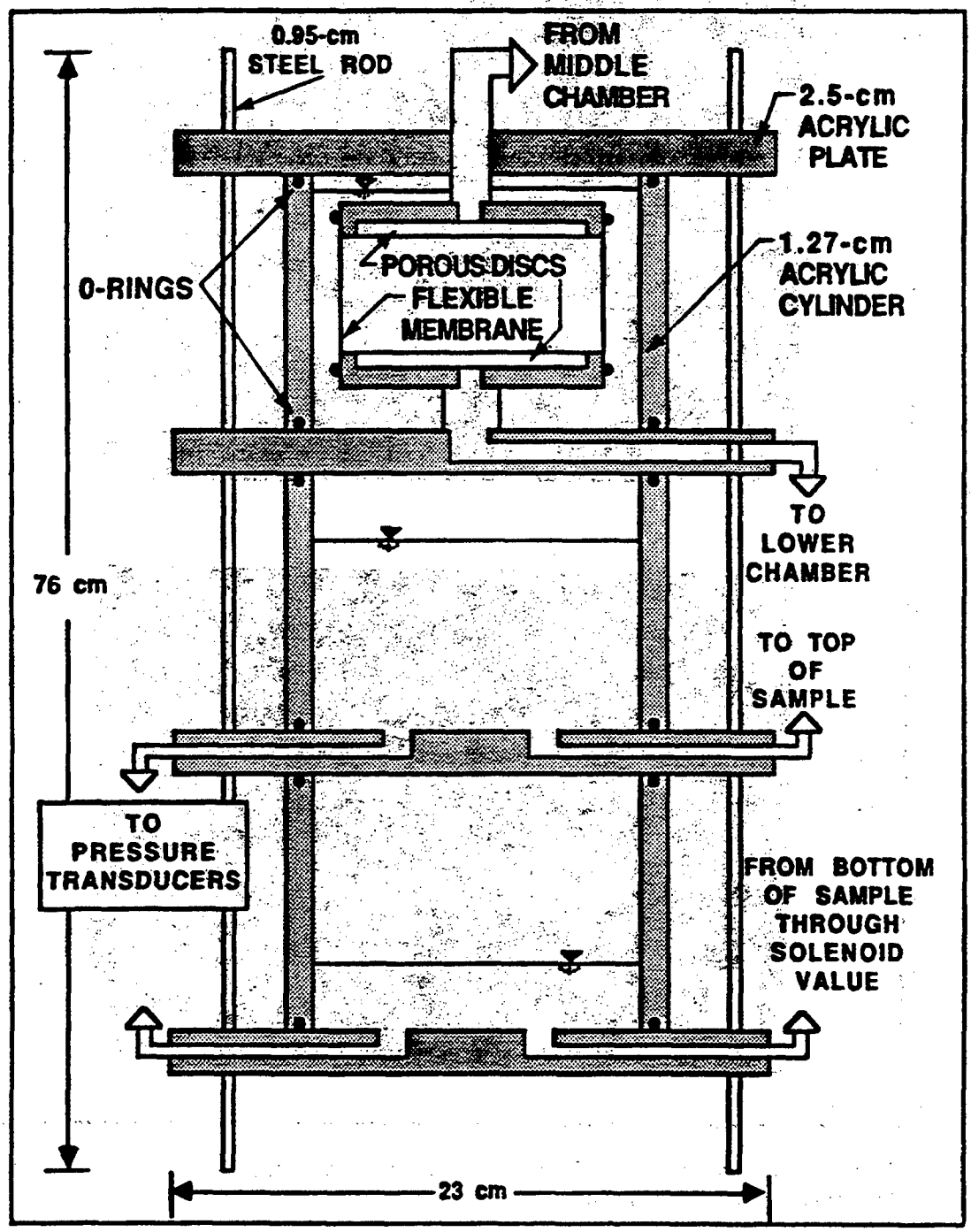

Figure 14. Schematic of Apparatus Used in the Saturated Hydraulic Conductivity Tests

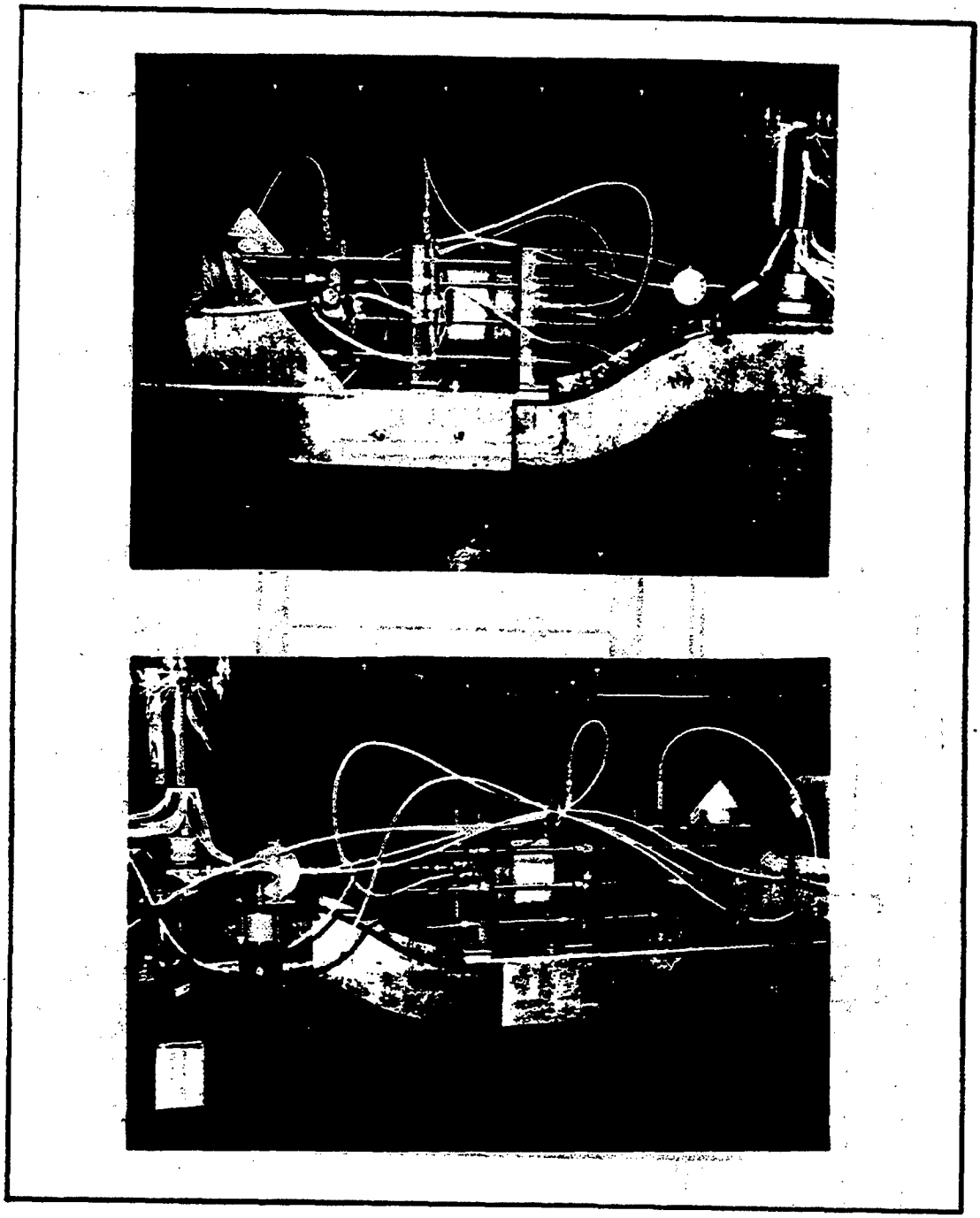

Figure 15. Photograph of the Saturated Hydraulic Conductivity Apparatus Attached to the Centrifuge Arm a) Front View; b) Rear View

the entire apparatus was unified by six 0.95-cm diameter steel rods. Permeant flow between the reservoirs and the soil sample was controlled by a three-way solenoid valve. Material and fabrication of the permeameter cost approximately $1000. Pressure transducers, attendant voltage meters, pressure controls and miscellaneous hardware cost an additional $4000.

The soil specimens were confined in a flexible membrane within the upper water-filled acrylic cylinder. Stainless steel porous discs and filter fabric were used to contain the soil sample, subject to the criterion that the pore sizes be small enough to prevent particle emigration from the sample, and yet large enough to avoid becoming limiting to flow. The flexible membrane must be free of leaks, nonreactive with the permeant and relatively impermeable to the confining fluid to ensure hydraulic isolation. Reactivity and permeability of the membrane can be tested by stretching a piece of the membrane over the top of a beaker containing the fluid in question, inverting, and monitoring the subsequent fluid loss (Uppot, 1984). Initial tests with decane revealed significant leakage and interaction between the latex rubber membrane and decane. After several hours of exposure to decane, the surface of the latex membranes was transformed into a wrinkled covering, similar in pattern to the convolutions on the surface of the brain. A similar wrinkle pattern was observed in a previous study using benzene with a latex membrane (Acar et al., 1985). It has been suggested that decane and other nonpolar hydrophobic organics penetrate the polymers comprising the latex membrane, resulting in molecular relaxation and hence an increase in the surface area of the membrane. The wrinkles result from the confining pressure restricting the volumetric expansion of the

membrane. As an intermediate solution to the leakage problem, a sheet of polyethylene food wrap was sandwiched between two latex membranes. However, this measure did not prevent the surface convolutions on the inner membrane. Single neoprene rubber membranes were subsequently utilized and found to be relatively nonreactive to decane. All of the saturated hydraulic conductivity tests reported herein using decane as the permeant utilized the neoprene rubber membranes.

The conduit system consisted of the tubing and valves connecting the sample cell to the pressure control and flow measurement components. Along with the energy loss induced across the soil sample, mechanical energy is lost in the permeameter due to friction along the tubing walls, and, of minor importance, due to flow contractions, expansions and bends. The conventional constant head saturated hydraulic conductivity test is conducted under steady flow conditions, and as such, the appropriate head loss can be obtained by pressure transducers located at each end of the sample; no correction is needed to account for other energy losses. However, hydraulic conductivity tests with variable boundary conditions, such as the falling head or variable head test employed here, result in transient boundary conditions, and the gradient across the sample is constantly changing; hence pressure transducers seldom are used at the ends of the sample. Rather, the transient boundary conditions are incorporated directly into the derivation of the equation for K. Generally the energy losses due to friction, etc., are neglected, which is acceptable when flow velocity in the tubing is small, as it may be for flow through clays and sand/clay composites as well as for gravity flow through sand. However, for sand samples under pressure and permeameters with small diameter tubing,

energy losses became significant as flow velocities increased. Extremely high energy losses due to friction were observed in the small (0.25 cm inside diameter) tubing of the commercial triaxial device. Larger tubing (0.64 cm inside diameter) was used in the new permeameter and as large as practical valves were employed in the permeameter to minimize energy losses due to flow restrictions. Nylon tubing, which is nonreactive to most organics, was used in the permeameter. The presence of decane did not noticeably affect the nylon tubing nor the acrylic chambers of the permeameter.

Elaborate multiphase systems have been utilized to accurately measure inflow/outflow rates (Dunn, 1983). However, visual observation of water surface elevations were utilized in this study to determine fluid flux in the current hydraulic conductivity device.

The air pressure system consisted of both vacuum and positive supplies, regulators, gages, pressure transducers and calibrated voltmeters. Deairing the permeants and the sample were facilitated by the vacuum. Appropriate pressure gradients were established and maintained across the sample via independent control of the air pressures in the influent and effluent reservoirs. Air pressure was introduced at the top of the influent and effluent reservoirs through the conduits in the upper acrylic plates. During preliminary testing, the inability of pressure regulators to hold constant pressures above the influent and effluent reservoirs as their water levels fluctuated resulted in inaccurate estimates of hydraulic conductivity. Adequate regulators were appropriated for subsequent testing. The accuracy of pressure gages, regulators and transducers is paramount due to their

role in establishing boundary conditions on the sample. Individual and differential pressure tranducers were utilized to monitor the "B" value of the sample before testing and the air pressure above the permeant surfaces during the tests. External confining pressure was maintained on the sample throughout the test by pressurizing the water in the surrounding chamber. This design allowed for flow-through back pressure saturation of the soil sample within the flexible membrane, reported to be the most efficient method of saturating the specimen (Dunn, 1983).

Bench Testing Procedures

Similar testing procedures were followed for all the saturated hydraulic conductivity tests. The saturated hydraulic conductivity tests of the sand and the sand/clay samples used for comparing bench and centrifuge results were conducted in the new permeameter. The clay samples were tested with water and decane in the triaxial apparatus. For the sand and sand/clay samples, the specimens were prepared dry. The initially dry kaolinite samples were prepared to designated water contents (29 and 32 percent by weight) and allowed to cure for six weeks. For each test, the clay samples were compacted to a specified volume, yielding bulk densities of approximately 100 pounds per cubic foot.

Several measures were performed to ensure that the samples were completely saturated. Prior to saturating the sample a vacuum was applied to the top of the water reservoir until the bubbling ceased. Water was subsequently introduced into the samples from the bottom while a vacuum of approximately 13 psi was maintained at the top. When air bubbles ceased to flow out the top of the sample, the pressures on the

influent and effluent reservoirs were increased to 40 psi for sands, 50 psi for the sand/clay mixtures and 70 psi for the clay samples. A slight gradient was established to allow flow through the sample. After a pressurization period of approximately one day for the sand and two to three days for the sand/clay and clay samples, "B" values of unity were recorded, indicating complete saturation.

A range of gradients was established during the saturated hydraulic conductivity testing. Of primary interest was the possibility of determining the critical value of the Reynolds number above which Darcy's law was invalid. Preliminary estimates of pore fluid velocities indicated that only the sand specimens could exhibit a deviation from Darcy's law. In fact, a previous investigation used gradients of over 800 on clay specimens to reduce the testing time, with no discernible deviation from Darcy's law (Uppot, 1984). Deviations from Darcy's law can be attributed to:

1. the transition from laminar to turbulent flow through the pores; and
2. the tendency for flow to occur in the larger pores as the velocity increases, thus decreasing the total cross-sectional area of flow.

When the desired initial pressure boundary conditions were established and fluid levels in the reservoirs recorded, the solenoid valve was opened and flow through the sample commenced. When the solenoid valve was closed, the elapsed time and fluid levels were recorded. For the sand specimens, the pressure differential during the test was recorded to quantify the friction and minor energy losses. This was not necessary for the slower fluid velocities present in the sand/clay and clay tests. The testing procedure was repeated until sufficient data were collected. Boundary conditions were verified and

real time data analysis was conducted on a microcomputer during the execution of the tests.

Tests with decane were performed immediately following tests using water. Water was removed from the influent lines and decane was introduced into the influent reservoir.

The viscosity of a permeant varies with temperature. The temperature of the main permeant reservoir was recorded during each test. The temperature in the air conditioned laboratory was maintained within a 5°C range throughout the duration of the testing program.

Centrifuge Testing Procedures

Saturated hydraulic conductivities were determined for sand and sand/clay soil specimens in the centrifuge. The high influent pressures, 120 psi, required for the clay samples were too high to safely perform replicate tests in the acrylic chambers within the centrifuge. The centrifuge tests were conducted on the same soil specimen immediately following the bench tests. The pressure transducers were recalibrated before each centrifuge test to compensate for line noise in the electrical slip rings. During the centrifuge tests, pressures in the sample and fluid reservoirs were controlled by regulators external to the centrifuge, which supplied air through hydraulic slip rings. When the desired initial pressure boundary conditions were established and fluid levels in the reservoirs recorded, the solenoid valve was opened and flow through the sample commenced. When the solenoid valve was closed, the elapsed time and fluid levels were recorded. For the sand specimens, the pressure differential during the test was recorded to quantify the friction and minor energy

losses. This was not necessary for the slower fluid velocities present in the sand/clay tests. The testing procedure was repeated until sufficient data were collected. Boundary conditions were verified and real time data analysis was conducted on a microcomputer during the execution of the tests.

Unsaturated Testing

Centrifugal techniques for physical modeling and material testing of unsaturated soil samples were evaluated in this study. A variety of applications were investigated, including several laboratory techniques for determining the relationship of hydraulic conductivity as a function of moisture content, as well as physically modeling the advection of a conservative leachate through a partially saturated soil profile. The results are presented below.

Physical Modeling

As the soil dries, the influence of gravity on the movement of pore fluid decreases. In fact, for the majority of the time, fluid flux in natural soils is dominated by suction gradients, which can typically be 1000 to 10,000 times the gradient due to gravity. In a uniformly dry soil, water movement below an influent source will occur in a radial pattern, reflecting the negligible influence of gravity. Thus, in the scenario of percolation of leachate from a hazardous waste site, the movement of fluid will be dominated by the extant suction gradients. Because the influence of gravity on the flow is small, there is no feasible advantage of physically modeling unsaturated flow conditions in the gravity-accelerated environment within the centrifuge.

Material Testing

Laboratory tests for determining the unsaturated hydraulic conductivity as a function of pore water content of soils have been developed for both steady and nonsteady flow conditions. Six of the most common methods were evaluated with the intention of determining a feasible centrifuge technique. The following criteria for assessing the different techniques were compiled:

1. The gravity component of the hydraulic potential gradient should be at least of the same order of magnitude as the suction component; preferably the gravity component will dominate.
2. The testing procedure should be appropriate for a wide variety of soil types.
3. The test should not present undue safety concerns with the use of decane as the permeant.

The results of the evaluation are summarized in Table 12

Table 12. Evaluation of Laboratory Tests for Determining Unsaturated Hydraulic Conductivity

Test	Gradient Dominated by Gravity?	Suitable For a Wide Range of Tests?	Allows Use of Decane?	Centrifuge Offers Advantage?
Steady Flow				
1. Impeding Crust	Yes	No	Yes	No
2. Sprinkler	Yes	No	Yes	Yes
3. Pressurized Steady	Yes	No	Yes	No
4. Ambient Steady	Yes	Yes	Yes	Yes
Transient Flow				
1. IPM[a]	Yes	Yes	Yes	Yes
2. Pressure Outflow	No	No	Yes	No

Note: a IPM refers to the Instantaneous Profile Method

Steady Flow Tests

Steady state methods of determining the hydraulic conductivity as a function of moisture content establish and maintain a constant pressure gradient (greater than or equal to zero) across the soil sample and monitor the rate and volume of discharge. The four tests evaluated herein were the impeding crust method, the sprinkler-induced steady flux method and two generic methods, the pressurized steady flux method and the ambient pressure steady flux method.

In the pressurized steady flux method, application of an air pressure to the sample can be used to increase the gas phase volume, and hence decrease the moisture content (Klute, 1965a). This technique is limited to soils with low permeabilities due to the restriction on the air entry value of the porous discs at the ends of the samples. The porous discs must have small enough pores such that the pressurized air in the soil sample cannot displace the liquid occupying the pores. However, as the pore diameter is reduced, the hydraulic conductivity of the disc also decreases. For example, a commercially available ceramic disc with an air entry value of 7.3 psi suction has an associated hydraulic conductivity on the order of 10^{-5} cm/sec (Soilmoisture Equipment Corporation, 1978).

In the ambient pressure steady flux method, atmospheric pressure is allowed to enter a horizontal or vertical sample through air holes in the rigid wall container. The water content is regulated by the soil suction at the entrance and exit (Klute, 1965a). This removes the restriction of limiting conductivity of the porous disc, but introduces the restriction that suctions must be less than the cavitation pressure of the fluid. For water this corresponds to a practical range of 200 cm

to 800 cm of water (Klute, 1965a). When the sample is vertical and the entrance and exit suctions are equal, the resulting soil moisture flux is driven by gravity.

Steady flow can also be achieved by placing a thin layer of flow-restricting material on top of the vertical soil and maintaining a shallow head of water (Green et al., 1983; Dunn, 1983). The crust material must have a saturated hydraulic conductivity less than the hydraulic conductivity of the test soil at the test suction. Plaster of Paris, gypsum and hydraulic cement have been used for this purpose. Extended periods of time are required to obtain steady flow, since the gradient is composed almost entirely of the gravitational potential gradient.

In the sprinkler-induced steady flux method, a constant rate of inflow is supplied by a source located above the vertical sample (Green et al., 1983). As long as the rate of application is lower than the saturated hydraulic conductivity the sample will eventually achieve a uniform soil moisture content, specific to the application rate. Since the gradient is composed almost entirely of the gravitational potential gradient, this method can be adapted for use in the centrifuge.

Unsteady Flow Techniques

Transient flow techniques for measuring the hydraulic conductivity have a time advantage over steady state methods in that they yield estimates of K over a range of moisture contents during a single test. Two nonsteady flow techniques were evaluated as a potential centrifuge candidate. The instantaneous profile method (IPM) entails monitoring the change in soil suction with time along the sample profile as the sample is exposed to specified boundary conditions (Green et al., 1983;

Olson and Daniel, 1981). Concurrent or independent information on the moisture retention characteristic is incorporated in obtaining estimates of K as a function of moisture content. Soil suction profiles can be obtained during drainage from initially saturated soil or during imbibition as water is introduced into a dry sample. When the test is conducted during the drainage cycle, the gravity component of the hydraulic gradient is greater than the soil moisture suction gradient; a comparison of these two components during a test of Lakeland Series soil is presented in Figure 16 (Dane et al., 1983). The soil moisture and potential data presented therein were collected during the redistribution of moisture following surface ponding. Thus the IPM test for the drainage cycle is a good candidate for adaptation to the centrifuge.

The other major transient flow technique is the pressure outflow method. The pressure outflow method relates the unsaturated hydraulic conductivity to the volume of water discharged from a sample resulting from an incremental increase in air pressure (Kirkham and Powers, 1972). Again, the restriction of porous discs with sufficient air entry values limits this procedure to materials with low conductivity. Alemi et al. (1976) proposed a theory for revising this test which utilizes a centrifuge to increase the hydraulic gradient via the gravitational head. However, no experimental results were available to assess this method.

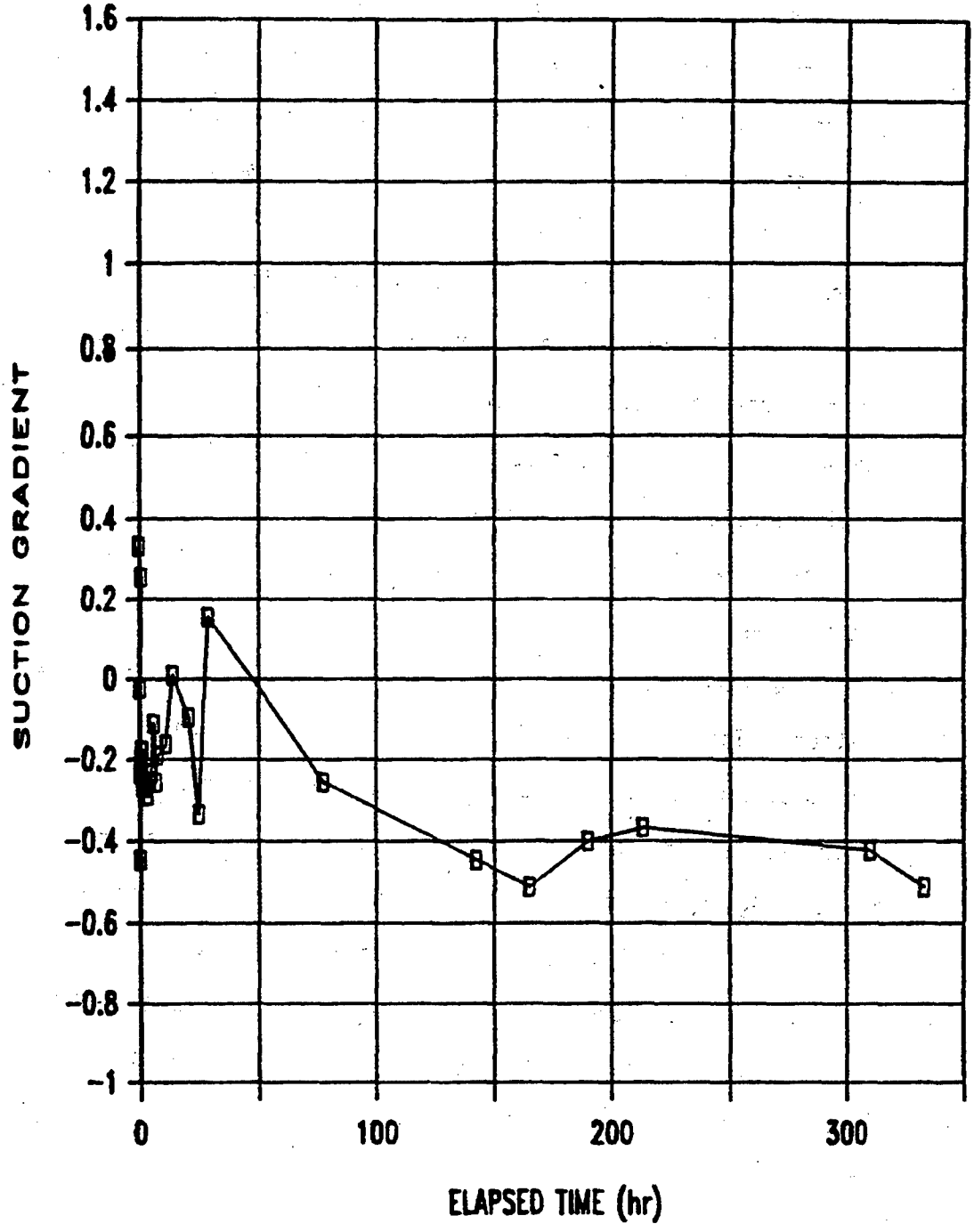

Figure 16. Time History of the Suction Gradient During the Drainage Test

Development of the Centrifugal Technique

The IPM was selected as the most feasible test procedure to determine the unsaturated hydraulic conductivity of a soil sample within the centrifuge. The apparatus utilized in the saturated test was readily modified for use in the IPM testing. A schematic of the apparatus is presented in Figure 17. Miniature pressure transducers were placed within the sample during preparation and monitored the soil moisture suction of the pore fluid during the test.

Computer Model

A computer program was developed and utilized to evaluate the influence of elevated and nonuniform acceleration levels on soil moisture movement in unsaturated soils. The model incorporated the centrifuge version of Darcy's law presented in equation 26 into the one-dimensional continuity expression referred to as Richard's equation

$$d\theta/dt = -dq/dz \qquad (29)$$

where $d\theta/dt$ is the time change in volumetric water content. The model assumes that the soil is homogeneous. A moisture retention curve and the relationship between the unsaturated hydraulic conductivity and the soil suction are entered as input data for each soil type of interest. The program can simulate the wetting and/or drainage of a soil sample under constant flux or constant potential boundary conditions. The model was designed to simulate bench (i.e., 1 g) or centrifuge acceleration levels, allowing direct evaluation of the influence of acceleration on soil moisture movement.

A fully implicit finite difference solution scheme was used. The resulting system of simultaneous equations forms a tridiagonal matrix, which was solved by the Thomas algorithm for each time step. The model

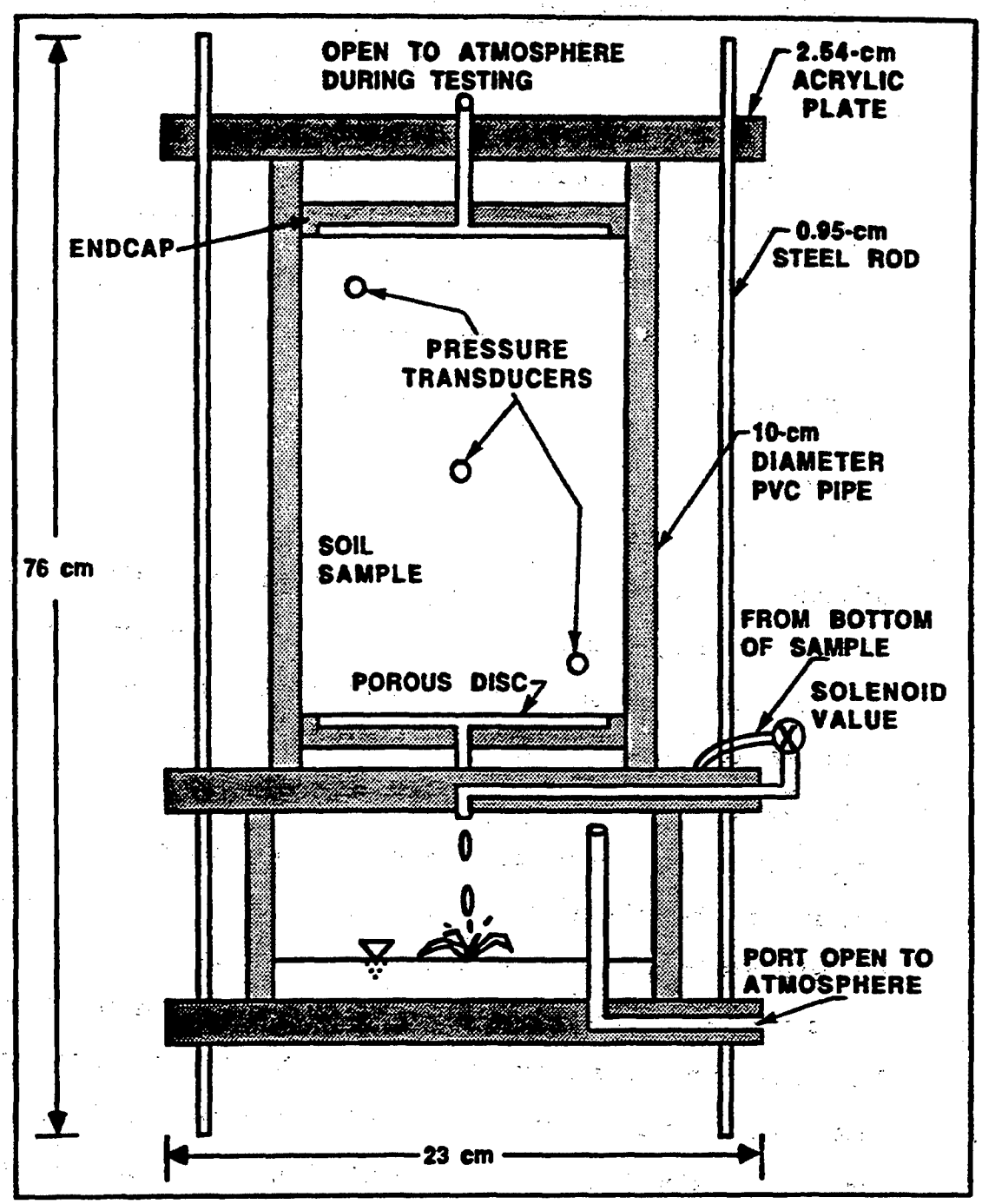

Figure 17. Schematic of the Proposed Test Apparatus for the Instantaneous Profile Method

was written in FORTRAN on a microcomputer using double precision variables and requires approximately five minutes to simulate an hour of soil moisture movement. The mass balance is checked each time step by comparing the total change in mass of the system with the net flux of mass from the system. Cumulative mass errors were consistently less than one-half of one percent for a one-hour simulation.

Accuracy of the model was determined by comparing the pressure profile after drainage ceased to the appropriate analytical expression of hydrostatic equilibrium. For bench tests, a linear relationship between sample depth and soil suction (expressed in cm of water), determined analytically as

$$h = h_0 + z \tag{30}$$

was reproduced by the model. Equation 30 states that, at hydrostatic equilibrium, the soil suction is equal to the height above a datum of fixed potential, e. g., a water table. For centrifuge tests, the pressure distribution at hydrostatic equilibrium was derived earlier as

$$P_2 = P_1 + pw^2 (r_2^2 - r_1^2)/2 \tag{31}$$

Results from the computer model agreed precisely with this relationship, thereby verifying the accuracy of the numerical technique.

Data Analysis

Analysis of the test results required initially deriving the appropriate flow equations based on the acceleration distribution and boundary conditions imposed during the tests. Because of the variable permeant levels in the influent and effluent reservoirs, traditional constant head and falling head permeability equations were inappropriate for the triaxial apparatus and new permeameter. The correct equation

for the bench tests was derived by incorporating the appropriate boundary conditions into the equation of motion. Referring to the definition sketch in Figure 18, the variable head equation for the bench tests is

$$K = \frac{aL}{2At} \ln(h_i/h_f) \tag{32}$$

where a = cross-sectional area of the influent line (L^2);

L = length of the sample (L);

A = cross-sectional area of the sample (L^2); and

t = duration of the test (T).

$$h_i = \frac{P_M - P_L}{pg} + (z_{MO} - z_{LO}) + H_L \tag{33}$$

P_M, P_L = air pressures at the permeant surface (M/LT^2);

z_{MO}, z_{LO} = initial permeant surface elevations (L); and

H_L = hydraulic energy loss due to friction, bends, valves, entrances and exits (L).

$$h_f = h_i + 2h \tag{34}$$

h = rise in the bottom container water surface (L).

Equation 32 has been written in a form similar to the conventional falling head equation, the differences being the factor of two in the denominator and the different definitions of h_i and h_f. Also, like the falling head equation, when the applied pressure gradient is high relative to the change in water levels during the test, equation 32 yields nearly identical results as the constant head equation. This was verified during data analysis. The complete derivation of the falling head permeability equation is presented in the Appendix. For comparison with the centrifuge test results and to investigate the influence of decane, the intrinsic permeability was calculated as

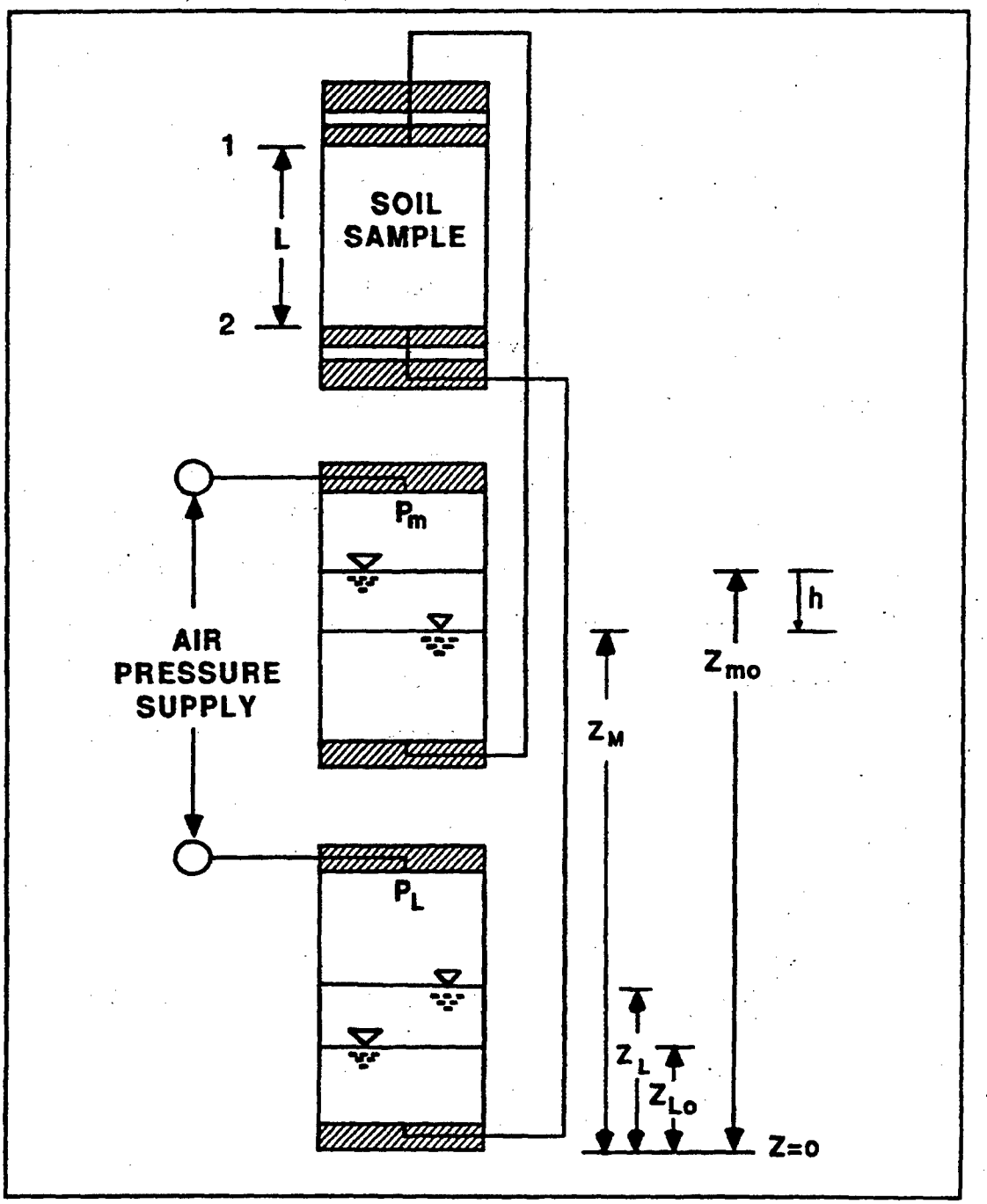

Figure 18. Definition Sketch for the Variable Head Permeability Equation - Bench Test

$$k = Kv/g \tag{35}$$

where v = kinematic viscosity of the permeant at the test temperature (L^2/T). As in the conventional falling head test, the variable head condition resulted in a deviation from steady flow, and hence, introduced an additional acceleration force acting on the fluid element. The fluid velocity during the test is proportional to the hydraulic gradient; hence, this acceleration term is proportional to the time rate of change in the gradient. During the bench tests, the gradients were nearly constant, hence this additional acceleration term was neglected. The derivation of the conventional falling head permeability test also neglects this term.

The derivation of the variable head hydraulic conductivity equation for the centrifuge testing necessitated derivation of the fundamental relationships of fluid flow under the influence of radial acceleration. Highlights of those derivations were presented in Chapter III. The appropriate equation for the variable head saturated hydraulic conductivity test in a centrifuge (see Figure 19) test is

$$K = \frac{aL}{Ath_0} \ln (h_1/h_2) \qquad \text{(in units of time)} \tag{36}$$

$$h_0 = w^2 (r_{LO} + r_{MO}) \tag{37}$$

where r_{LO}, r_{MO} = the initial radii of the water surfaces (L).

$$h_1 = \frac{P_L - P_M}{p} + \frac{w^2}{2} (r_{MO}^2 - r_{LO}^2) + H_L \tag{38}$$

$$h_2 = h_1 + h_0 * h \tag{39}$$

where h = increase in radius of the upper fluid surface (L).

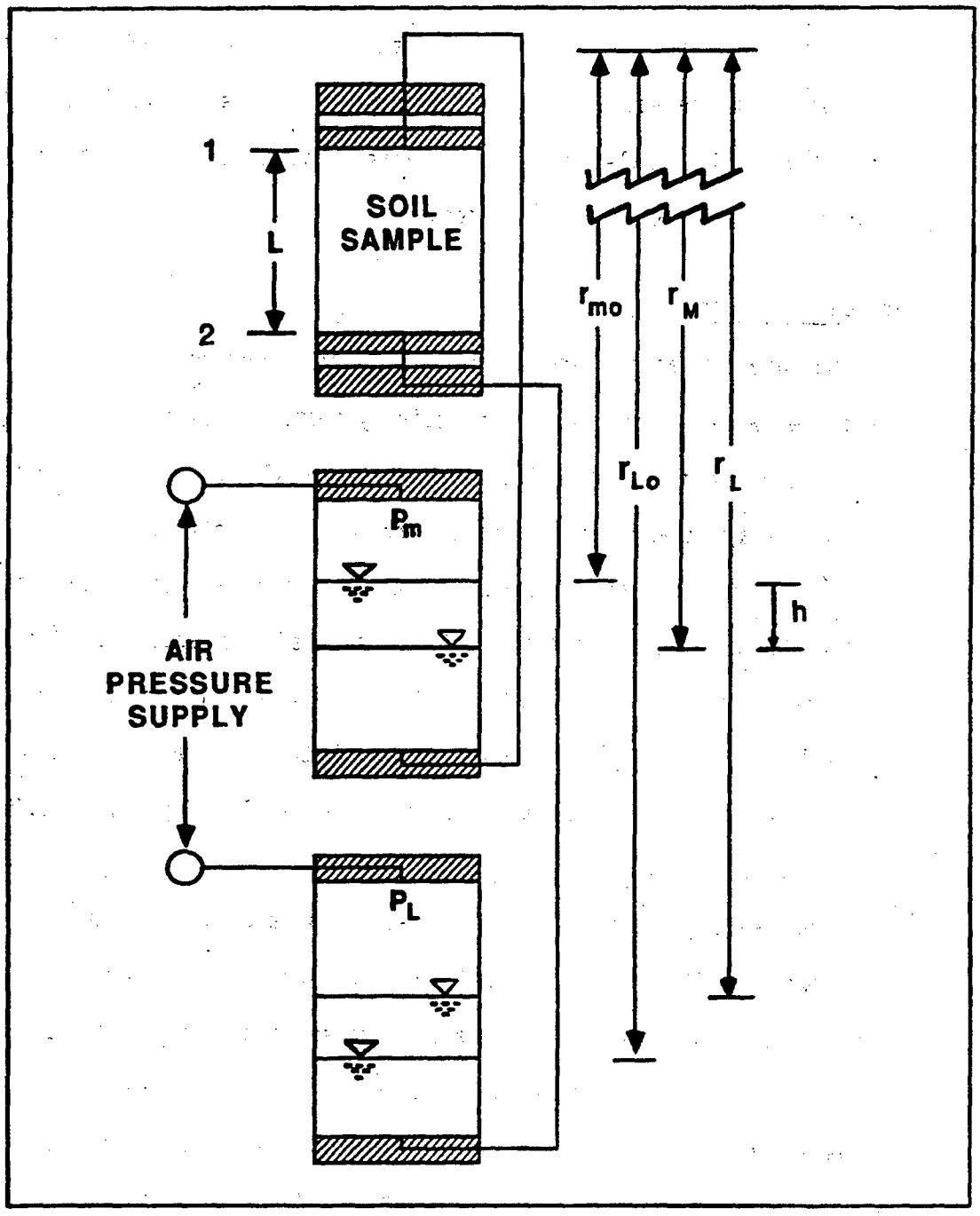

Figure 19. Definition Sketch for the Variable Head Permeability Equation - Centrifuge Test

Here, HL has the dimensions of energy per unit mass. The complete derivation of the falling head permeability equation is presented in the Appendix. Estimates of the intrinsic permeability were calculated from

$$k = Kv \qquad (40)$$

The data analysis worksheet for the centrifuge tests included information on the acceleration and hydrostatic pressure profiles in the permeameter. The real-time data analysis facilitated the establishment of proper initial boundary pressures.

Sources of Error

Measurement errors are inherent in most laboratory tests. Errors associated with the hydraulic conductivity tests are discussed below.

During the tests, the flux through the soil sample was determined as the average change in volume of the inlet and effluent reservoirs. The levels in the reservoirs were recorded before and after each test. In the centrifuge, a strobe light illuminated the apparatus directly below the window in the housing, allowing direct observation of the water levels in flight. Fluctuation of the permeant surfaces was observed at all rotational speeds, with severe sloshing (0.5 - 1.0 cm) occurring below 150 RPM.

The use of high gradients across the clay and sand/clay samples may have caused differential consolidation during the test. Also, the exit end of the sample had higher effective stresses acting on the particles as a result of the gradient. To minimize the influence of these transient phenomena, the sample was allowed to equilibrate for a period of one to ten minutes after changing the boundary conditions before measurements began.

A sensitivity analysis of the measurement errors was performed by recording the variation in K as the input parameters were varied. Maximum practical errors in determining the sample dimensions and the test duration resulted in a variation of less than 5 percent in estimates of K. The height of the meniscus varied from zero to 0.2 cm during the course of the tests. The pressure transducers were calibrated regularly and had a sensitivity of 0.02 psi. Obviously, the lower the gradient and smaller the flux during the test, the more sensitive the estimates of K are to errors in reading the water level and pressure gradient. To compensate for this sensitivity, tests with small gradients were run long enough to register at least a one cm change in the effluent reservoir.

Another possible source of error was the equation used to calculate K. Both the bench and centrifuge variable head equations were derived during this study and have not been independently tested. For comparison, estimates of K were determined using the standard constant head equation. Under high pressure gradients, the variable head equation yielded similar results, since under these boundary conditions, the change in elevation of the permeant reservoir surfaces were negligible compared to the pressure gradient. The validity of the variable head equations was carefully scrutinized, and eventually verified under the extreme range of hydraulic conductivity values, boundary gradients, acceleration levels and test durations experienced during the testing program. The validity of the equations and the permeameter was also supported by nearly identical estimates of the saturated hydraulic conductivity obtained by performing a conventional falling head permeability test on the sand.

CHAPTER V
RESULTS AND DISCUSSION

The objective of the laboratory research program was to develop centrifugal testing methods for determining saturated and unsaturated hydraulic conductivity of soil samples. The testing program encompassed:

1. the design, fabrication and analysis of permeameters for use in the centrifuge;
2. execution of hydraulic conductivity tests using water and decane in a 1-g environment to provide a benchmark for comparing centrifuge results;
3. derivation of the appropriate equations of motion for fluid flow in a centrifuge;
4. execution of hydraulic conductivity tests using water and decane in the centrifuge at various accelerations;
5. comparison of centrifuge results with 1-g test results; and
6. (if necessary) modification of the centrifuge device, testing procedures and/or data analysis based on results of the comparison.

These were successfully accomplished during the course of the study. Analysis of the current technology in permeameters resulted in an appropriate design of apparatus to be utilized in centrifuge testing. The apparatus was fabricated, tested and employed during the course of the study. Saturated hydraulic conductivity tests were conducted on the laboratory bench using commercial triaxial apparatus

and the apparatus designed during the study. Four soil types and two permeants were utilized to cover a broad range of saturated hydraulic conductivity values. Centrifuge testing was carried out using the same soil types, permeants and hydraulic gradients. For the unsaturated hydraulic conductivity analysis, the influence of acceleration levels on soil moisture redistribution was evaluated by means of a computer model. Results of these tests are discussed below.

Saturated Hydraulic Conductivity Tests

Sand Samples

Influence of acceleration level

The saturated hydraulic conductivity testing with sand exposed several interesting facets of permeability testing and flow through porous media in general. The initial testing was performed on the commercial triaxial apparatus. However, after analyzing the results, it was realized that significant energy losses occurred during the tests. High energy losses due to friction occurred in the small diameter tubing (inside diameter of 0.15 cm), which rendered the commercial triaxial apparatus unsuitable for determining saturated hydraulic conductivity of sand samples. Results presented herein were obtained from the new apparatus which was designed with larger diameter tubing to decrease the frictional energy losses. The hydraulic energy losses which occurred during the tests were monitored with a differential pressure transducer. A typical hydraulic energy distribution during a centrifuge test is presented in Figure 20. The derivation of the variable head conductivity equation incorporated the energy loss term directly.

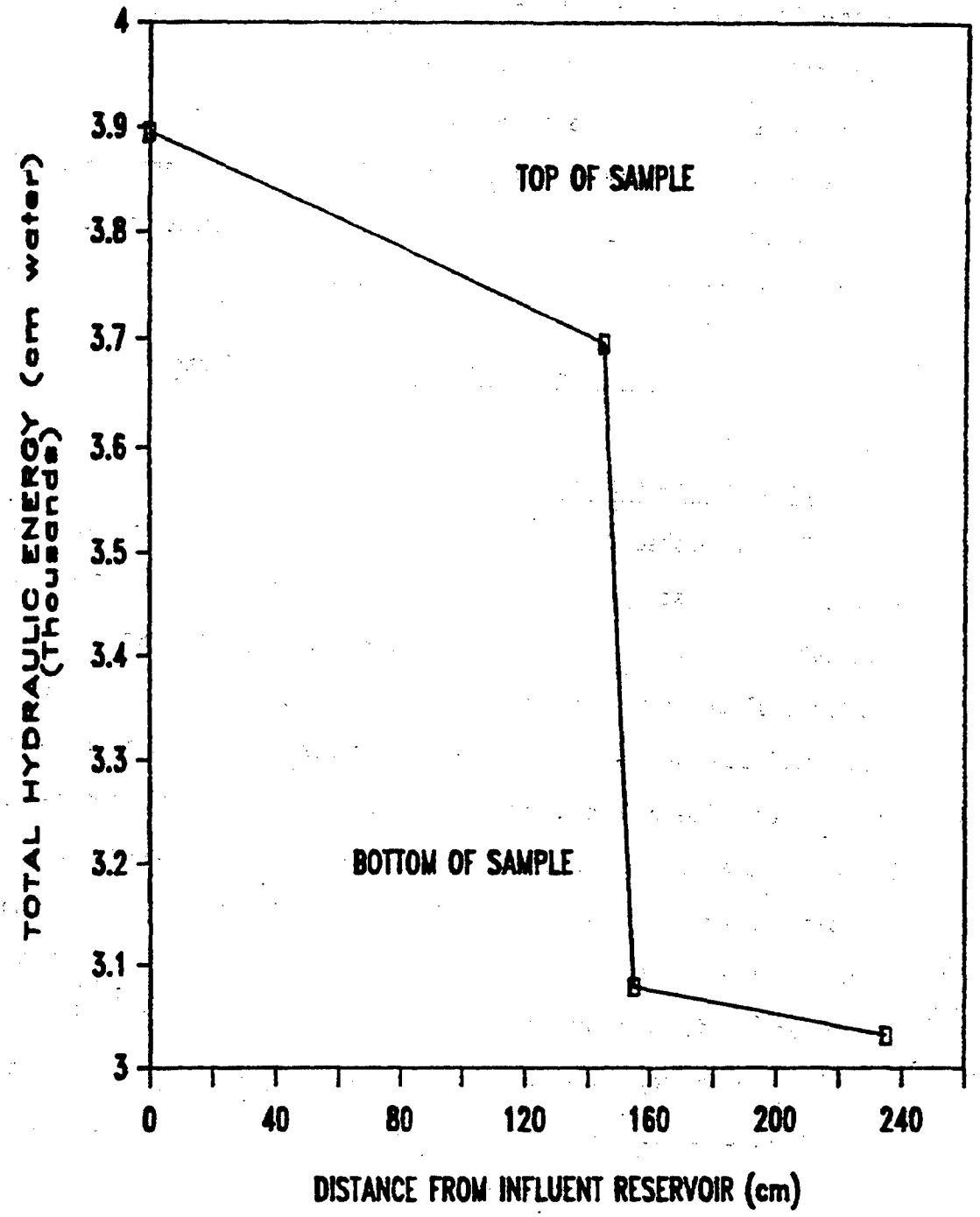

Figure 20. Hydraulic Energy Profile During the Variable Head Test

The tests were conducted on the bench and then transferred to the centrifuge for subsequent testing. Approximately 30 minutes were required for assembly in the centrifuge. Similar gradient ranges were established in the centrifuge as on the bench. As the permeant shifted from the influent reservoir to the effluent reservoir, the hydraulic pressure gradient changed during the course of the tests. Changes in the gradient of 10 were commonly observed in the centrifuge, while gradient changes on the bench were rarely greater than 1.

Departure from Darcy's law was observed in both the 1-g and multiple-g tests with sand. Estimates of the intrinsic permeability, k, are presented in Figure 21. The extreme variation in estimates of k were explained when the same data were plotted versus the initial gradient (see Figure 22), exhibiting a strong dependence on the hydraulic gradient. An independent estimate of k was obtained by performing a conventional falling head permeability test on the sand sample using a low gradient. An average gradient of 2.8 yielded an average value for k of 8.56×10^{-8} cm^2, which corresponds to a hydraulic conductivity value of 9.44×10^{-3} cm/s. These results verify the accuracy of the new permeameter as well as the variable head equation. As Figure 23 demonstrates, this deviation from Darcy's law was reproduced in the centrifuge at accelerations of 14.7 and 24.4 g's. The greater scatter observed in the centrifuge results is attributed to the observed fluctuations in the reservoir surfaces. Below a gradient of around ten, somewhat constant values of k were determined. However, increased gradients resulted in decreased magnitudes of the intrinsic permeability. Constant values of k were obtained below hydraulic gradients corresponding to soils Reynolds number of approximately 0.2.

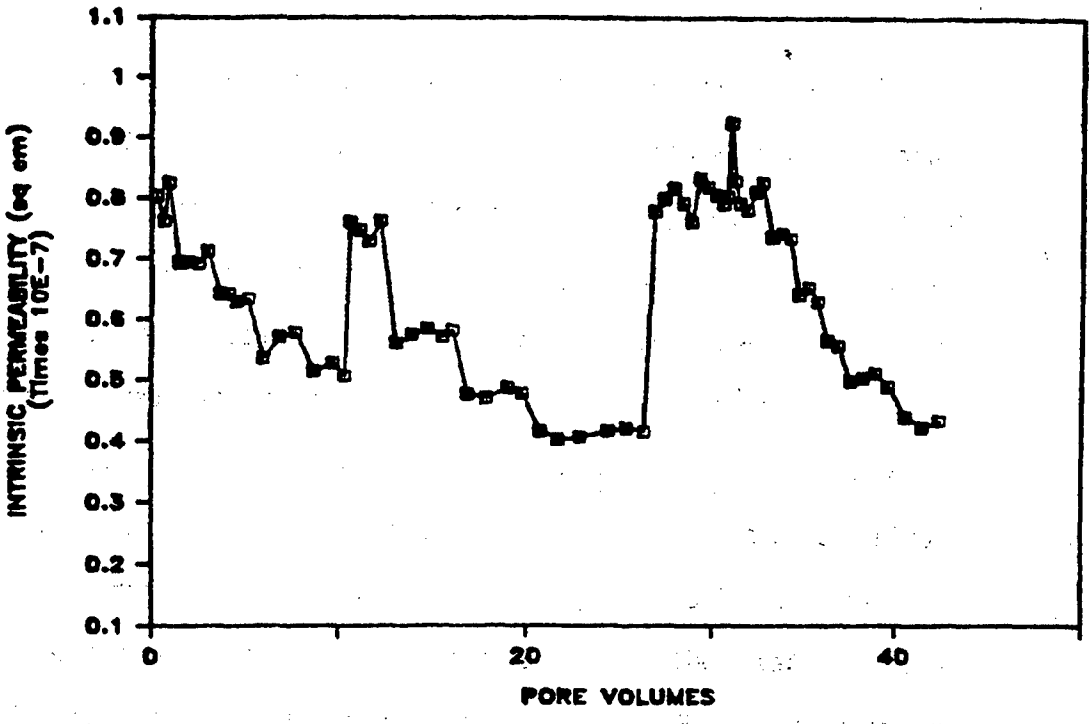

Figure 21. Permeability of Water Through Sand as a Function of Pore Volume

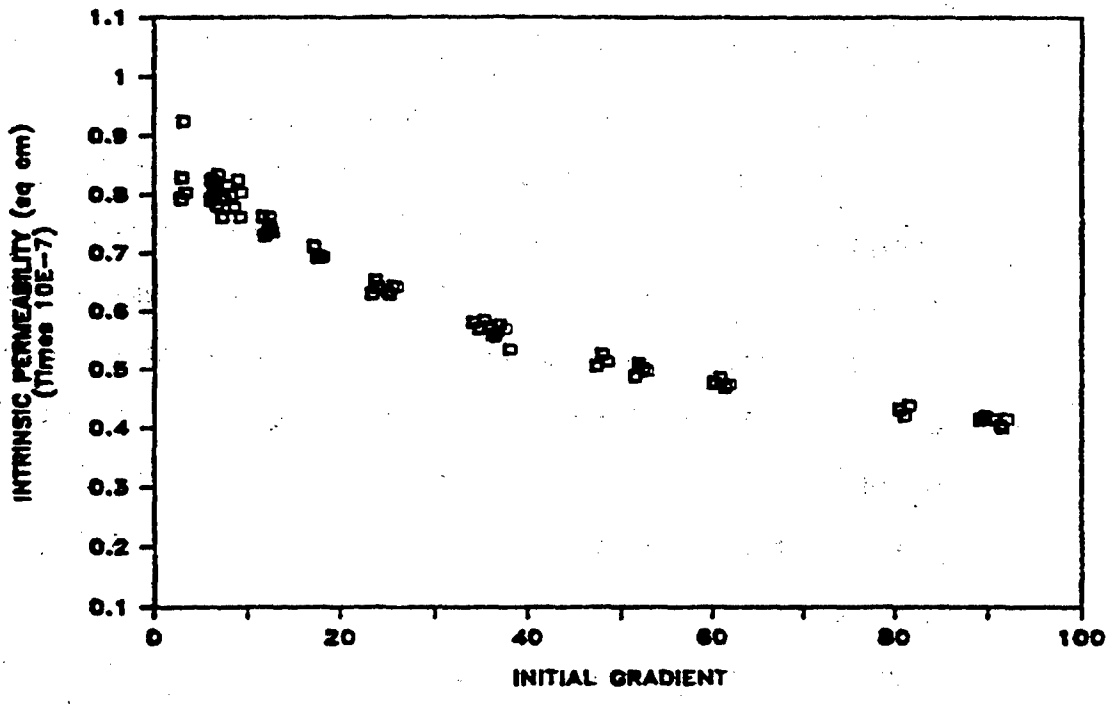

Figure 22. Permeability of Water Through Sand as a Function of Initial Gradient

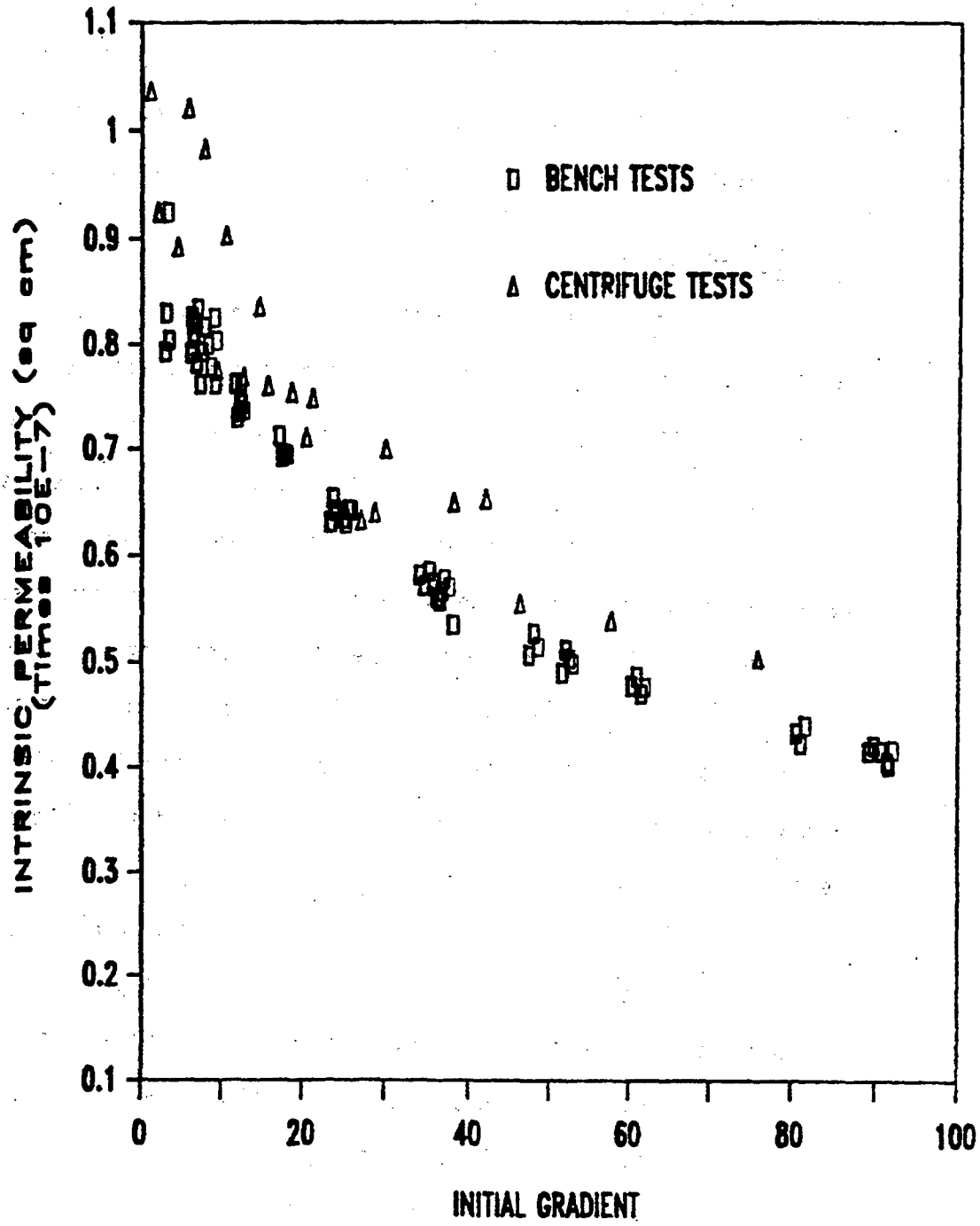

Figure 23. Comparison of Centrifuge and Bench Results of Permeability of Water Through Sand for 1, 14.7 and 24.4 g's

This value is almost an order of magnitude smaller than the reported limits of between one and ten (Bear, 1979). Deviations from Darcy's law can be attributed to:

1. the transition from laminar to turbulent flow through the pores; and
2. the tendency for flow to occur in the larger pores as the velocity increases, thus decreasing the total cross-sectional area of flow.

Influence of decane

During the hydraulic conductivity testing with decane as the permeant, the fluid and soil system experienced binary phase flow. Decane is nonpolar hydrophobic and immiscible in water. In the fluid reservoirs the decane floated on top of the water. During the tests the water was displaced from the sand in a plug flow fashion; very little water was discharged after decane appeared in the effluent reservoir. In the soil sample the decane displaced the majority of the pore water; the amount of water that remained adjacent to the soil particles is referred to as the irreducible water content (Schwille, 1984). The irreducible water content for the sand was estimated to be less than 5 percent of the total void volume.

The saturated hydraulic conductivity of decane through sand was determined on the bench and in the centrifuge at 24.4 g's. The results are presented in Figure 24. Unlike the results for water, estimates of intrinsic permeability of decane did not exhibit a strong relationship with the gradient, as demonstrated in Figure 25. Observed values ranged from 30 to 50 percent less than values with water.

The frictional losses observed during the testing with decane were less than those observed during the water tests. This was unexpected since the decane is approximately 33 percent more viscous. Apparently

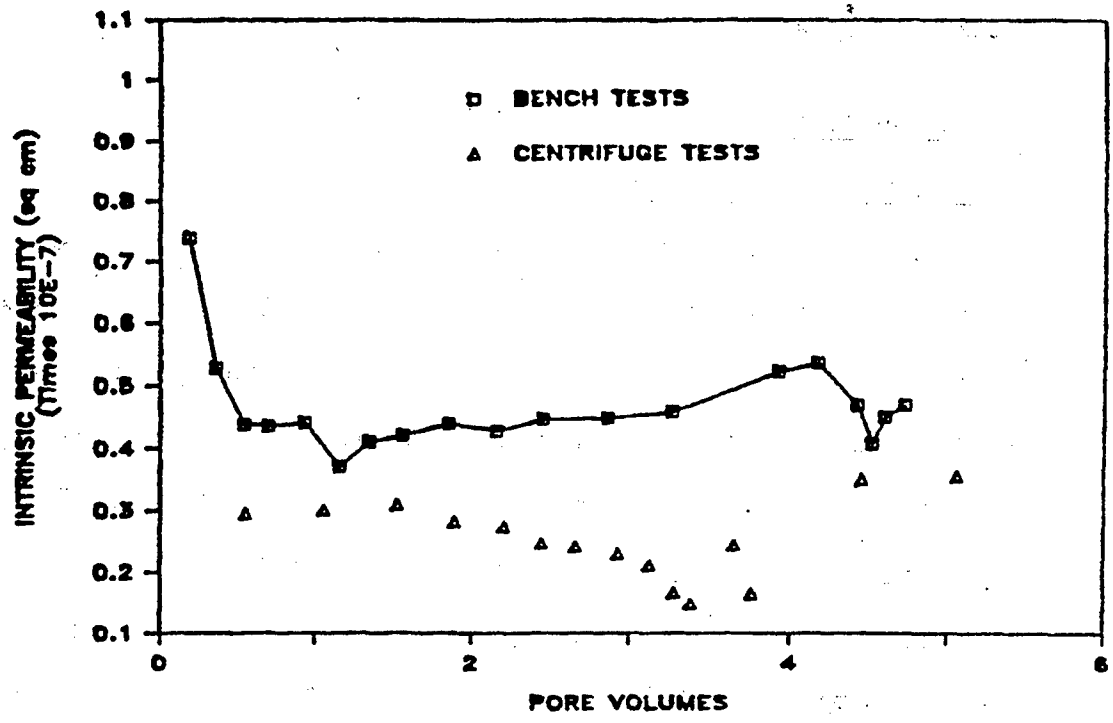

Figure 24. Comparison of Centrifuge and Bench Results of Permeability of Decane Through Sand for 1 and 24.4 g's

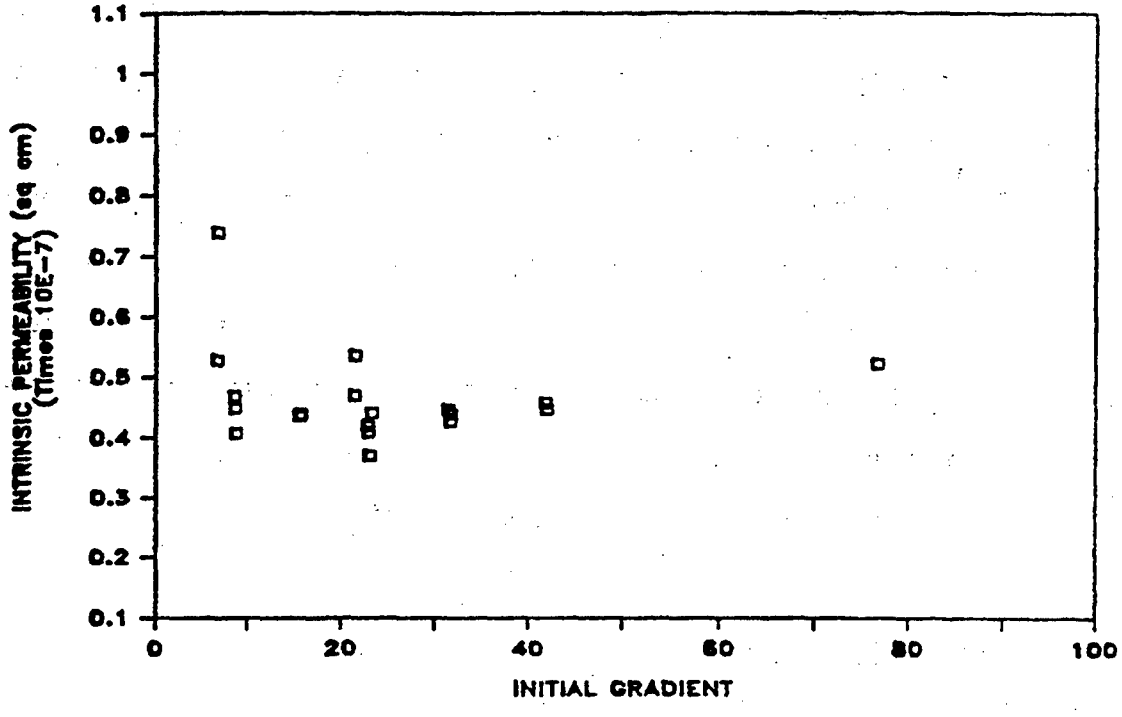

Figure 25. Permeability of Decane Through Sand as a Function of Initial Gradient

the adhesion between the nonpolar decane and the nylon tubing is less than that between the polar water molecules and the tubing.

Sand/Clay Samples

Influence of acceleration level

Saturated hydraulic conductivity tests were performed on sand/clay samples on the laboratory bench and in the centrifuge. Acceleration levels of 19.3 and 24.4 g's were established during the centrifuge tests. Energy losses due to friction were determined to be negligible during the tests due to the low velocities in the tubing. Figure 26 compares the results obtained in the centrifuge with those determined on the bench. Initial gradients of 90 to 200 were established across the 4.8 cm samples during the tests. By regulating the pressures at the upper and lower ends of the specimen, the direction of flow was reversed during the course of the centrifuge tests, such that the fluid moved against the radial acceleration forces. The variable head equation correctly handled this case as long as the direction of the hydraulic pressure gradient remained constant throughout the test.

Estimates of the intrinsic permeability of water through a sand/clay sample obtained in the centrifuge at two rotational speeds are presented in Figure 27. The lower estimates observed at the higher acceleration level suggest that the greater confining pressures, and consequently, greater effective stresses on the sample, influenced the rate at which water moves through the soil pores.

Influence of decane

Test results using decane after water are presented in Figure 28. Gradients of 45 to 160 were used during the tests. Decane was

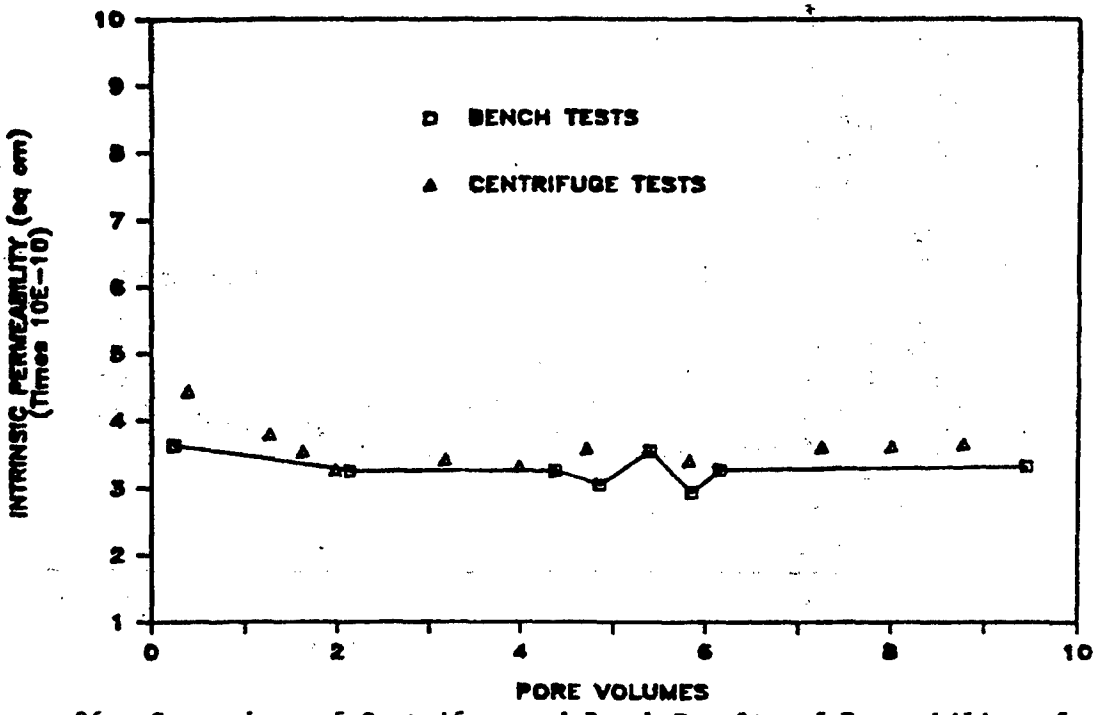

Figure 26. Comparison of Centrifuge and Bench Results of Permeability of Water Through Sand/Clay for 1, 19.3 and 24.4 g's

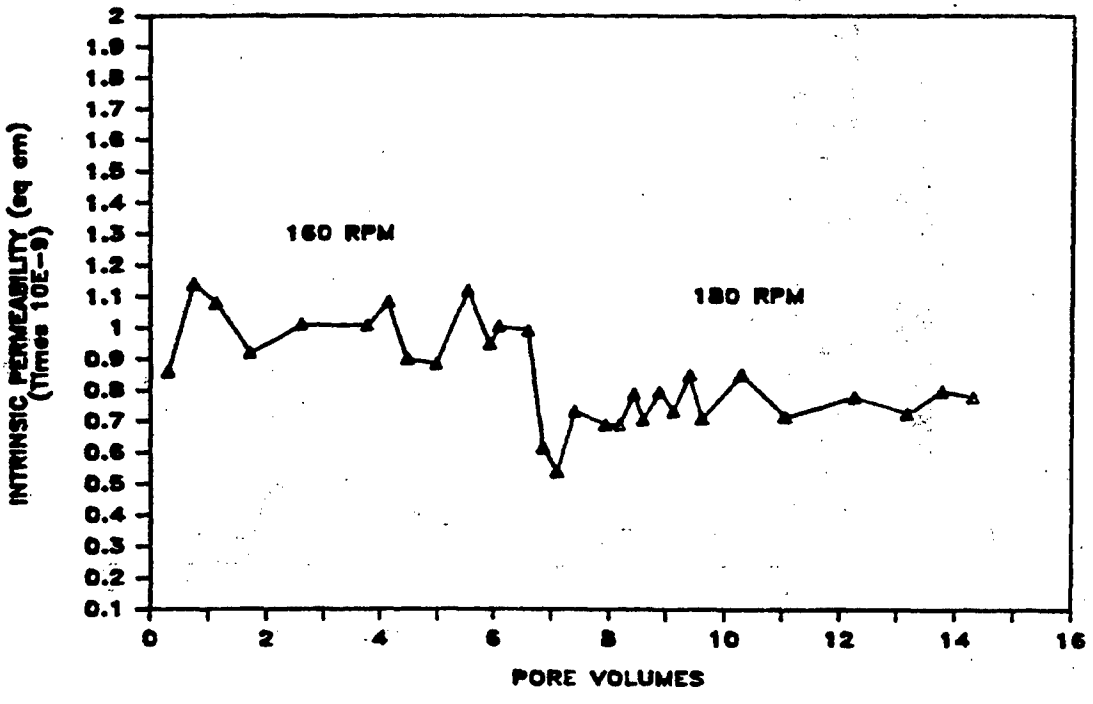

Figure 27. Comparison of Permeability of Water Through Sand/Clay as a Function of Acceleration Level at 19.3 and 24.4 g's

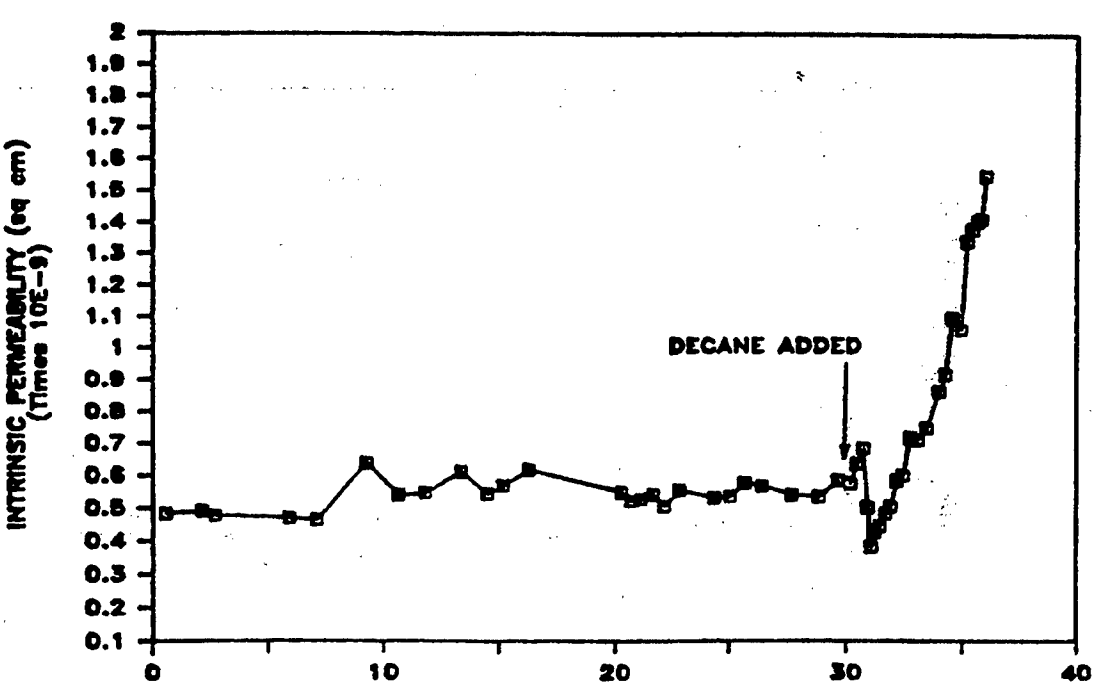

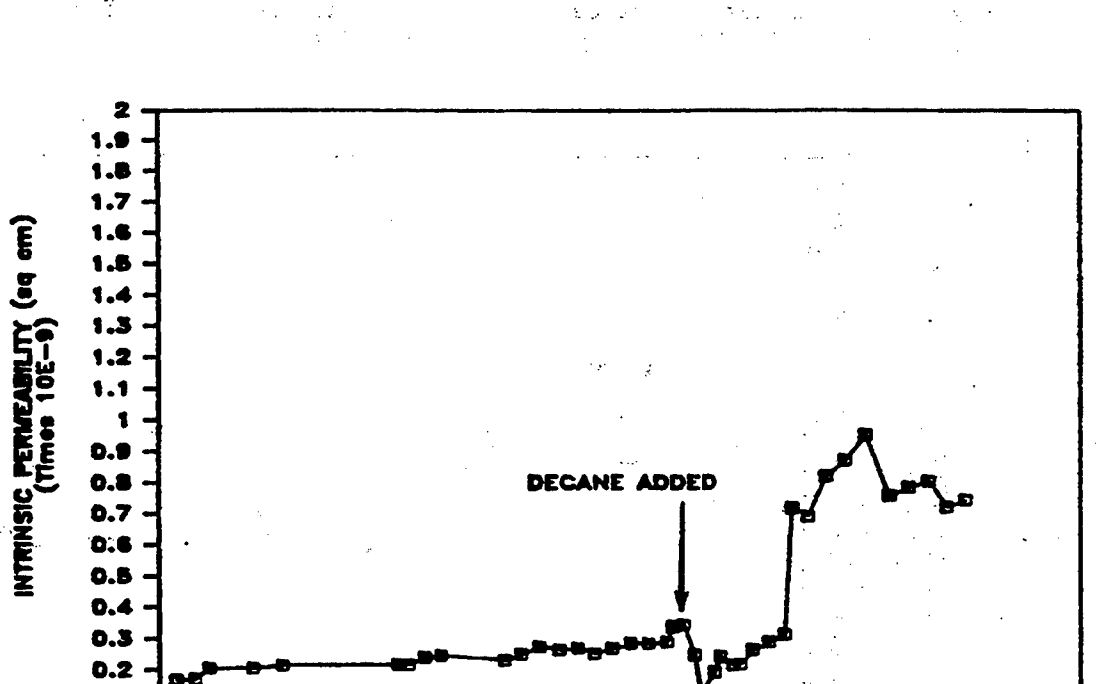

Figure 28. Comparison of the Permeabilities of Decane and Water Through Sand/Clay a) Sample 1; b) Sample 2 for 1 g bench tests

introduced to the top of the soil sample. Since the decane has a lower density than water, a bouyant force was present which acted against the hydraulic potential while pore water was present. Estimates of the intrinsic permeability dropped dramatically with the introduction of decane. However, definite trends of increasing k were observed as the specimens were permeated with decane. Similar patterns have been reported in prior studies of organic permeants through fine grained samples (Acar et al., 1985; Daniel et al., 1985). This trend suggests the formation of channels within the samples. It is hypothesized that the decane caused preferential agglomeration of the clay particles within the sand/clay mix. Visual inspection of the samples after the tests supported this, revealing a grainy appearance in the decane-soaked samples, as opposed to the smooth appearance of samples exposed only to water. This agglomeration may have occurred as a result of the adhesive and cohesive forces between the polar water molecules within the electric double layer of the clay particles. The nonpolar hydrophobic decane could not replace the adsorbed water and determined the path of least resistence to be around the agglomerations.

The decane displaced the water in a plug-like fashion. Very little water was discharged once the decane entered the effluent reservoir. The irreducible water content was found to be less than 5 percent of the void volume. Estimates of the intrinsic permeability did not exhibit a discernible relationship with gradient, as presented in Figure 29. The existence of hydraulic channeling is supported by the non-unique relationship between k and the gradient as the gradient was increased and then reduced during the tests.

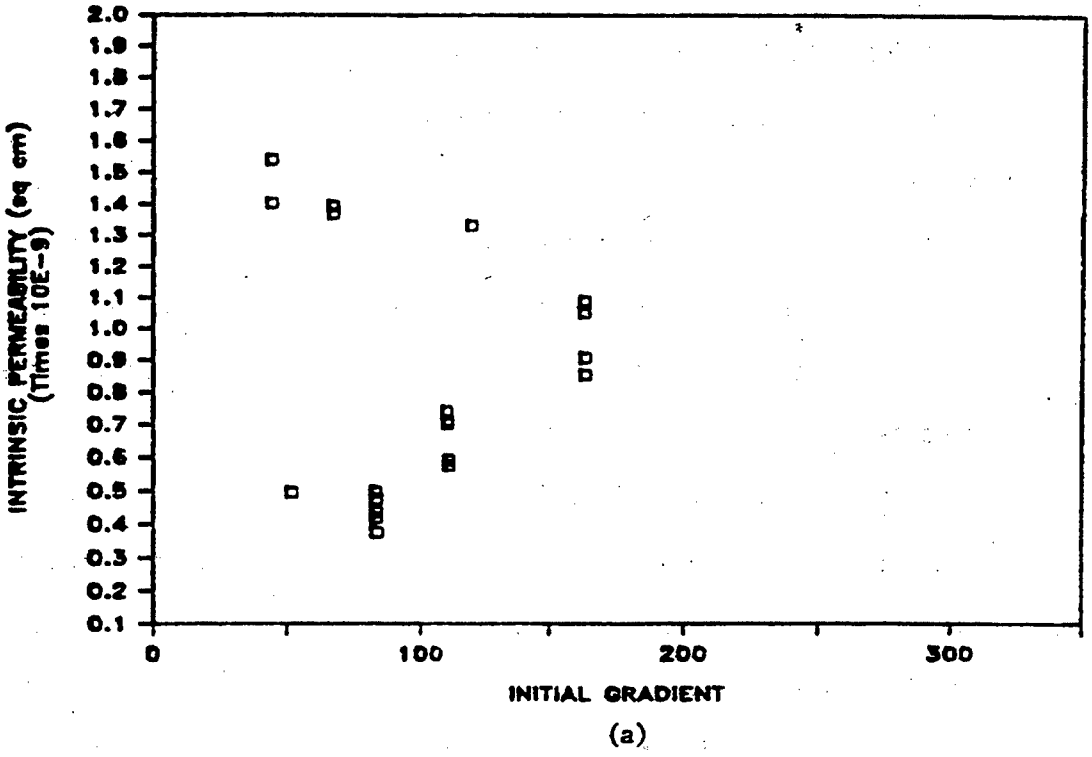

(a)

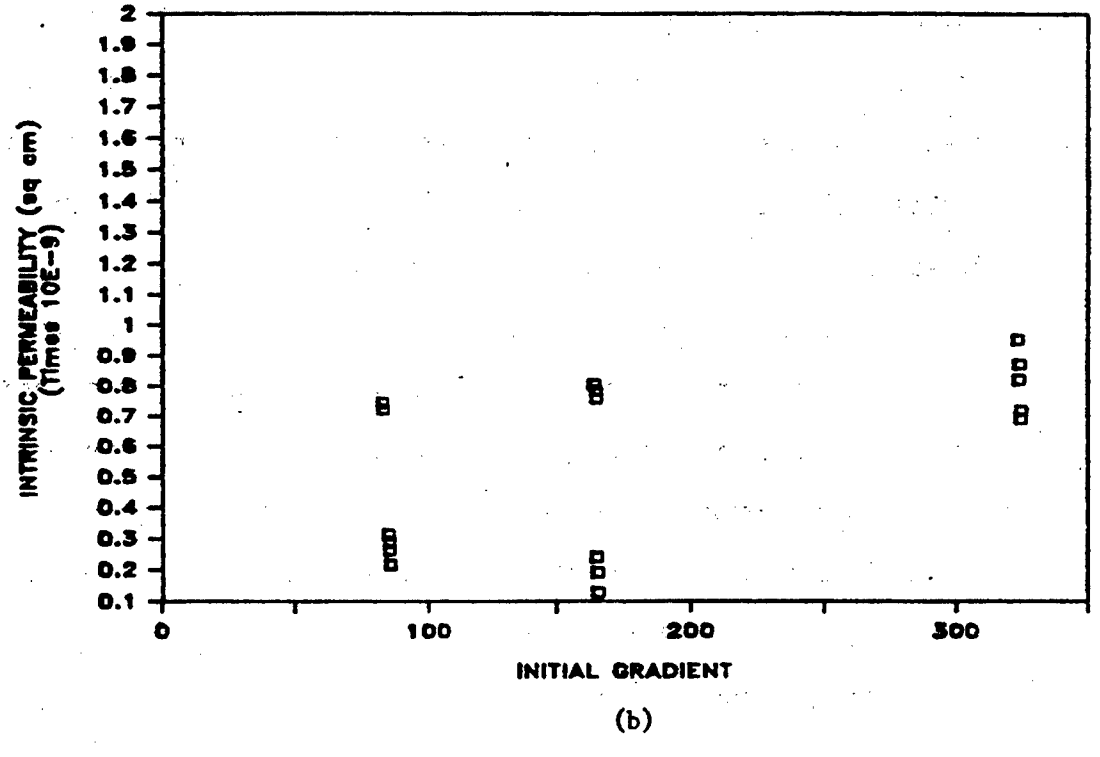

(b)

Figure 29. Permeability of Decane Through Sand/Clay as a Function of Initial Gradient a) Sample 1; b) Sample 2 for 1 g bench tests

Clay Samples

Safety considerations prevented the execution of the saturated hydraulic conductivity tests on clay within the centrifuge. Inlet pressures of 100 psi were required on the bench tests; however, to overcome the reduction in pressure as the fluid moves toward the center of rotation to the top of the sample would require approximately 120 psi in the lower chamber at 24.4 g's in the centrifuge. The acrylic apparatus was successfully pressure tested at 120 psi, but in light of the successful data collection using sand and sand/clay samples, the risk of a seal failure and consequential damage was not warranted.

Influence of Decane

Saturated hydraulic conductivity tests were performed on kaolinite samples using distilled water followed by decane. The tests were performed on a commercial triaxial apparatus after a backpressure saturation period of 3-4 days produced a "B" value of unity. Energy losses due to friction were determined to be negligible. The results of the tests are presented in Figs. 30 and 31. A pressure differential of 10 psi across the 2.54-cm high samples was used with the water, producing a gradient of 277. Consistent estimates of the intrinsic permeability between 1.8 and 3.2 x 10^{-13} cm^2 were obtained, which correspond to hydraulic conductivity values between 2.1 and 3.7 x 10^{-8} cm/s. Slightly higher values were obtained for the samples prepared at an initial water content of 32 percent by weight. The flux through all the clay samples decreased significantly following the addition of decane. Complete cessation of flow was observed in three of the four samples after approximately 0.2 pore volumes entered the permeant lines. The volume of the permeameter influent lines between the reservoir and

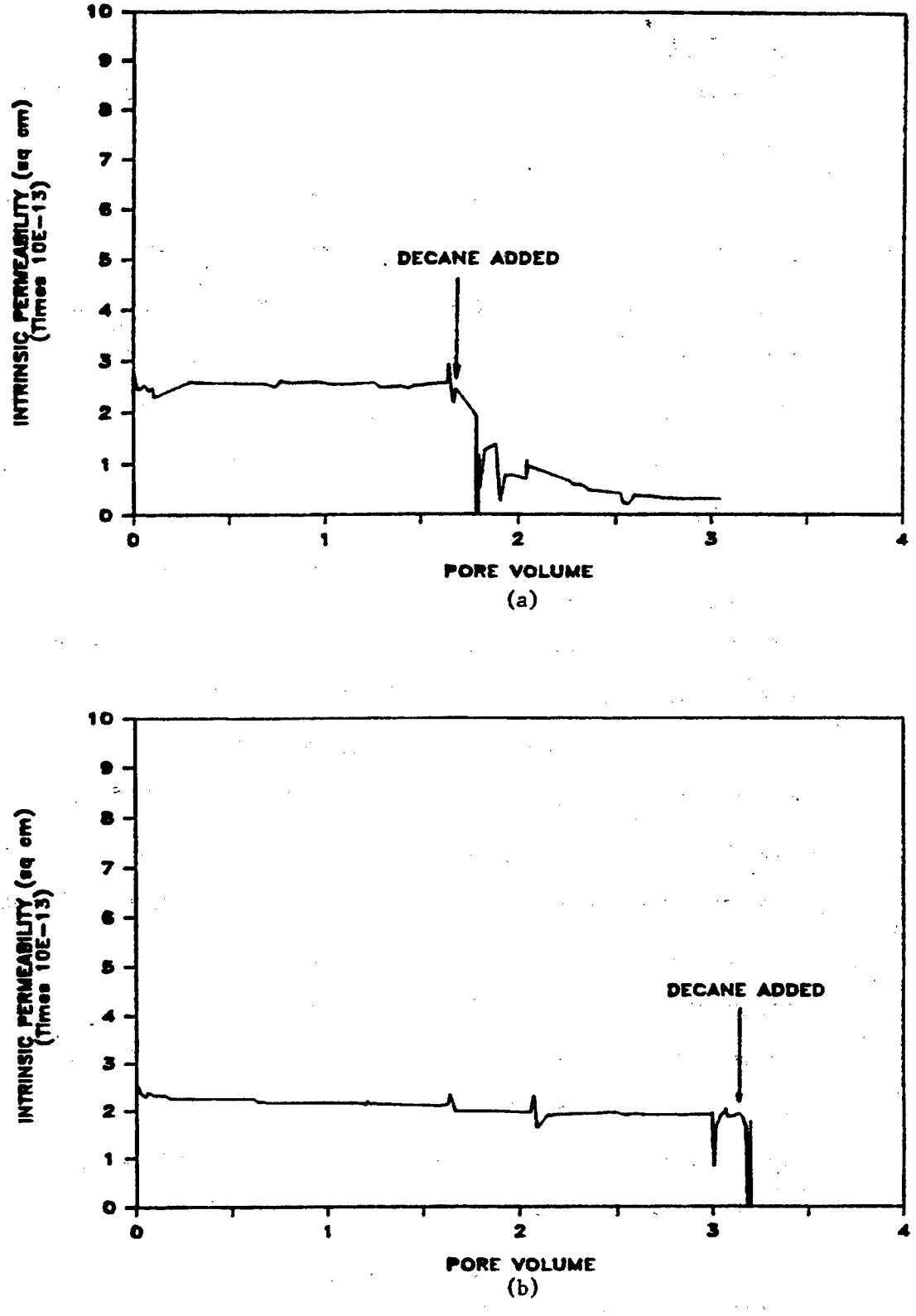

Figure 30. Comparison of the Permeabilities of Decane and Water Through Clay; Initial Water Content 29% a) Sample 1; b) Sample 2

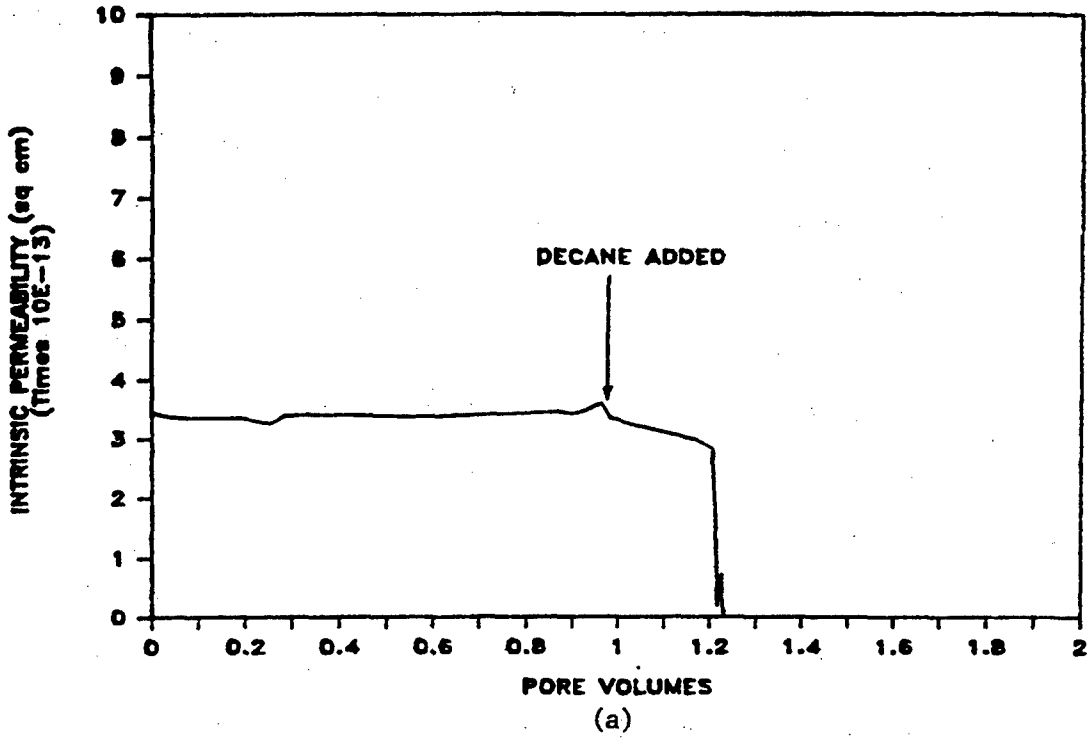

(a)

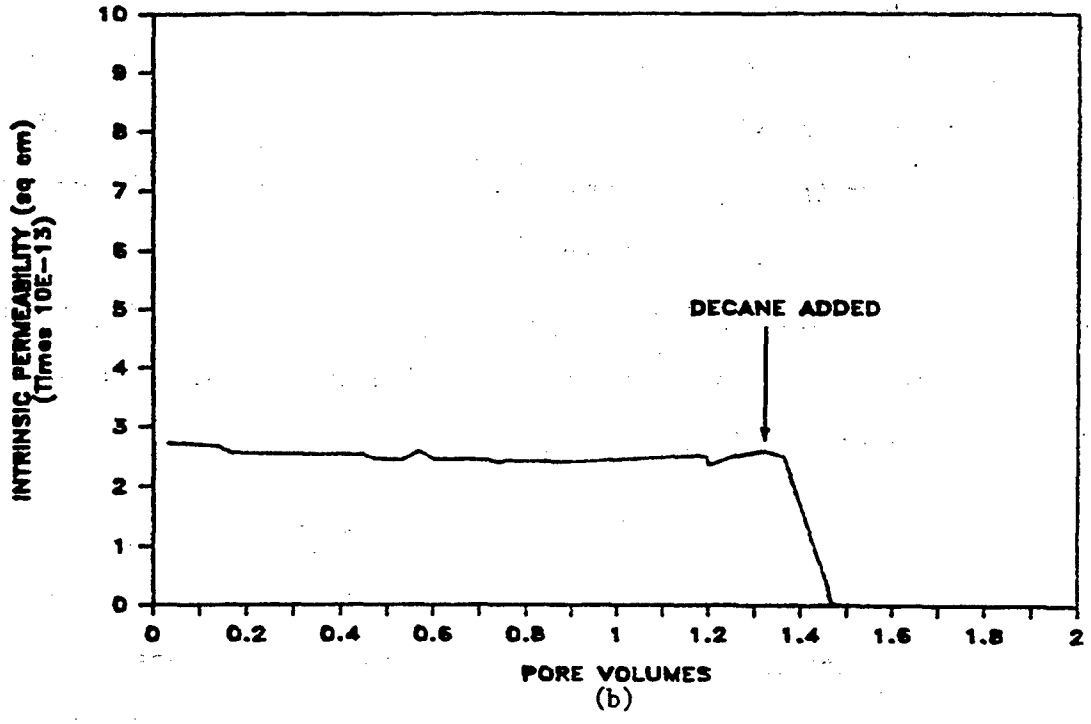

(b)

Figure 31. Comparison of the Permeabilities of Decane and Water Through Clay; Initial Water Content 32% a) Sample 1; b) Sample 2

the top of the sample is 8.5 cc, which corresponds to approximately 0.2 pore volumes of the 2.54-cm high specimens. Hence, there was little if any penetration of the decane into the clay samples before the flow ceased. Similar results were obtained in an earlier study with aniline and xylene through kaolinite (Uppot, 1984). Like aniline and xylene, decane is nonpolar, and hence, does not possess any electrostatic mechanism to displace the polar water molecules from the charged clay particles surface. Decane, aniline and xylene are immiscible in water; hence, the only way these fluids can flow through the clay pores is to physically displace the water.

The pressure gradient was tripled in an effort to overcome the interfacial energy of the water-decane interface. The flow through the samples resumed in two of the four samples under the higher gradient. However, the flux dropped off again in one sample, while estimates of the intrinsic permeability were about an order of magnitude lower than with water in the remaining sample. Even though the confining pressure was increased along with the inlet pressure, volume change of the sample within the flexible membrane was not monitored and could account for the apparent fluid flux through the sample.

These results suggest that for this range of gradients clays saturated with water are impermeable to a nonpolar immiscible hydrocarbon like decane.

Unsaturated Soil Tests

Based on the preliminary analysis, the most feasible test for unsaturated hydraulic conductivity was the Instantaneous Profile Method (IPM). During the IPM test, the soil suction is recorded at a fixed location in the soil profile as the sample drains. The computer model

was utilized to compare the IPM under bench and centrifuge acceleration levels. Physical dimensions of the sample were obtained from the centrifuge apparatus developed for the unsaturated tests (see Figure 16). The soil type used in the computer analysis was a hypothetical sand with moisture retention and hydraulic conductivity characteristics as presented in Figure 32. For the computer tests, the initially saturated sample was drained under the influence of gravity for the bench test, and under the influence of radial acceleration in the centrifuge at speed of 120, 180 and 240 RPM.

From the drainage test results presented in Figures 33 and 34 and summarized in Table 13, the centrifuge technique offers two obvious advantages over the bench test:

1. the method covers a much wider range of soil moisture and suction; and
2. the testing time, i.e., the time required to reach hydrostatic equilibrium, is reduced.

An additional advantage of the centrifuge technique is the possibility of expeditiously obtaining moisture retention characteristics of soil samples. These could be obtained by spinning initially saturated samples until drainage ceases and subsequently determining the moisture content at discrete locations along the profile. The pressure distribution presented in equation 20 could be correlated to the moisture content at specific elevations, providing the information needed for the moisture retention curves. The redistribution of soil moisture due to suction gradients after the sample stops spinning may present a problem for soils with high rates of unsaturated hydraulic conductivity.

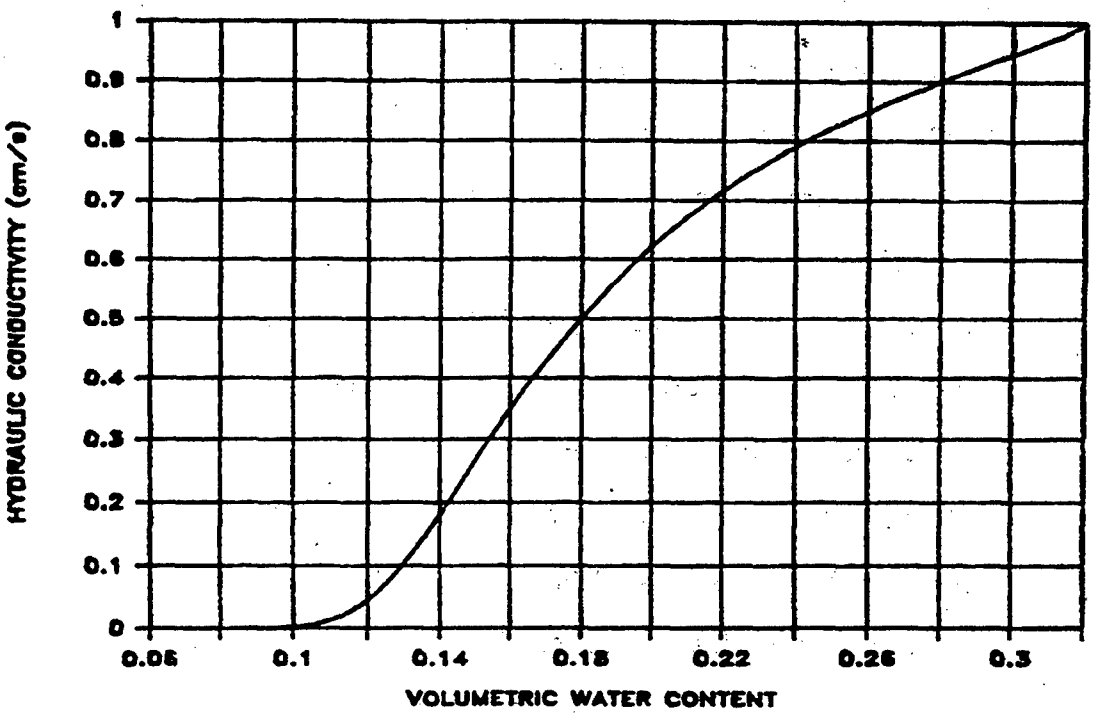

(a)

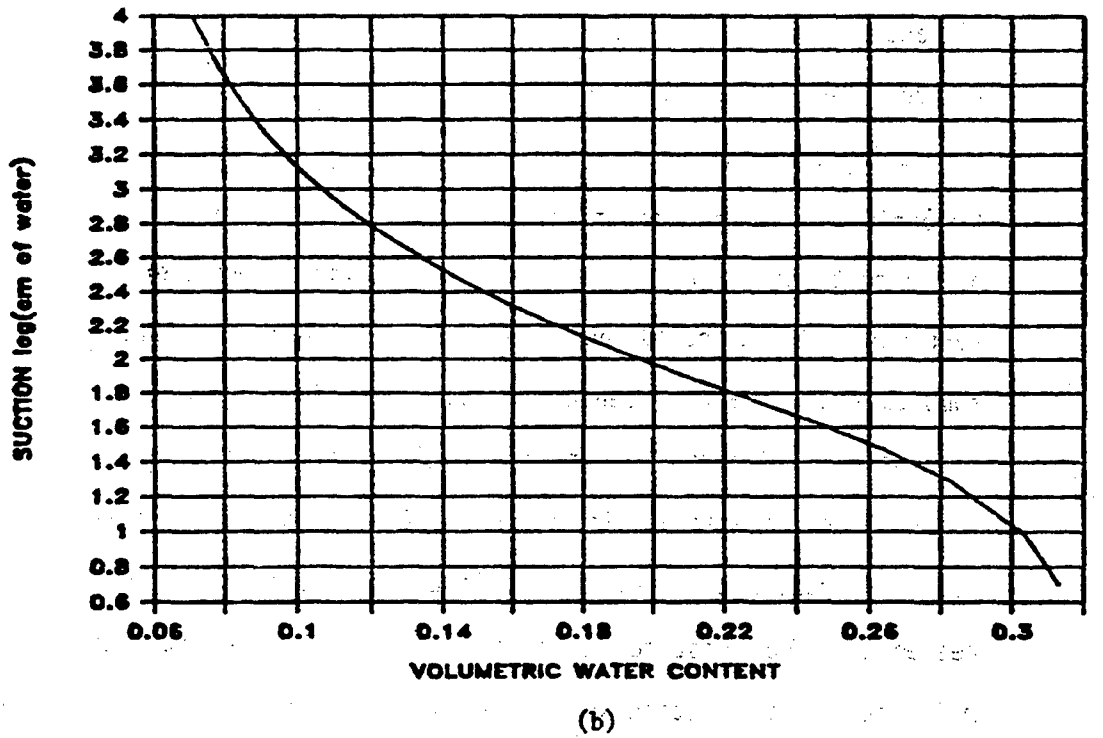

(b)

Figure 32. Characteristics of the Sand Used in the Drainage Simulations a) Hydraulic Conductivity; b) Moisture Retention Characteristic

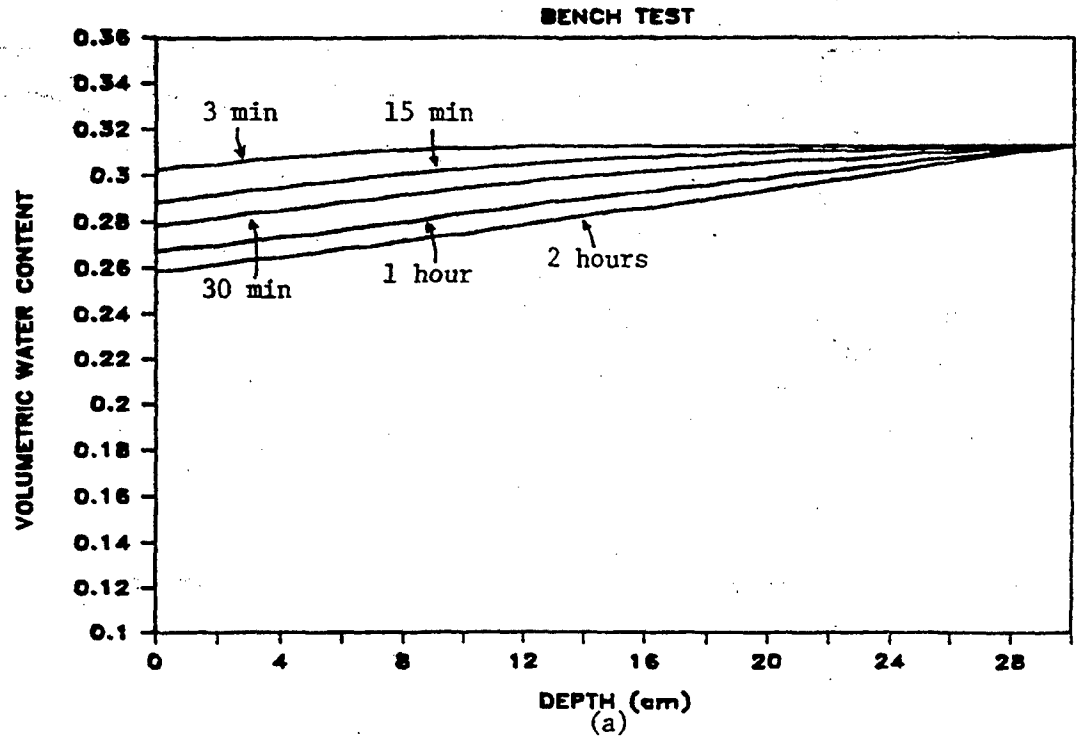

(a)

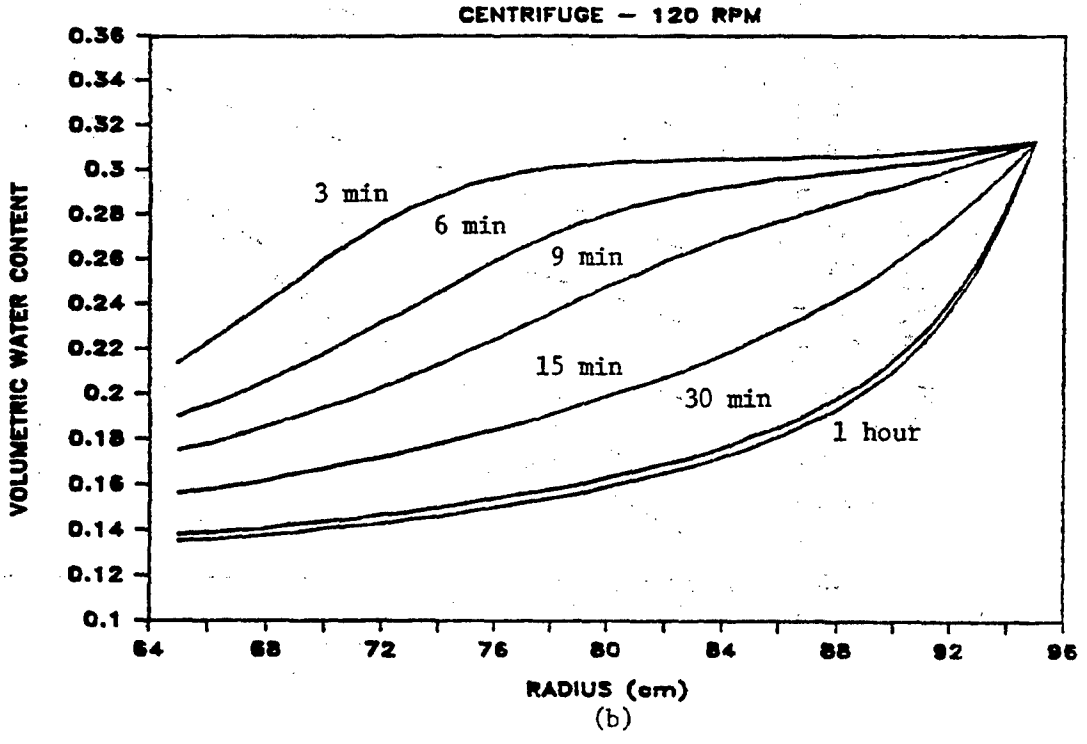

(b)

Figure 33. Comparison of Drainage Sequence in a Soil Sample a) Bench Simulation Results; b) Centrifuge Simulation Results

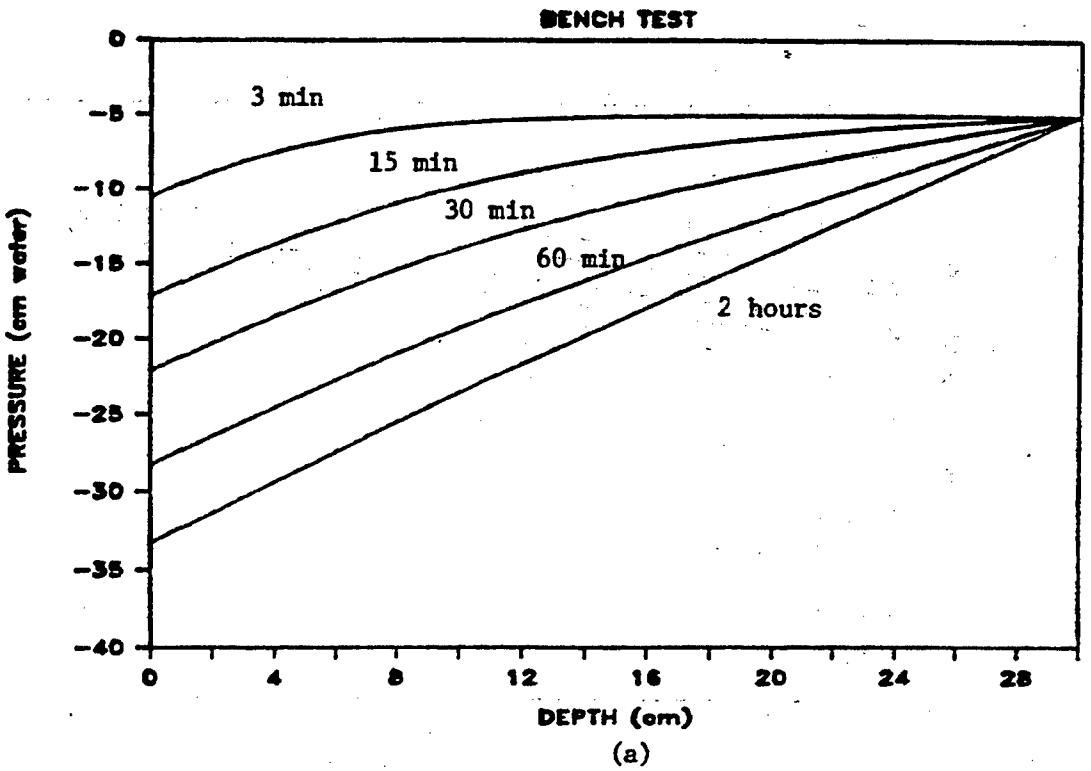

(a)

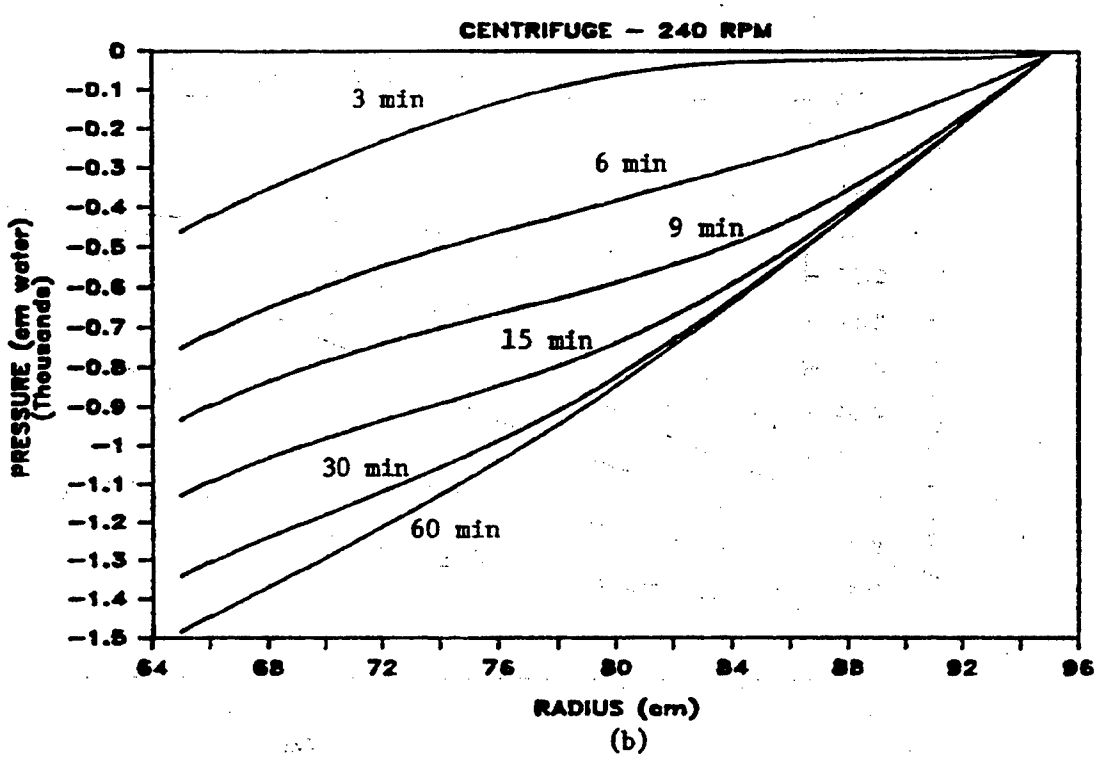

(b)

Figure 34. Comparison of the Pressure Profiles in a Soil Sample a) Bench Simulation Results; b) Centrifuge Simulation Results

Table 13. Summary of Simulated Drainage Test Results

Test Number	RPM	Acceleration Level (g's)	Moisture Content Range (%)	Moisture Suction Range (cm water)	Test Duration (min)
1	1	1.0	26 - 31	5 - 33	120
2	120	15.3	14 - 31	5 - 380	60
3	180	34.4	11 - 31	5 - 875	60
4	240	61.2	10 - 31	5 - 1475	60

Discussion

The total hydraulic energy of a fluid in a centrifuge is composed of four elements:

1. air pressure at the surface of the fluid;
2. submergence pressure of the fluid;
3. potential energy associated with the elevation (radius) difference between two points in a fluid; and
4. kinetic energy of the moving fluid.

The delineation of these components is essential when describing the effect of centrifugation on a fluid system, for it is only the latter three which increase significantly with the angular velocity of the centrifuge arm. The increase in air pressure is limited to the increase in weight of the gas; with a mass density of 0.00129 g/cc^3, an increase of 50 g's on a volume of one liter of air results in a pressure increase of less than 0.01 psi. Hence the total energy difference does not increase proportionately with the increase in radial acceleration.

Inspection of the equations of motion for a fluid in a centrifuge indicates the interchangeable relationship between the air pressure differential and the increase in centrifugal acceleration. This

relationship is a critical factor in comparing centrifugal techniques with conventional laboratory tests. In the saturated hydraulic conductivity testing, the increase in the hydraulic gradient due to the increased acceleration levels was reproduced in a triaxial apparatus by increasing the pressure gradient across the sample.

CHAPTER VI
LABORATORY TESTING OF UNSATURATED SOIL

Introduction

Hydraulic conductivity tests for unsaturated soils are carried out by subjecting the soil to a wide range of suctions and measuring the flow of fluid through the soil as a function of suction. By correlating soil suction to soil water content, a curve relating hydraulic conductivity to soil water content (by weight) may be produced. The range of suctions required to test a particular soil is a function of that soil's moisture-suction characteristic curve (moisture release curve), which itself is a function of the soil's type, texture and drainage history. This range starts at atmospheric (positive pressure) and may extend to many atmospheres suction (negative pressure). For sands the extreme suction value seldom exceeds 1 atmosphere.

Required suctions are normally achieved in one of two ways. The easiest method is to allow a saturated soil column to drain under the influence of gravity into a reservoir at the base of the column. Another method is to apply a differential pressure gradient across the sample and allowing a soil column to drain while keeping one end completely saturated. While this second method is not exactly producing suction, the effect is the same.

For simple drainage under the influence of gravity the suction, and hence the water content, at any point within the soil column is determined by the distance that point is above the surface of the

reservoir. Unfortunately, for soil columns much greater than one meter (about 0.1 atm suction) this method is too cumbersome. It may also require larger amounts of soil sample than are available. Also, since drainage is driven by gravity only, testing times can run into weeks. This is because hydraulic conductivity falls off steeply with decreasing water content.

Draining a soil column under pressure gradients is advantageous over the method discussed previously because it requires much less sample, and because the entire range of soil moisture contents may be produced. This, however, is contingent upon keeping one end of the soil saturated completely. Normally, this is done by supporting one end of the sample by a porous plate which, once saturated, will not allow air to pass through under the maximum pressure investigated. This maximum pressure is termed the plate's blow-out pressure. Unfortunately, a plate with a high enough blow-out pressure to be useful for these tests, will necessarily have a very low hydraulic conductivity.

Table 14 compares typical blow-out pressures and conductivity values for several plates available commercially, with the range of hydraulic conductivities expected for Edgar sand. Ideally, a plate should be chosen such that its blow-out pressure is high enough to allow the soil to drain completely, while its hydraulic conductivity equals or exceeds that of the saturated soil. Note that none of the plates in Table 14 meet both requirements.

These problems can be eliminated in the centrifuge which uses acceleration as a driving force rather than externally applied suctions or pressure differentials. A support platform having very high permeability may be chosen because blowout is unimportant. The

Table 14. Hydraulic Conductivities as a Function of Blow-out Pressures for some Metal Filters and Water Content of Edgar Sand

Nominal Pore Size (mm)	Blow-out Pressure (cm water)	Filter Thickness (mm)	Gradient	k (cm/hr)	Edgar Sand w (%)	Edgar Sand k (cm/hr)
0.0005	114.3	1.19	589.7	1.12E-01	3.20	1.22E-03
0.0020	45.7	1.57	447.0	8.75E-01	25.23	1.38E+00
0.0050	35.6	1.57	447.0	1.37E+00	33.54	3.88E+00
0.0100	20.3	1.57	447.0	8.75E+00	41.84	9.84E+00
0.0200	12.7	1.57	447.0	2.02E+01	43.05	1.17E+01
0.0400	7.6	1.98	355.3	6.88E+01	43.27	1.22E+01
0.1000	1.3	2.36	298.0	2.46E+02	43.30	1.24E+01

NOTE: Conductivity values for metal filters were calculated based on data supplied by the manufacturer. Conductivities for Edgar sand were calculated using methods presented in this paper.

centrifuge has an added advantage in that it induces high gradients to form in the soil sample, thus not only accelerating the test but also providing a wide range of moisture contents to be evaluated in a relatively short time.

The simulation results presented earlier in this report demonstrate the utility of the centrifuge for obtaining drainage curves. The remainder of this report describes the steps taken to investigate the validity of these initial simulations as well as determining the technical feasibility of the geotechnical centrifuge as an instrument to measure the drainage curves of granular soils.

The steps undertaken during this phase of the investigation are as follows:

1. Drainage was simulated for the soil used in these experiments using the finite difference scheme mentioned earlier.
2. The soil test apparatus for the centrifuge tests was designed and constructed.

3. Unsaturated conductivity tests were carried out in the centrifuge.
4. Conductivity curves for the sand were plotted based on the experimental results and compared with expected curves based on unsaturated flow modeling theory.

Each of these steps will now be discussed in more detail.

Simulation

Determination of Unsaturated Flow Parameters

A combination of theoretical and empirical techniques are generally used to simulate conductivity curves for soils. Different methods work best with different soils and there is generally no way of determining which function works best without actually testing the soil. Mualem (1976) reviewed several of the most widely used methods and compared them with experimentally obtained drainage curves for a variety of soils. One of these methods seemed more generally applicable to a wider variety of soils than the others. The method was a modification of that proposed originally by Childs and Collis-George (Childs and Collis-George, 1950). Van Genuchten (1980) presented a modified form of this equation which permits the simulation of moisture release curves as well as conductivity curves but does not otherwise differ from Mualem's model. He also suggested a method to back calculate the moisture release curve parameters from experimentally obtained moisture release curves. The parameters used to construct the moisture release curve are the same as those used in the conductivity curve simulation. This is most advantageous since the moisture release curves are relatively easy to measure. These reasons combined make the van Genuchten model attractive and are why this method was chosen for this study.

The experimentally obtained curve for the Edgar sand used in this study is shown in Figure 35. The curve is typical of a uniform granular soil and shows how rapidly water content falls with increased suction. This data was used to back calculate the van Genuchten parameters for the moisture release curves presented in Figure 36. This figure shows the simulated curves calculated from three sets of van Genuchten parameters compared with the actual data points from the curve in Figure 35. The parameters representing the center curve (a = .0224, n = 3.85) were arbitrarily chosen as best representing Edgar sand and were used in the ensuing drainage simulations. The simulated curve is reasonably accurate down to a moisture content of 5 percent.

Figure 37 depicts hydraulic conductivity as a function of water content by each of the three sets of parameters used to generate the curves in Figure 36. Note that there is not a lot of difference between these curves and hence small errors in choosing parameters should not effect the results significantly. This outcome is supported by the results shown in Figure 38 which show hydraulic conductivity as a function of matric suction for the three sets of van Genuchten parameters of Figures 36 and 37.

Conductivity versus water content curves were also generated by two other methods which are often cited in the literature. One of these is another variation of the original Childs and Collis-George model as proposed by Jackson (Jackson, 1965). The other is a less accurate but much more straightforward approach by Irmay (Bear, 1979). These are presented in Figure 39 with the van Genuchten curve selected for Edgar sand. Here again the differences are small.

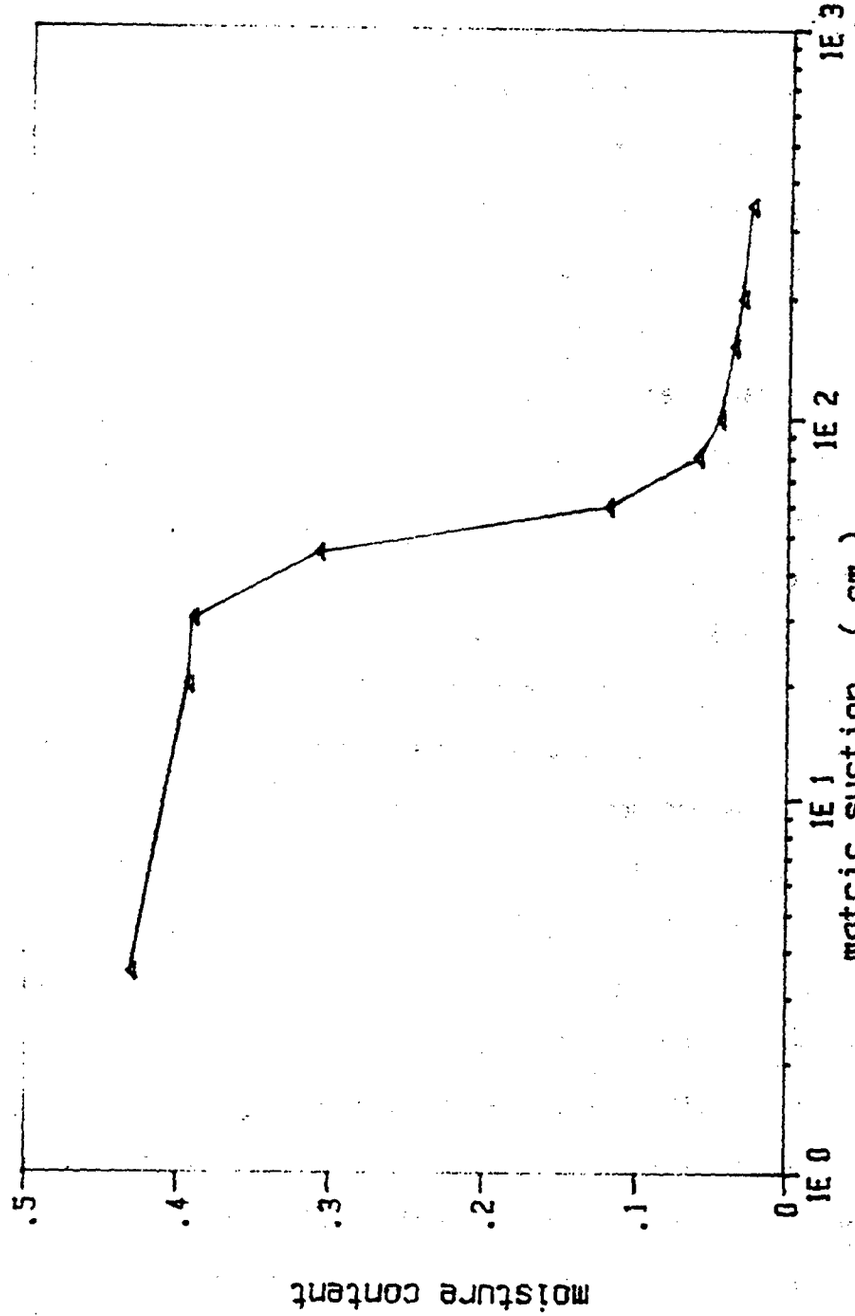

Figure 35. Experimental Moisture Content versus Suction Curve for Edgar Sand

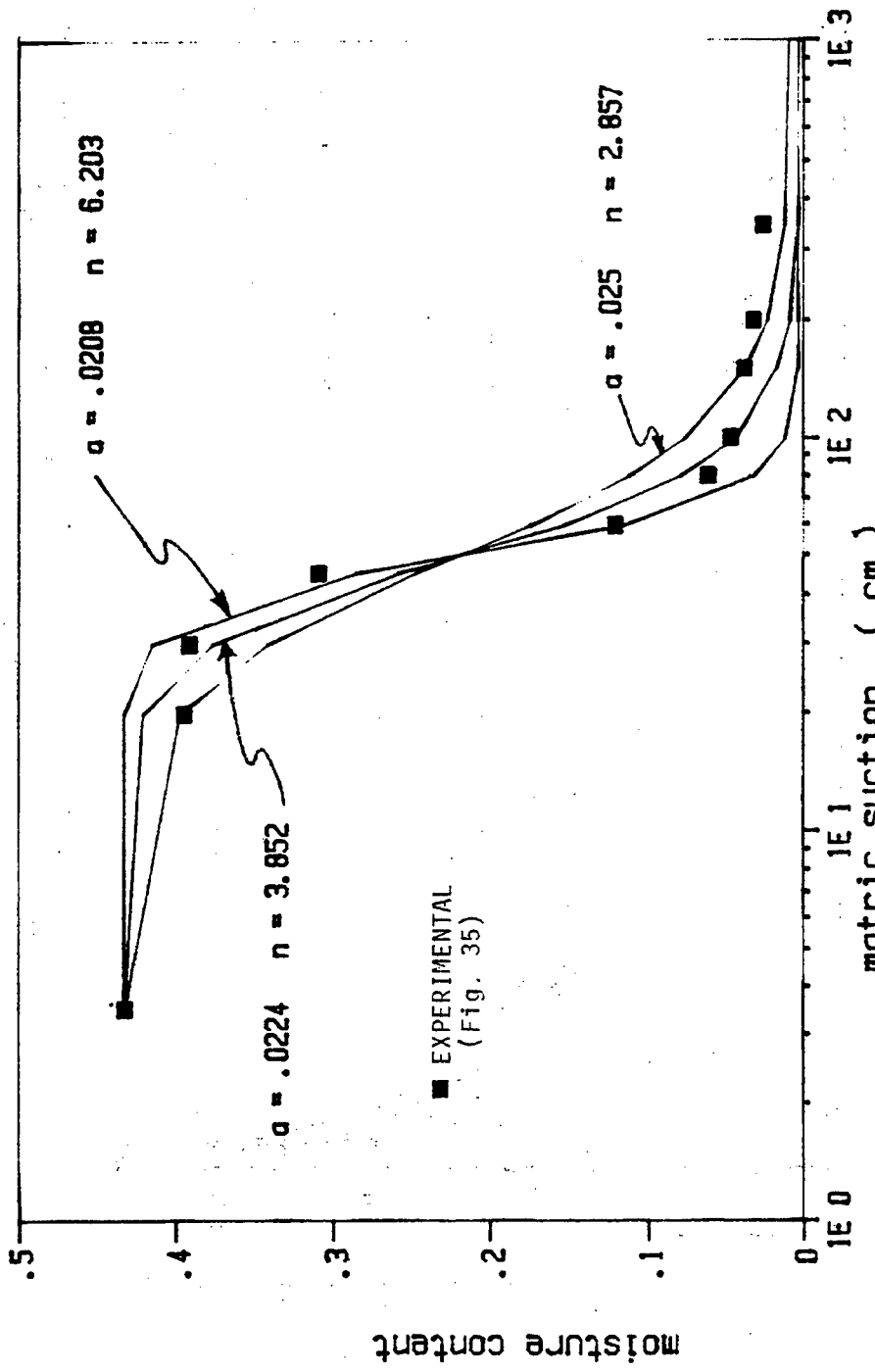

Figure 36. Comparison of van Genuchten Parameters for Edgar Sand

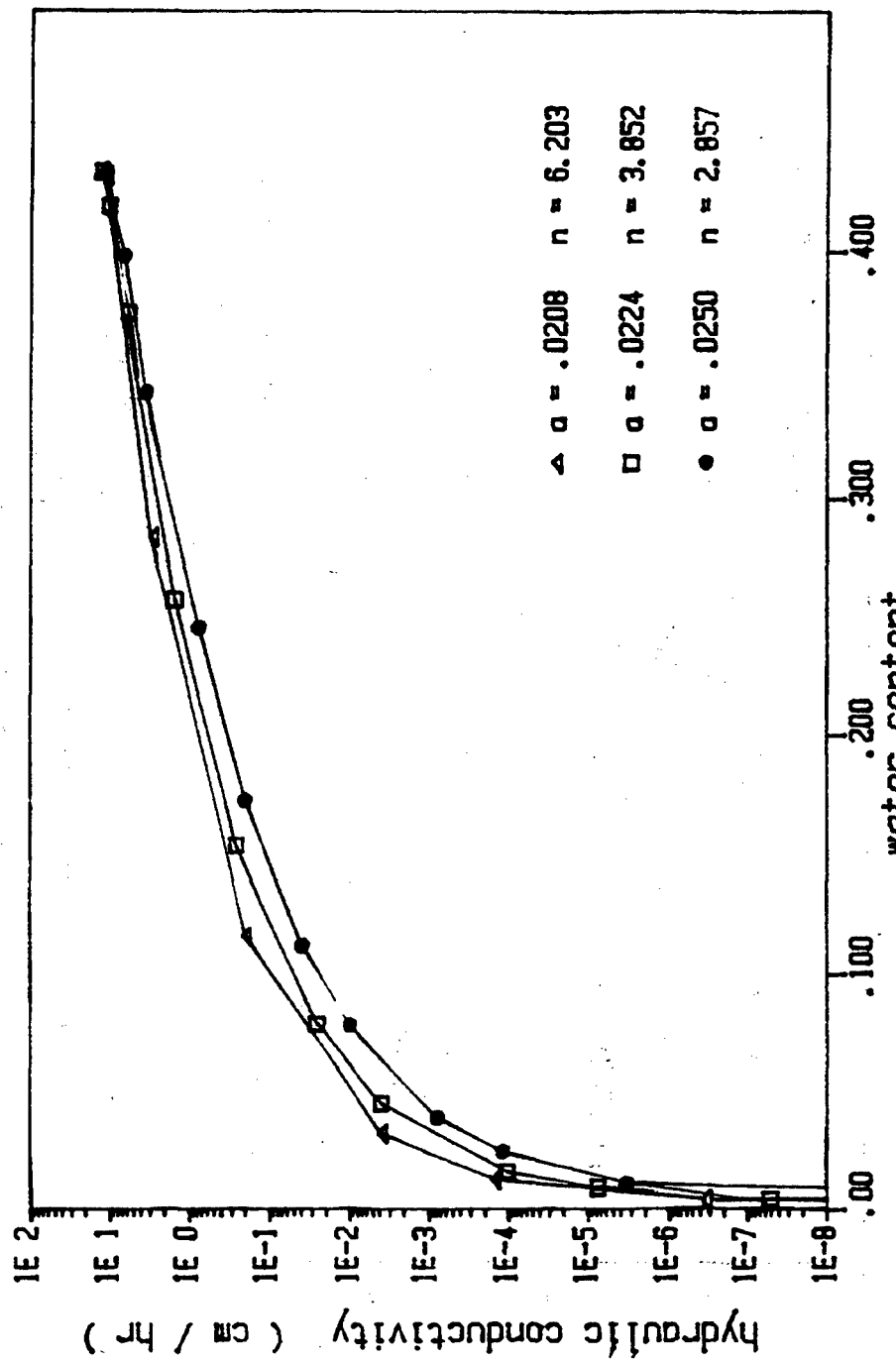

Figure 37. Hydraulic Conductivity versus Water Content Using van Genuchten Parameters for Edgar Sand

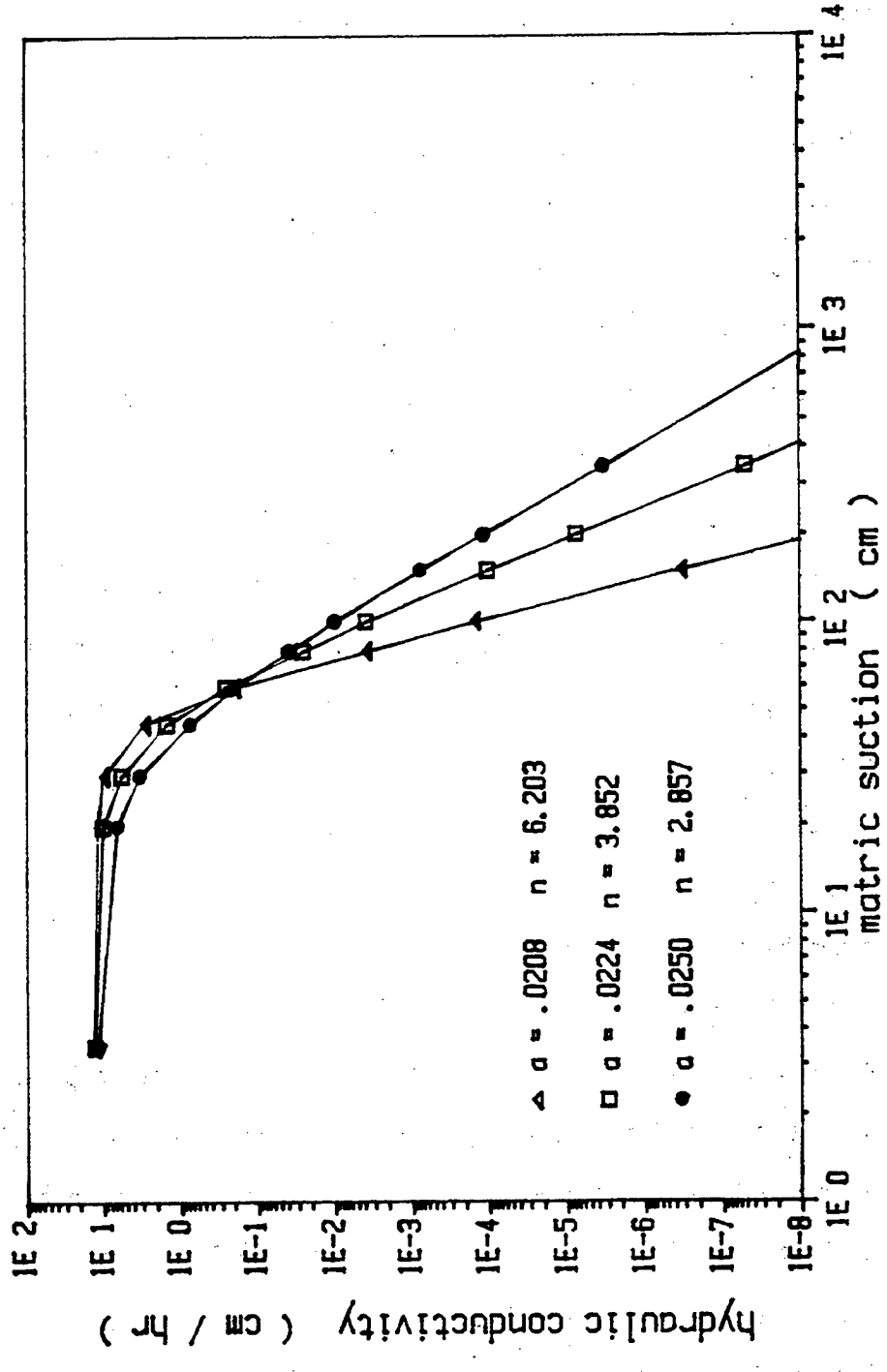

Figure 38. Calculated Hydraulic Conductivity versus Suction Relationships for Edgar Sand

Finite Difference Model

The finite difference program discussed earlier in this report was written using fixed flow parameters intended to represent a "typical" sand. Modifications have since been made which allow the substitution of different soil parameters so that any soil may be studied. Also the original version did not use the identical simulation methods as was chosen for the Edgar sand so additional modifications were made to include this. Simulations were then run for the centrifuge at 150 rpm using the dimensions of the designed testing apparatus (discussed later). A parametric study was performed by altering both the time and distance steps in the finite difference simulation in order to minimize the error. Once the time and distance steps had been optimized, simulations were run at 150, 100, and 0 rpm (1-g bench simulation). Unfortunately, the program is not capable of simulating the initial conditions expected for the centrifuge run which included an initial hydrostatic pressure distribution varying by the formula:

$$h_p = \rho g z$$

for the bench simulation and:

$$h_p = 0.5w^2[r_0^2 - r_1^2]$$

for the centrifuge simulation. Here h_p = the hydrostatic pressure head; ρ = mass density of water; g = the earth's gravitational acceleration; z = the depth under the water surface; w = the angular velocity of the centrifuge (radians/sec); r_0 = the rotational radius of the water surface; and r_1 = the rotational radius at any depth in the soil column. The simulation program could only model a constant pressure distribution which had to be less than or equal to zero as an initial

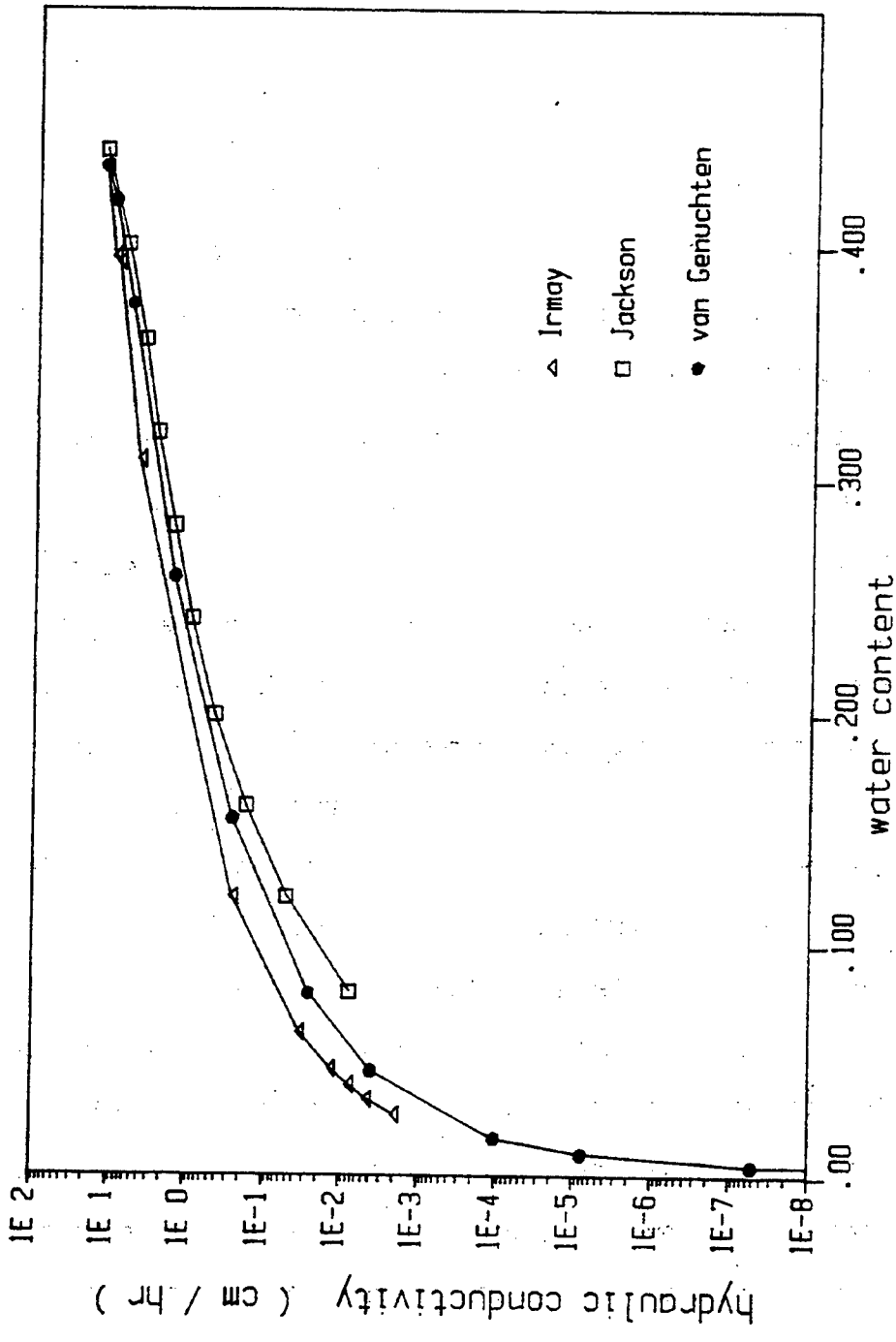

Figure 39. Comparison of Calculated Hydraulic Conductivity versus Water Content Relationship for Edgar Sand

condition. For this reason the simulation results should not be expected to agree completely with actual test results, however comparisons between the two should give a qualitative feel of the effectiveness of the experimental procedures and the validity of the model.

Laboratory Tests

The Instantaneous Profile Method of measuring hydraulic conductivities of unsaturated soils is used commonly by soil scientists and has the advantage over other methods in that an entire drainage profile of a soil may be obtained in the course of a single test. The test is also rapid since it is not necessary for the soil water to reach equilibrium with its matric suction as it is with steady state tests.

The apparatus used for these tests is depicted in Figure 40. The basic frame was the same as that used for the saturated tests and consisted of a lower chamber/reservoir and an upper chamber for housig the soil sample. The reservoir consisted of a hollow acrylic cylinder clamped between two acrylic plates using o-rings to provide for a leak proof seal. The soil chamber was simply an 18-inch piece of schedule 40 pvc pipe and was clamped to the top of the reservoir by a third acrylic plate. Rubber gaskets were used to seal the pvc against the acrylic. The soil was supported in the sample chamber on the same scintered metal disk used in the saturated studies. The disk was supported by a partially hollowed acrylic disk which channeled the sample effluent through attached brass fittings and tubing which lead to the lower chamber.

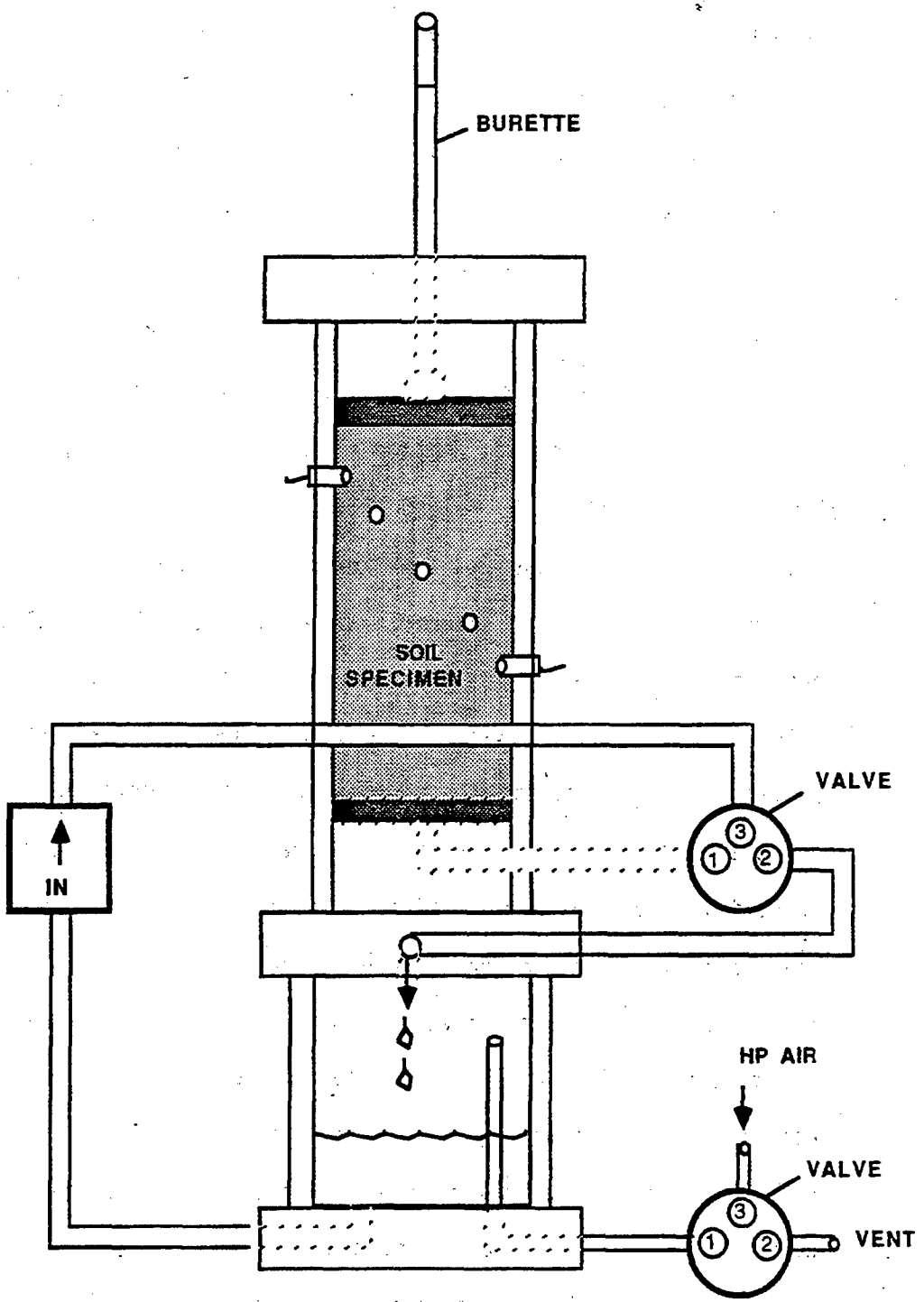

UNSATURATED FLOW APPARATUS FOR THE CENTRIFUGE

Figure 40. Schematic of Apparatus used in Partially Saturated Hydraulic Conductivity Tests

Water and high pressure air flow during the experiment was controlled by two 3-way and one 2-way solenoid valves as shown in Figure 40. These enabled the soil to be saturated with water in the reservoir while the centrifuge was spinning. With solenoid 1 and 2 on (see Figure 40), high pressure air could be furnished to the top of the reservoir to force water out of the bottom of the reservoir and up through the sample bottom. The progress of saturation could be monitored visually using a strobe light to observe water levels in both the reservoir and in a calibrated burette attached to the top of the sample chamber. The burette also allowed recording the height of the water surface above the sample so that pressure readings could be "zeroed" at the start of each test.

Once the sample was saturated solenoid 1 and 2 were closed which shut off the water supply to the sample and vented the reservoir to the atmosphere. Once the level in the burette was recorded, the test was started by opening solenoid 3 which allowed the sample to drain freely into the reservoir. Pressure/suction changes throughout the test were recorded from 5 transducers inserted in the walls of the soil chamber. Transducers were manufactured by Druck, Inc., and had a minimum sensitivity of 0.05 volts per centimeter of water head. Readings were recorded on magnetic disk by an HP 3497A data acquisition unit every 10 or 15 seconds for the centrifuge test and every 60 seconds for the bench test. Readings were also sent directly to a printer during testing as a backup in case of failure of the magnetic media. Photographs of the apparatus as installed in the centrifuge are shown in Figure 41. Bench tests were performed with the apparatus in the upright position and ran approximately 0.5 hour. Centrifuge tests were run at 100, and 150 rpm (7.5 and 16.9 g's) and lasted no longer than 15 minutes each.

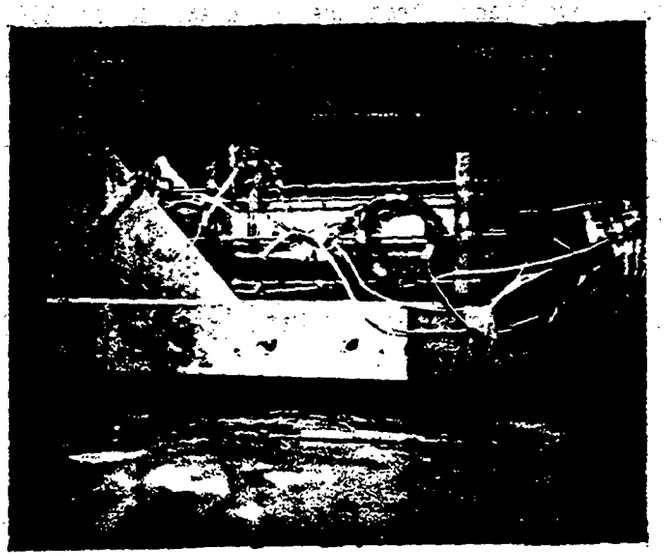

Front View

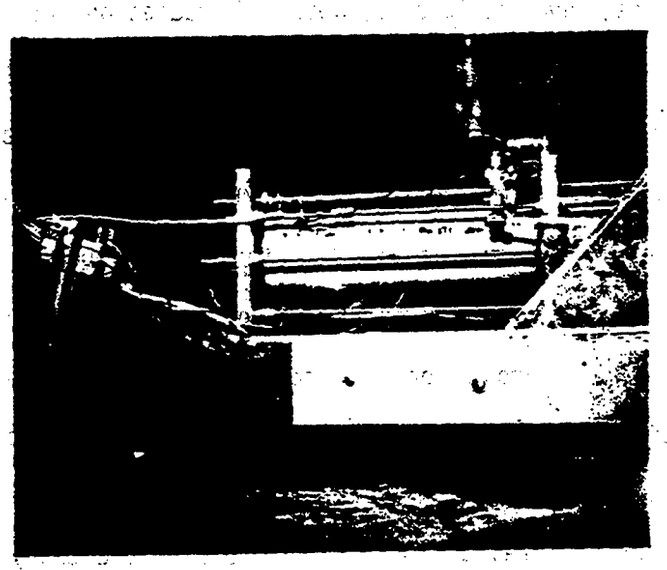

Back View

Figure 41. Photograph of Partially Saturated Hydraulic Conductivity Apparatus on Centrifuge

Data Reduction

Data was down-loaded from the HP disks to an 8088 microprocessor based personal computer for disk storage in MS-DOS format and analysis on MS-DOS computers. Data files listed elapsed time into each test and the corresponding voltage output of each transducer. Matric suction values were calculated from the voltage output using the appropriate multipliers for each transducer. Water contents were determined using the matric suction values by either the method of van Genuchten (described earlier) or by direct interpolation from the experimentally obtained moisture release curves (Figure 35). Ideally, it is best to have a separate estimator of water content by some non-destructive means such as gamma ray attenuation or neutron back scattering. However, these devices, due to the amounts of radiation involved, were too dangerous to be used in the centrifuge during the developmental stages of this method. Therefore, for the purposes of the feasibility study, moisture contents were determined from matric suctions alone.

A FORTRAN program was written for data reduction and determines hydraulic conductivities by dividing the sample into 5 sections, each of which is centered around one transducer. At each point in time water contents of each section are considered to be constant and are determined by the transducer reading for that section. Flow from the bottom of each section is calculated from the sum of the changes in water contents of all sections above. Gradients between sections are calculated by the change in total head between two adjacent transducers divided by the distance between them. The water content at the bottom of a section is determined from the matric suction at that point which is determined by interpolating linearly between the two adjacent transducers.

While these assumptions of linearity are usually valid for bench tests where gradients are linear, they must be justified for the centrifuge where gravitational acceleration varies with the spin radius (R) and both gradients and moisture distributions can be far from linear. To test these assumptions, suction output data from the finite difference simulations were fed into the data reduction program to represent actual data from the five transducers of the testing apparatus. Output from the data reduction program was then compared with permeability curves calculated by the van Genuchten method. This data is presented graphically in Figures 42, 43 and 44 for a bench simulation, a 100 rpm (7.5 g) centrifuge simulation and a 150 rpm (16.9 g) centrifuge simulation, respectively. The figures show excellent agreement between reduced data and the actual curves that they represent. Thus the assumptions used in the data reduction formulation are valid for the transducer spacings used in this set-up for centrifuge speeds of at least 150 rpm.

Test Results

A series of bench tests were performed to test the apparatus and to calibrate the electronics of the system. Typical bench test results are presented in Figures 45 and 46. Figure 45 shows matric suction as a function of drainage time. The first 4 data points showing negative suction (positive pressure) were taken before drainage began and were used to zero the electronics using the state head values in the column. Note that 3 of the 4 transducers had already established equilibrium at a moisture content only slightly below saturation.

Typical results form the early centrifuge runs are presented in Figures 47 and 48. Figure 47 shows matric suction versus drainage time

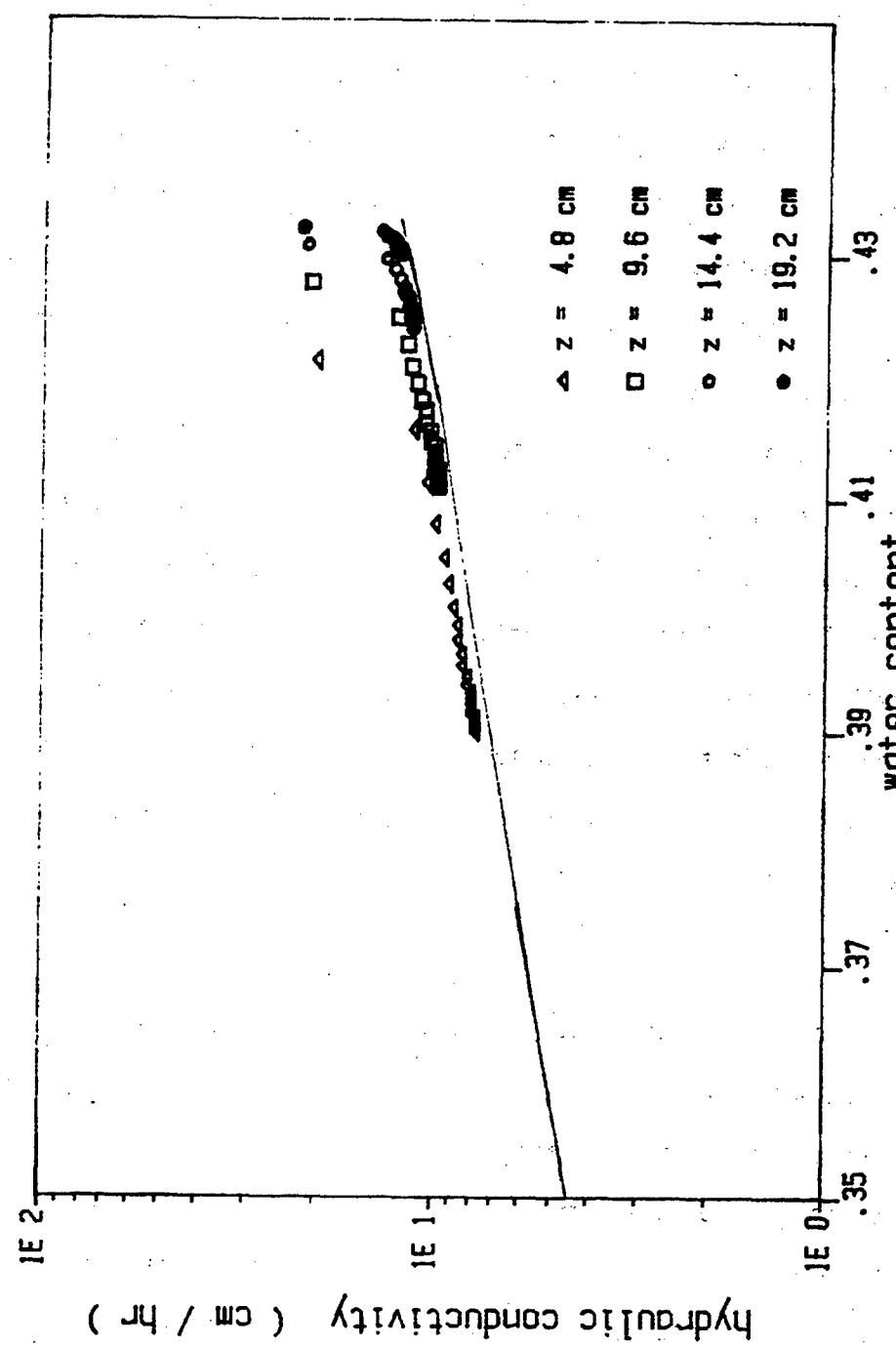

Figure 42. Simulation of Hydraulic Conductivity - Water Content Relationship for Edgar Sand at 1g (z from specimen top)

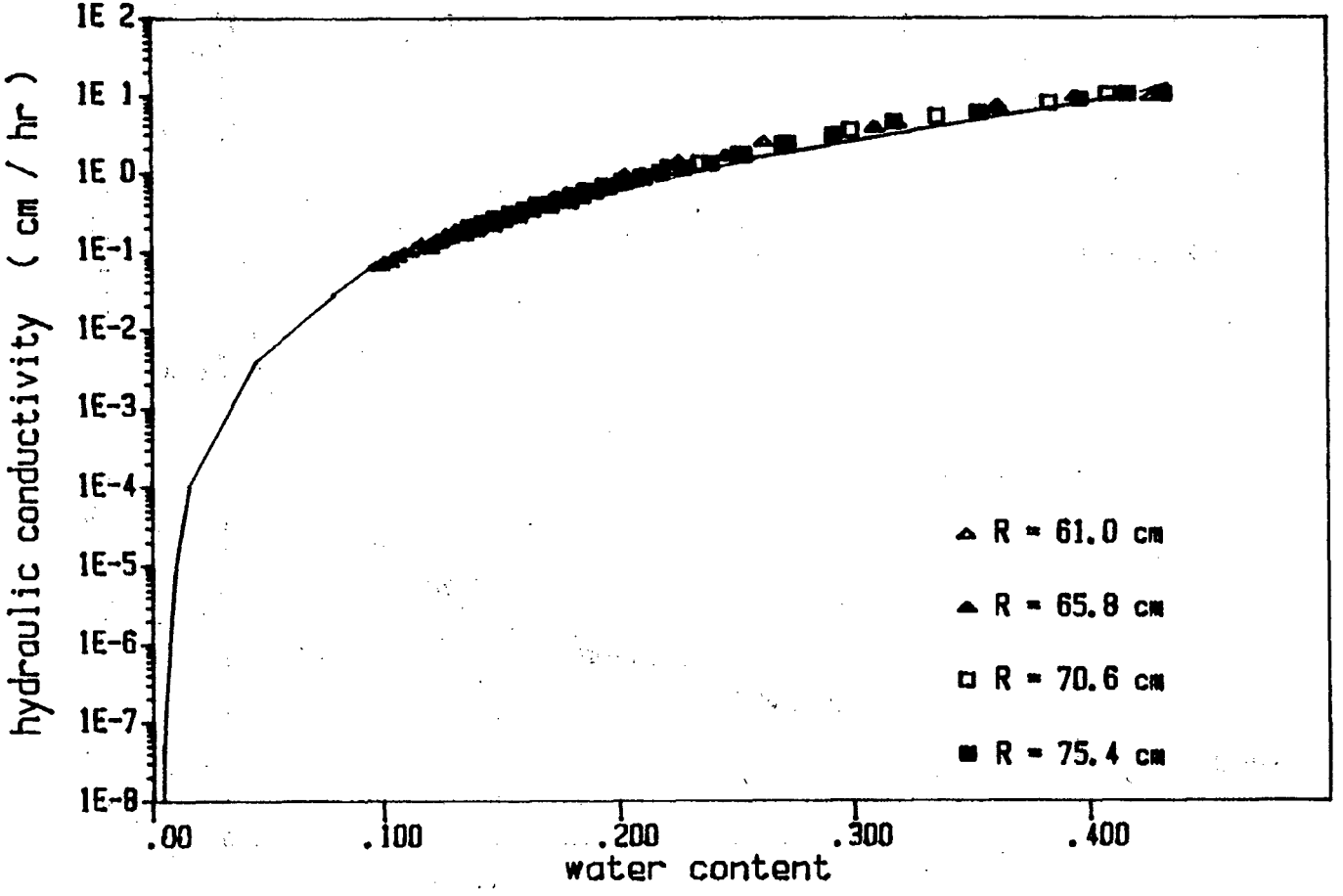

Figure 43. Simulation of Hydraulic Conductivity - Water Content Relationship for Edgar Sand at 100 rpm (R = Centrifuge radius)

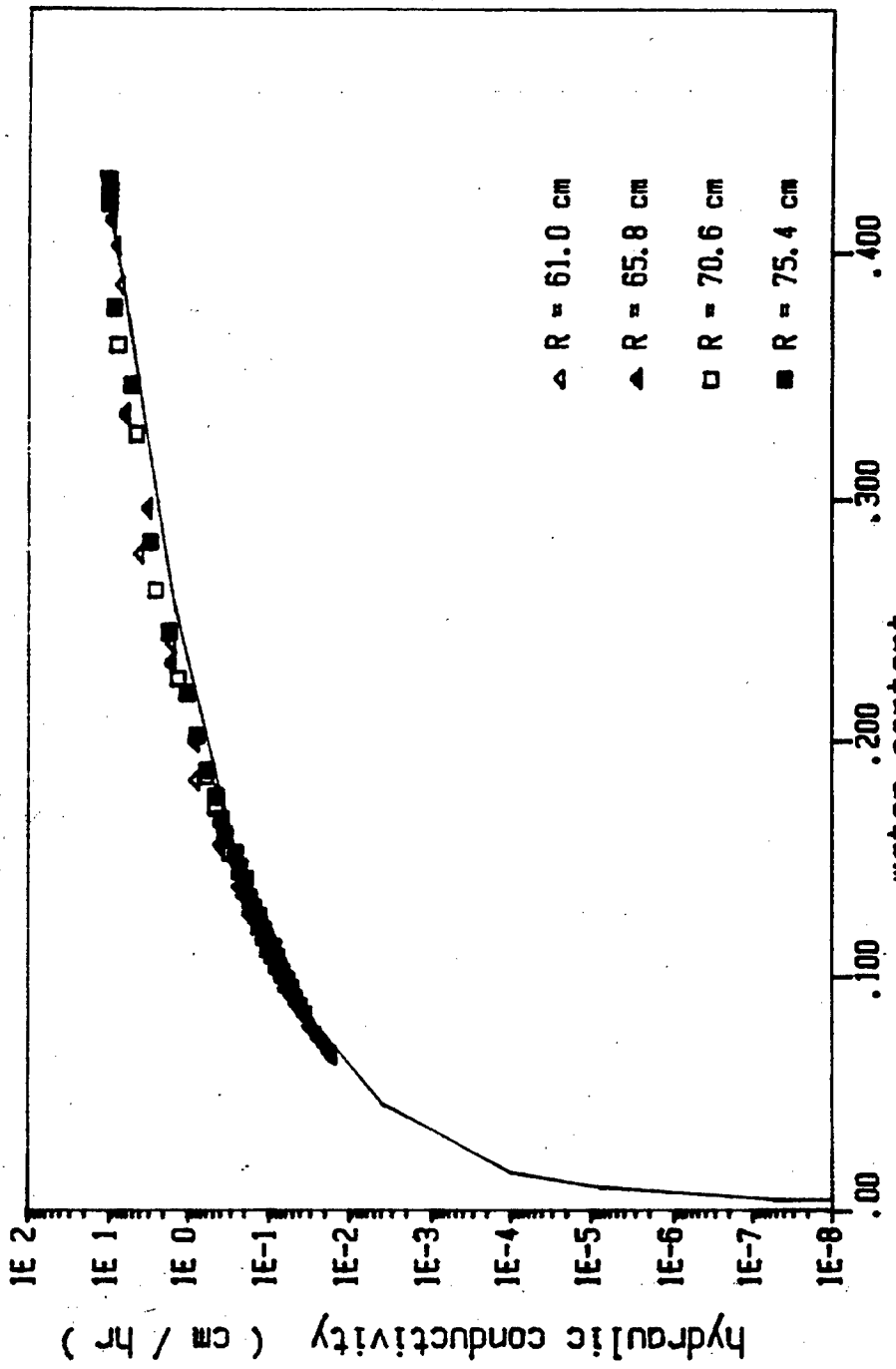

Figure 44. Simulation of Hydraulic Conductivity - Water Content Relationship for Edgar Sand at 150 rpm (R = Centrifuge radius)

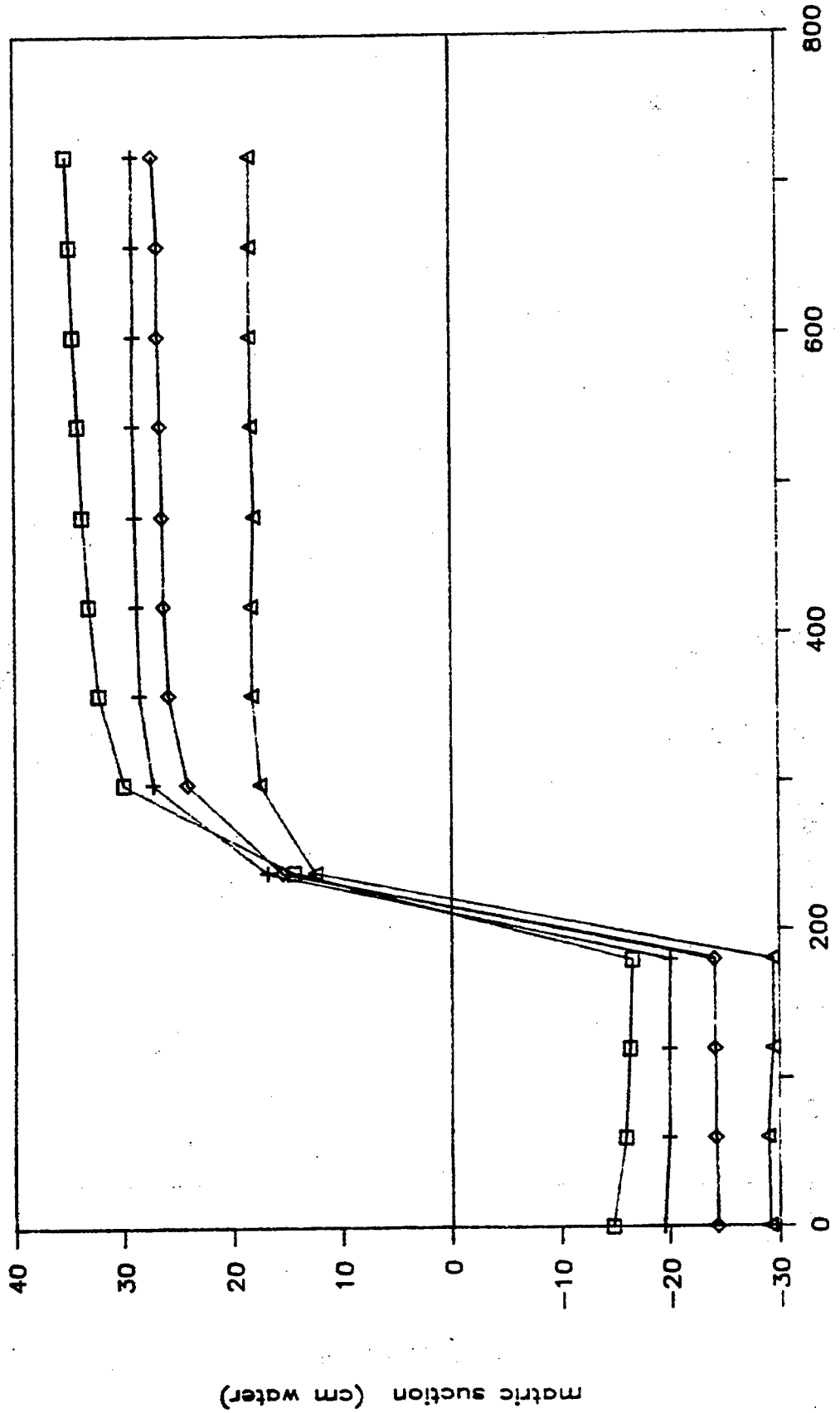

Figure 45. Matric Suction - Time Relationship for 1g Bench Tests

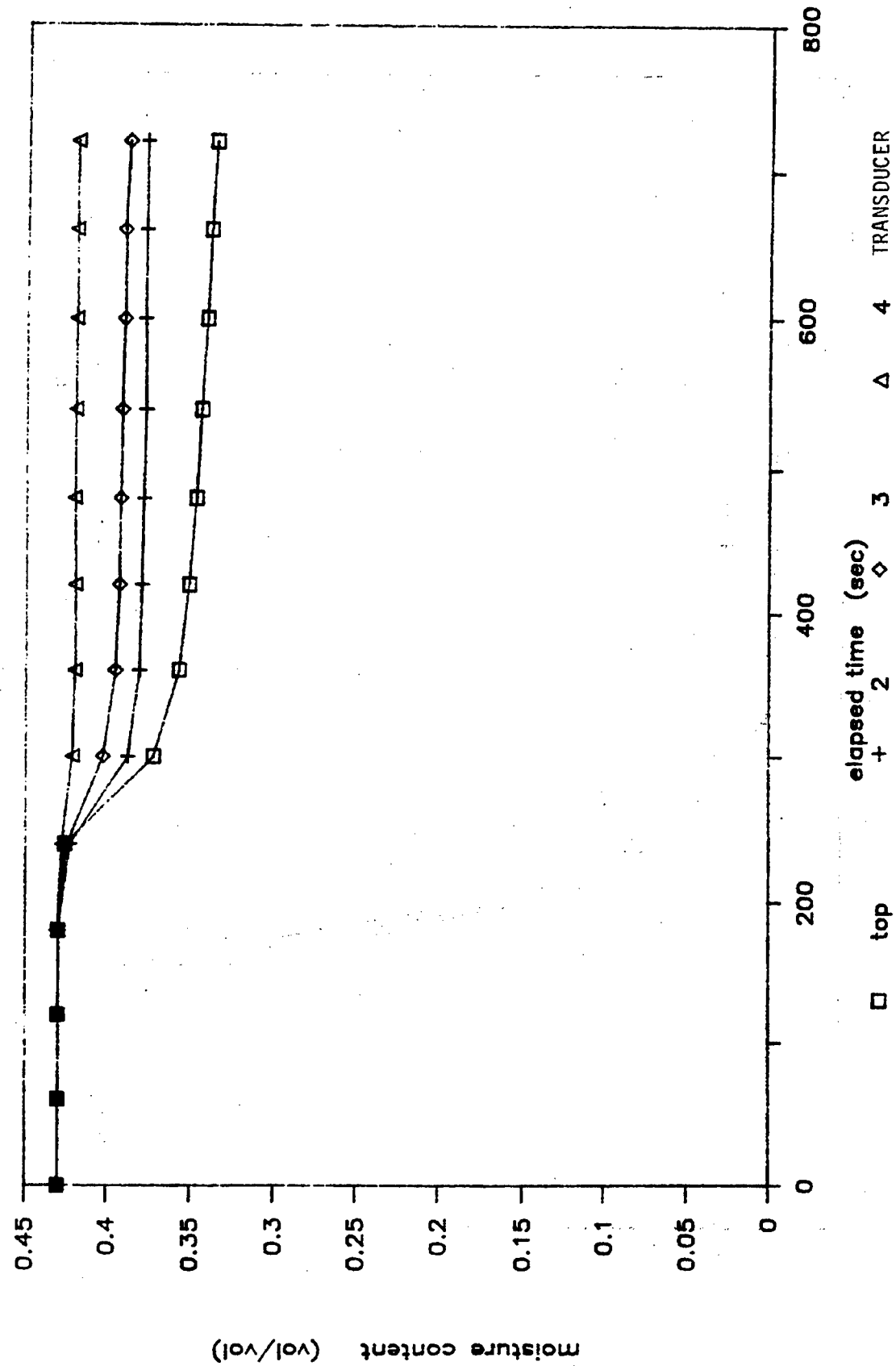

Figure 46. Moisture Content - Time Relationship for 1g Bench Tests

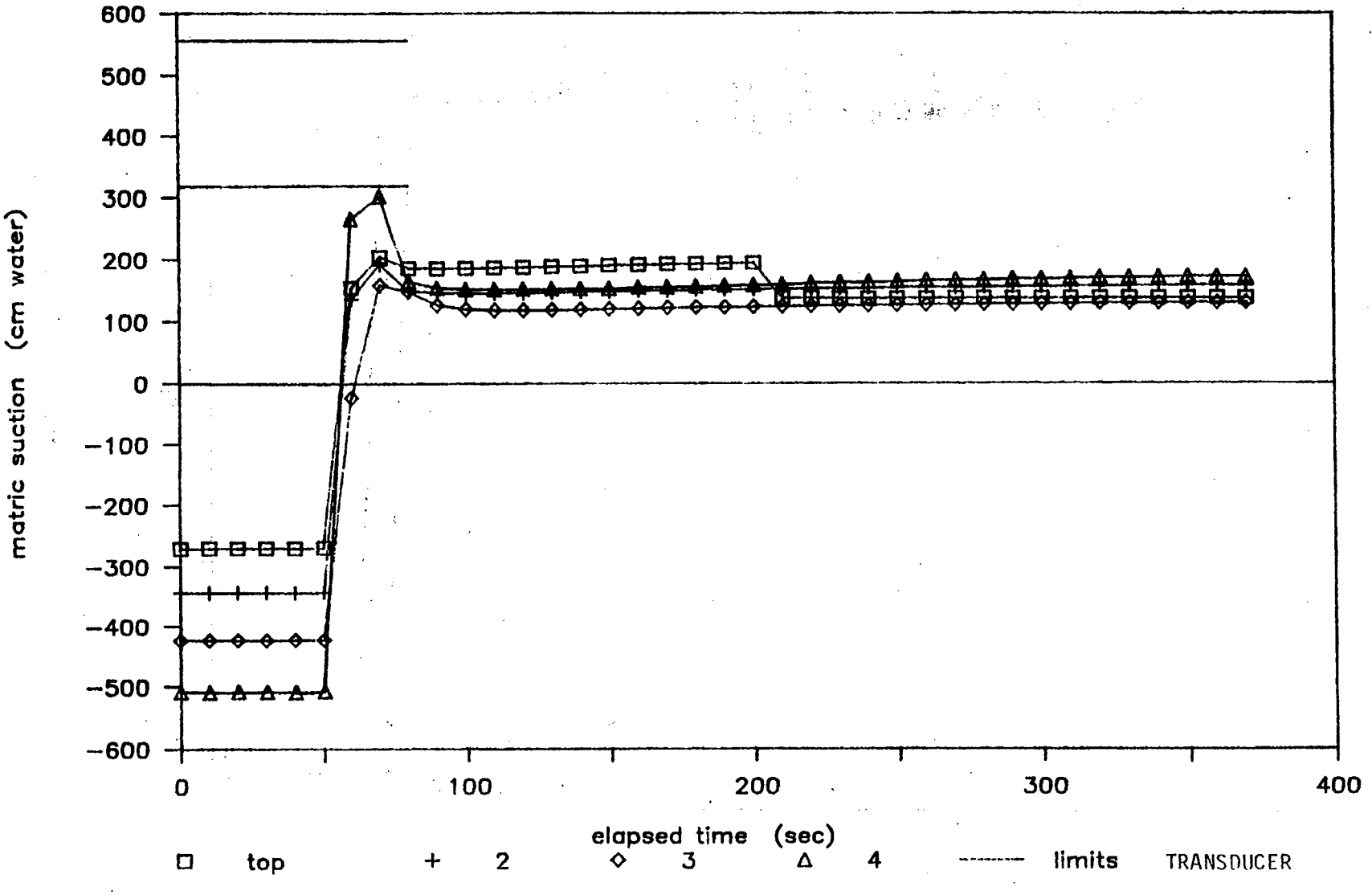

Figure 47. Matric Suction - Time Relationship for 150 rpm Centrifugal Test

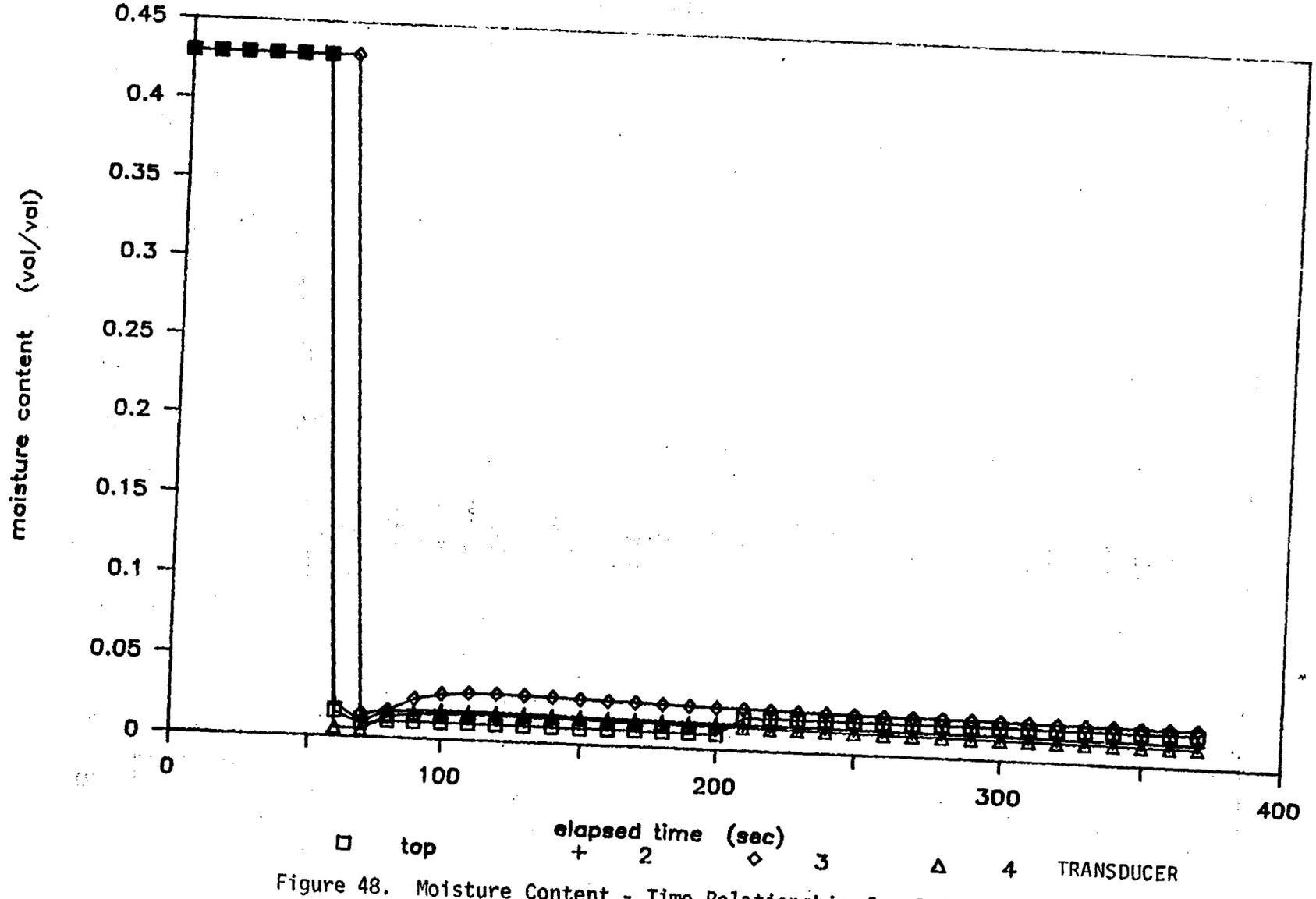

Figure 48. Moisture Content - Time Relationship for 150 rpm Centrifugal Test

for the first run at 150 rpm. Again the early points showing negative suction were read before drainage began to allow zeroing the electronics to the inital static head. The two horizontal lines in the upper left hand corner of the plot represent the theoretical equilibrium values for the top and bottom transducers at the test speed. Notice that the initial suction change is immediate but that it appears to reverse its upward trend and then come to an equilibrium value which is the same for all 4 transducers. This phenomenon is interpreted in Figure 48 as a sudden decrease in water content followed by a slight inrease to an equilibrium suggesting a constant water content throughout the column. This false interpretation is the result of the transducers fluid phase loosing contact with the matric fluid phase. All centrifuge runs at lower speeds had similar results.

An attempt was made to compact the soil around the transducers more tightly and improve matric contact with the transducers by increasing the rotational rate to 180 rpm. Testing at this speed was not possible due to limitations of the compressed air supply within the centrifuge, but it was hoped that the temporary increase in centrifugal induced effective stresses within the soil would improve later results.

Figure 49 shows suction curves at 150 rpm after first spinning at 180 rpm. These curves show a more gradual increase in matric suction as drainage progresses. They also show the rate of change for suction decreasing with time, as would be expected since conductivity decreases with increasing drainage. Drainage curves corresponding to Figure 49 are presented in Figure 50. The drainage boundary is quite sharp. At any point in time, the soil at one transducer can be saturated completely, while the soil at the transducer just above it is nearly drained.

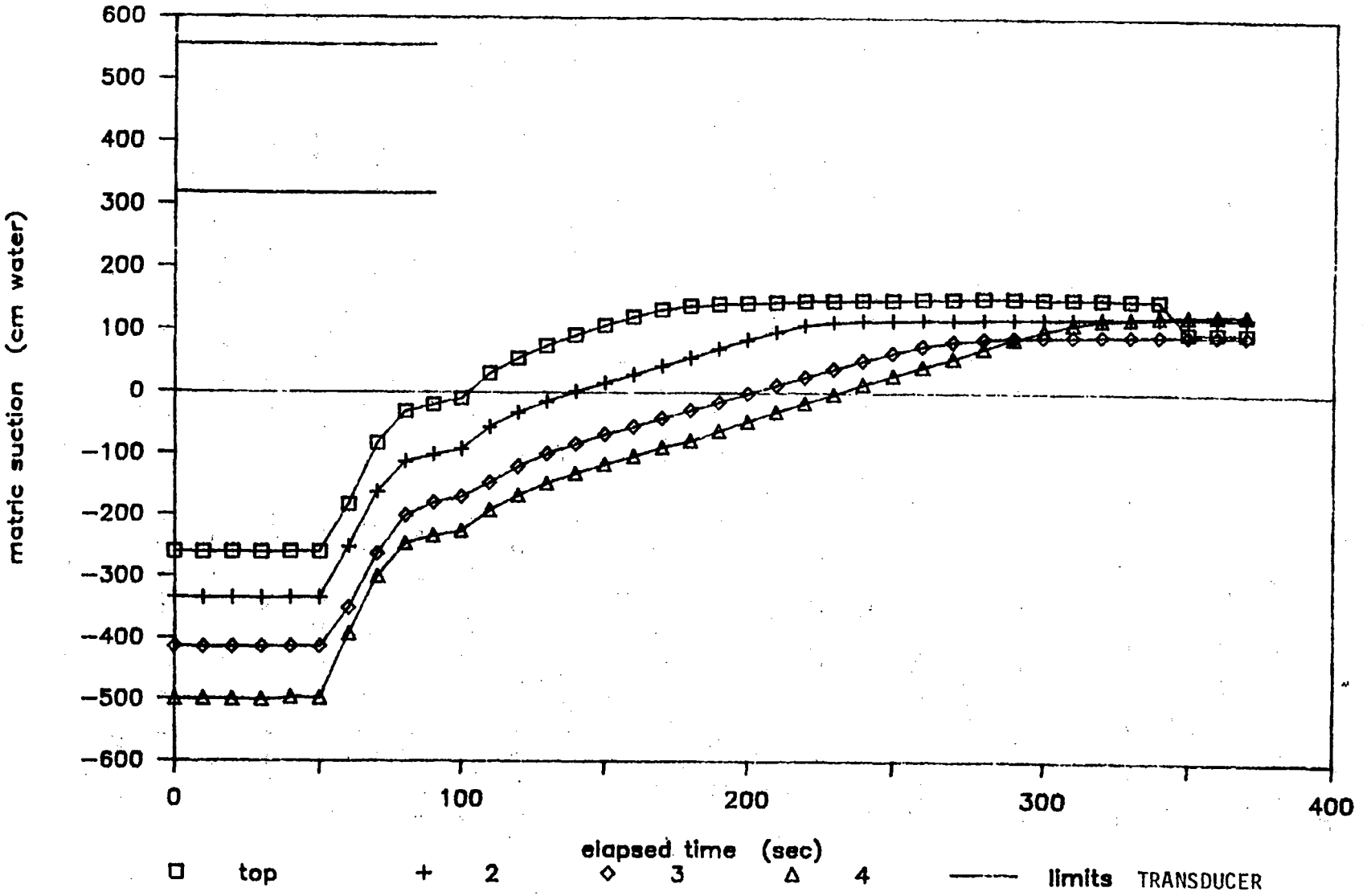

Figure 49. Matric Suction - Time Relationship for 180/150 rpm Centrifugal Test

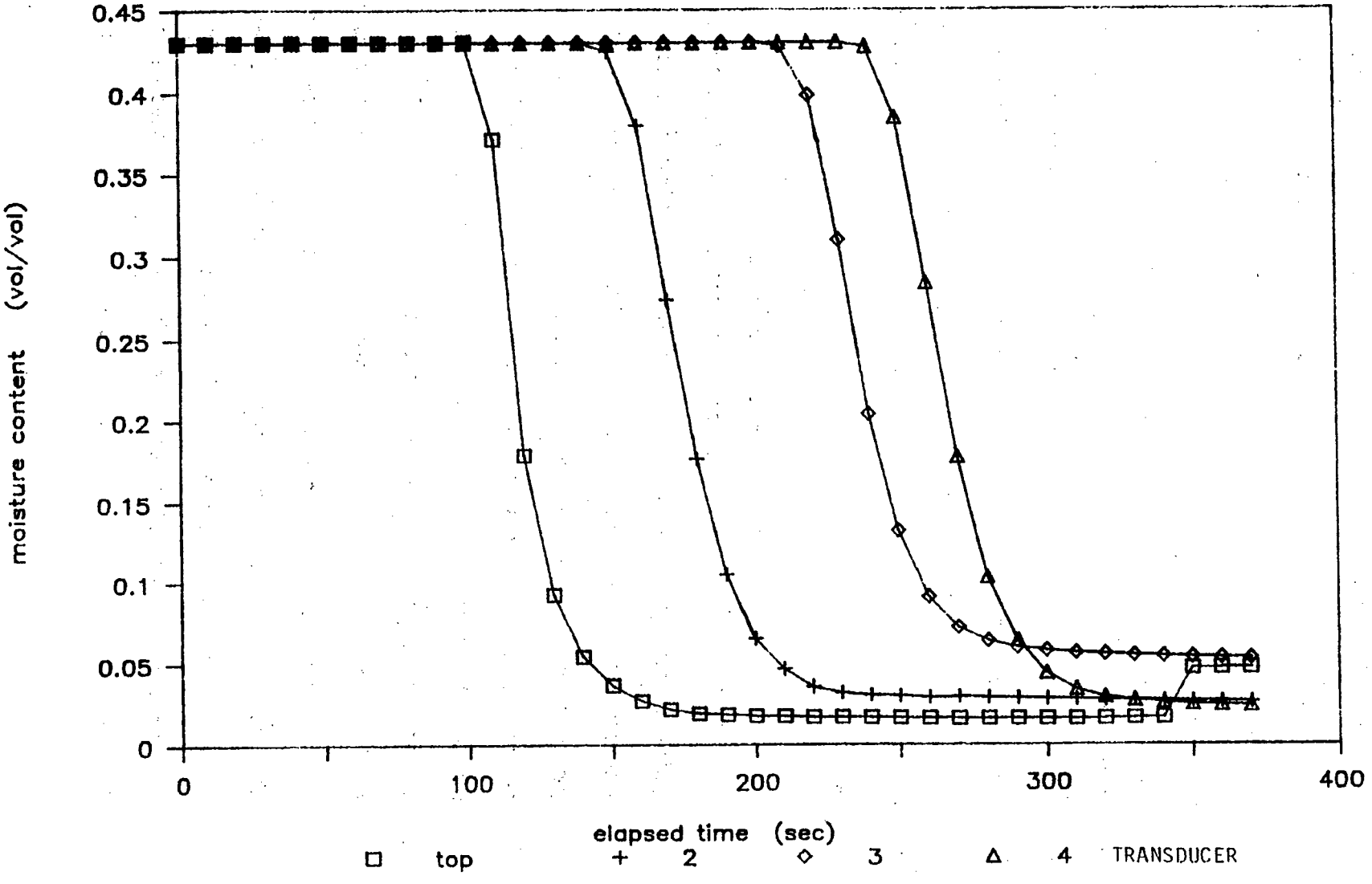

Figure 50. Moisture Content - Time Relationship for 180/150 rpm Centrifugal Test

An approximate shape of the drainage boundary can be seen in Figure 51. In this figure the moisture profile within the soil column is represented by a separate curve for drainage times of 1, 2, 3, and 4 minutes. Note that the entire column is drained completely within 4 minutes.

The resultant conductivity curve is shown as a function of water content in Figure 52 along with the curves which were simulated by the method of van Genuchten. Similar representations relating conductivity directly to suction are presented in Figure 53. For completeness, conductivity versus water content for the test is also plotted in Figure 54 to compare with the same curves predicted by the Jackson and Irmay methods.

Discussion of Results

Testing at low rpm's produced no significant results; that is, the apparent drainage curves were unreasonable. The first test at 150 rpm produced similar results. It was only after the specimen had been subjected to spinning at 180 rpm that the second run at 150 rpm produced reasonable results. This is most likely the result of insufficient compaction of the soil around the transducers initially. In order for the transducers to maintain intimate contact with the fluid phase of the sample matrix during drainage, the spacing between soil particles (void spacing) and the transducer's porous stones must be on the same order as the inter-particle spacing throughout the specimen. If voids were too large around the transducers initially, that space would drain first leaving the transducers isolated from the rest of the specimen's fluid phase. The high effective stresses resulting from the 180 rpm spin were

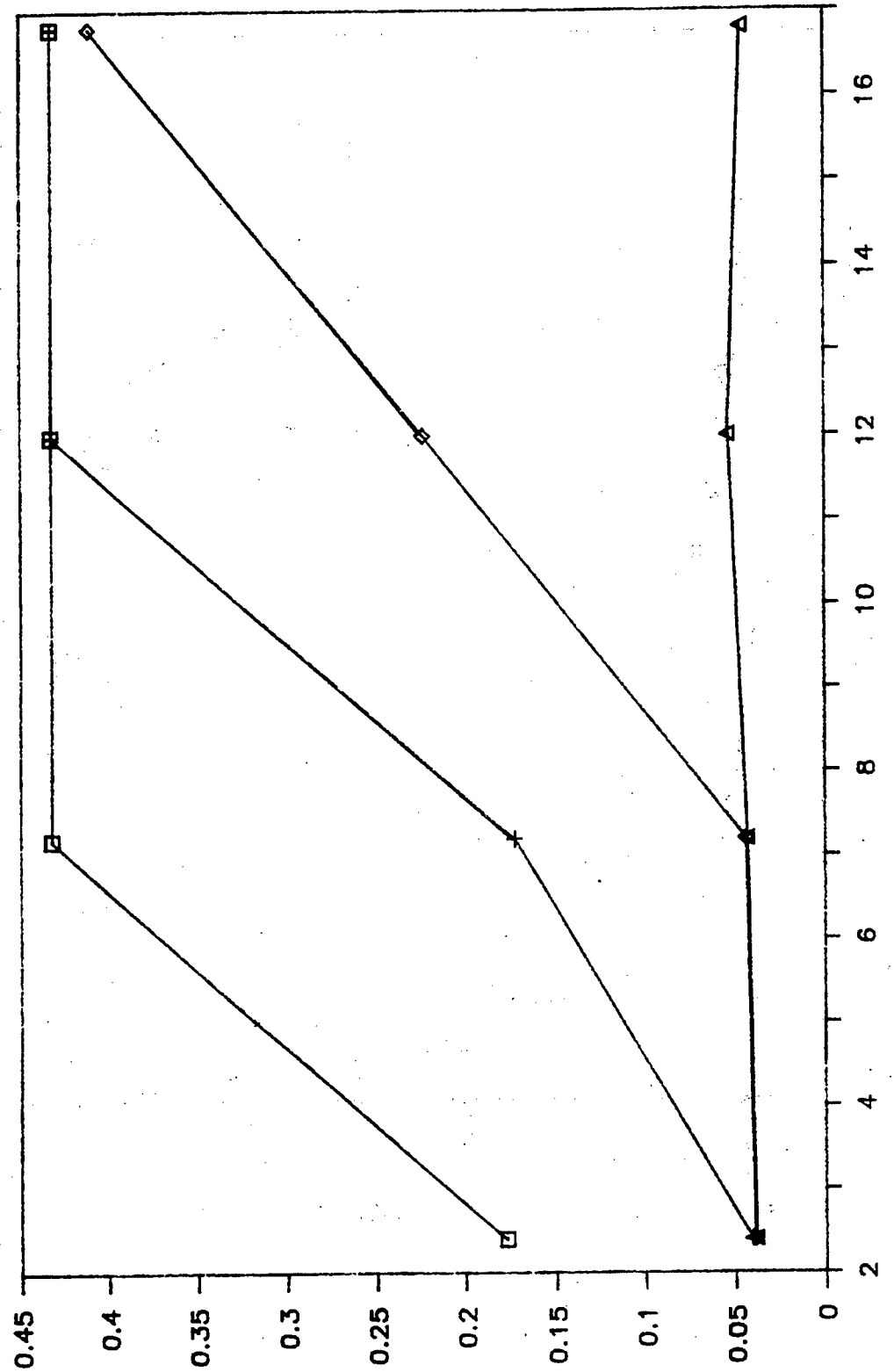

Figure 51. Water Content Profile - Time Relationship for 180/150 rpm Centrifugal Test

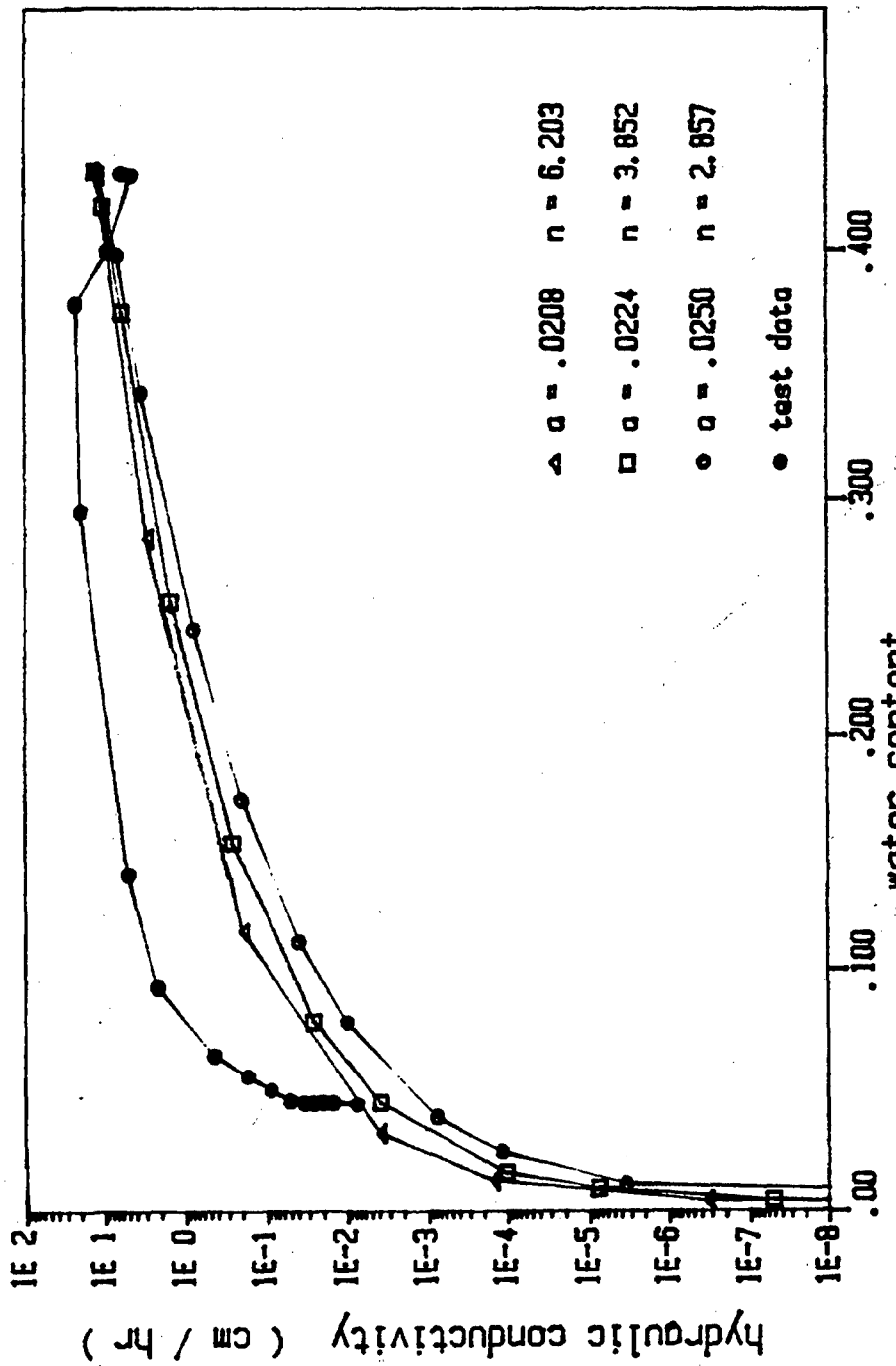

Figure 52. Comparison of Observed and Calculated Hydraulic Conductivity - Water Content Relationship from Centrifugal Test

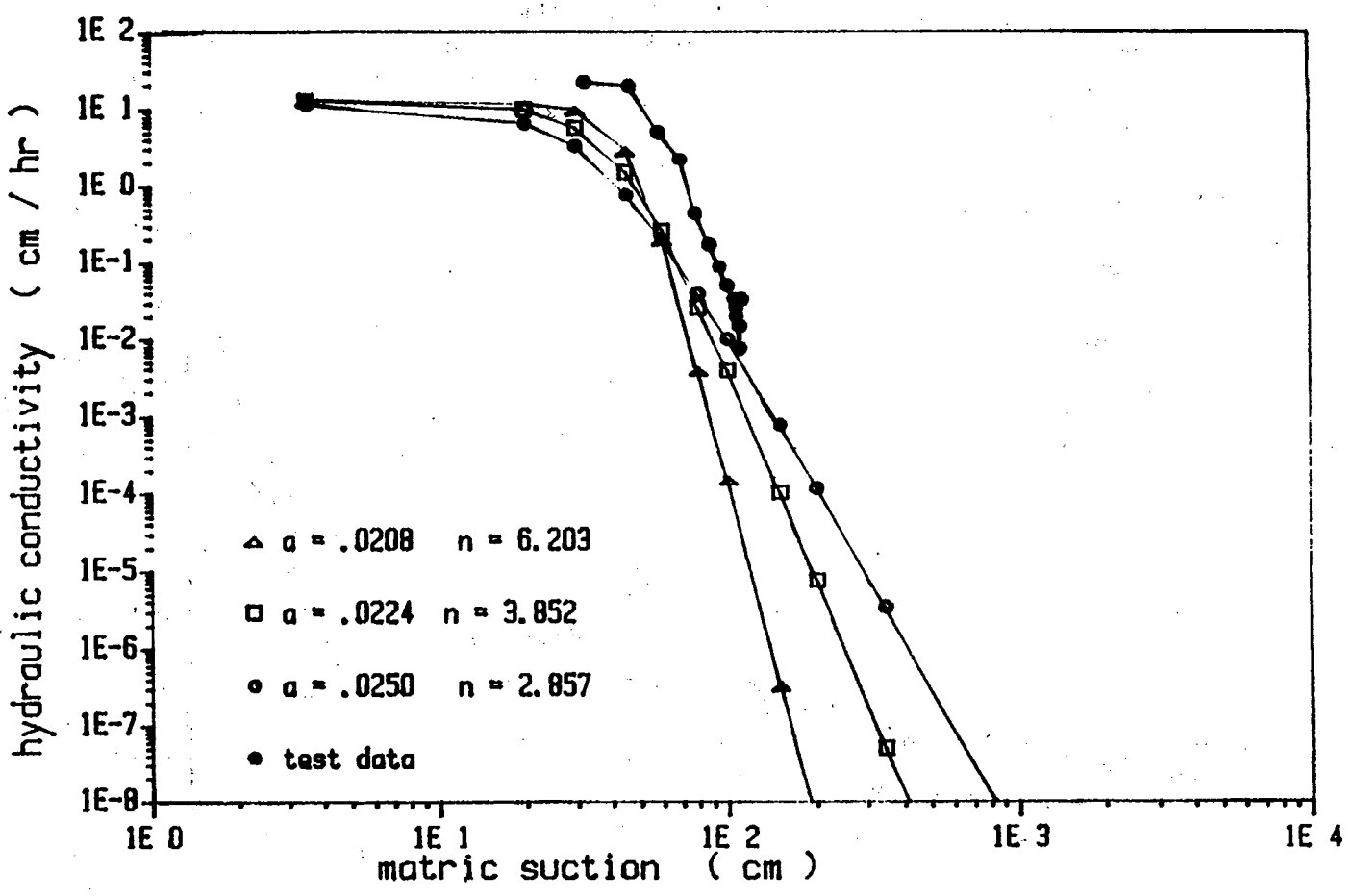

Figure 53. Comparison of Observed and Calculated Hydraulic Conductivity - Suction Relationship from Centrifugal Test

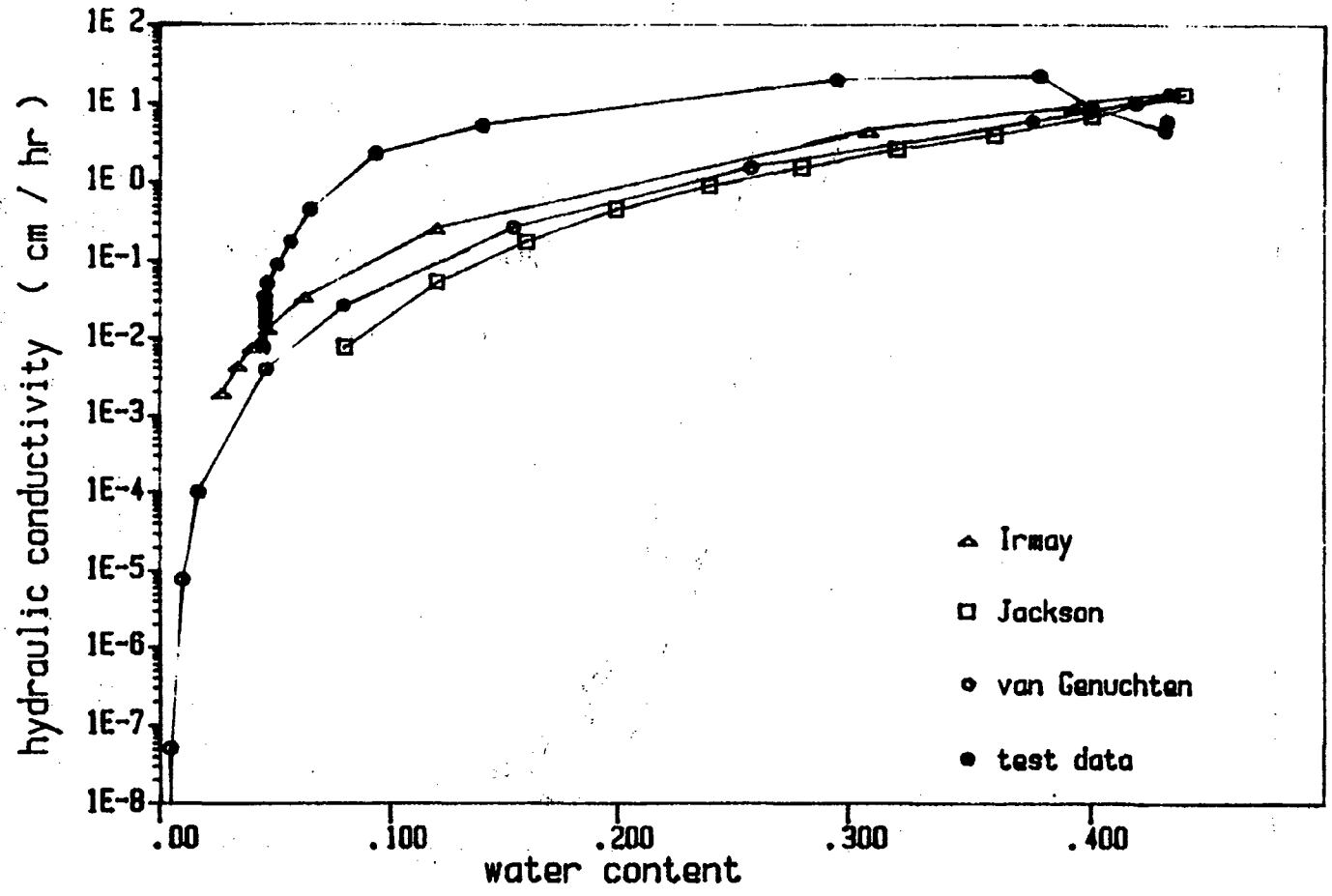

Figure 54. Comparison of Various Calculated and Observed Hydraulic Conductivity - Water Content Relationships from Centrifugal Tests

apparently sufficient to compact the soil against the transducers so that subsequent testing at 150 rpm produced reasonable results.

The moisture release function and parameters chosen for this sand (Figure 36) are representative as evidenced by the good match between the simulated curve and the experimental points. The relationship breaks down however for water contents below about 5 percent. Since water contents in the finite difference simulations never reached that point, the results of those simulations will be unaffected. However, during laboratory testing the soil very quickly reached these water contents. Therefore, during data reduction, water contents were determined by direct interpolation from the experimentally obtained moisture release curve (Figure 35).

The simplifying assumptions used in the data reduction program appear to be valid for speeds of at least 150 rpm for the transducer spacing used in this apparatus. As with any numerical linearization of a non-linear process, caution should be exercised when either distance or time steps become large. When in doubt it is recommended the accuracy of the data reduction scheme be testetd against results from a numerical simulation as was done here.

Unfortunately, the simulation results cannot be compared directly with the experimental results due to the inability of the finite difference program to model accurately the initial conditions within the centrifuge. The model requires a constant suction everywhere in the sample initially, while the actual initial conditions are hydrostatic.

With the apparatus used, the number of tests performed was limited by the fact that the flow solenoid eventually became contaminated with sand and was unable to seal properly. At that point initial conditions

could no longer be established since a steady water level above the sample could not be maintained. Unfortunately, any filter fine enough to prevent the smallest particles from reaching the solenoid might restrict drainage and reduce the quality of the experimental results. Care should therefore be used in selecting a filter. Table 14 can be used as a rough guide in filter selection.

The similuation methods used are generally quite good for a variety of soils and especially for sands. They are most accurate in the early stages of drainage, but all tend to overpredict hydraulic conductivity in the lower moisture content ranges. The experimental data plotted in Figures 52 and 54 confirm this overprediction. The measured drop in hydraulic conductivity is much more pronounced than that predicted by any of the simulation methods.

The early stages of drainage are a different matter. Here the experimental results, while farily close to the simulated values, do not match them exactly. This is where the simulated curves should be most accurate, and suggests that the hydraulic conductivities measured in the centrifuge are actually greater than they would be if measured at 1 g. This overprediction of conductivities by tests has been reported previously (Figures 53 and 54) and is apparently a function of test gradients. High test gradients such as those encountered in the centrifuge have the effect of shifting the moisture release curve to the right. This may help explain why the experimental drainage rates were so much faster than those predicted with the finite difference model.

Based on these results a new moisture release curve was constructed and its parameters were used in finite difference simulations to see if

the numerical model could duplicate the experimental results. Unfortunately, the time and distance steps required to keep mass balance errors in the simulation within acceptable limits were so small that this approach became impractical. One computer run which was attempted ran for 12 hours to simulate the first 30 seconds of flow and the resulting mass balance errors were still unacceptable. This difficulty is undoubtedly the result of the sharp drainage boundary which was observed during testing. Numerical techniques, such as finite difference, are inherently bad at modeling sudden transitions.

The results from the second 150 rpm test show that ths method is workable as a means of rapidly measuring drainage curves for granular soils. Although the high gradients tend to shift the apparent moisture release characteristics, the predictions resulting from centrifuge testing are conservative. That is, if values obtained from testing are used to predict hazardous waste migration, they will tend to overpredict the flow. If more accuracy is desired the centrifuge would be the ideal device to study the effects of varying gradients on unsaturated media flow. With some improvements in the apparatus design, drainage curves for the entire moisture range of a soil similar to the one tested can be measured in five minutes. Since the testing time is short, multiple runs can be made on the same sample for verification purposes. The short test duration is most useful in areas such as contaminant transport through soils. Since the soil can be drained almost completely in such a short time, different solution combinations can be tested simply by draining the sample and changing the fluid in the reservoir.

The only major drawback with the methodology as it stands is the lack of an independent means of determining moisture content. Even with this limitation, the test results still agree with the theoretical curves to within an order of magnitude or so and given all of the other problems encountered with these first trials, that is not bad. The present method is most useful for pollutant migration studies where unsaturated theory is at its weakest. "Moisture release" curves for various solvent/solute combinations can either be measured directly by conventional means or be back-calculated from the moisture release curve of pure water. The test can then be run with the contaminant solution and the results compared with similar test results for pure water to obtain relative hydraulic conductivities. In any event, the results presented here indicate that the proposed method is worth considering as an extremely rapid method for obtaining the unsaturated conductivities of granular soils.

CHAPTER VII
CONCLUSIONS

The technical feasibility of utilizing a large-scale centrifuge for estimating the hydraulic conductivity of fluids in a wide variety of soil types was demonstrated. Conclusions regarding centrifugal techniques and the migration behavior of decane are summarized below.

1. Equations were derived and verified to describe the influence of nonuniform acceleration levels on fluid motion within a centrifuge. Their application removes the restriction of thin samples in centrifugal modeling and testing procedures. The equations allow accurate determination of the total or individual components of the hydraulic potential at any location in the sample, thereby facilitating the verification of scaling factors applied in physical models.

2. A centrifugal technique was developed for performing saturated hydraulic conductivity testing. A flexible wall permeameter was designed and tested which allowed determination of saturated hydraulic conductivity estimates for a wide range of soil types on the laboratory bench and also in the centrifuge. The equations of fluid motion in conduits and porous media within a centrifuge were derived and incorporated into a variable head permeability equation. Excellent agreement was demonstrated between estimates of intrinsic permeabilities obtained on the bench and in the centrifuge. Acceleration levels ranged from 14 to 25 g's.

3. The centrifugal technique for determining saturated hydraulic conductivity does not offer any savings in time over similar bench tests. Although the gravitational component of the total hydraulic potential was significantly increased during the tests, an identical increase in the total hydraulic energy was obtained on the bench by increasing the pressure component by means of air pressure regulators. Fluctuations of the permeant reservoir surface were observed during the centrifuge testing, apparently due to a minor imbalance of the rotor arms. As a result, the accuracy of the centrifuge technique was probably less than the bench testing.

4. One advantage of centrifugal techniques over bench methods is the ability to accurately reproduce the effective stress profile when physically modeling a prototype field sample. For example, when testing the permeability of a six-foot thick clay liner for use under a landfill, a scaled-down model in the centrifuge will experience the actual increase in effective stress with depth, whereas a bench model will experience an almost uniform effective stress distribution. Accordingly, the test method having greater effective stresses in turn can cause densification resulting in lower rates of leaching and can influence design decisions. However, the confining pressures used in the bench tests and acceleration levels of the centrifugal models were in sufficient concert that agreement was obtained between the two methods.

5. Caution should be exercised when extrapolating advection rates determined in a centrifugal model to field conditions. A nonlinear response of fluid flux to increasing hydraulic gradient, indicating a deviation from Darcy's law, was observed in the sand samples at a soil Reynolds number greater than 0.2 or gradient > 10.

6. A thorough analysis of the total hydraulic energy should be conducted as part of centrifugal modeling and testing programs dealing with fluid movement.

7. Estimates of saturated hydraulic conductivity for nonaqueous permeants cannot be extrapolated from values determined using water as the permeant, based on differences in kinematic viscosity. Saturated hydraulic conductivity tests using decane and water in a fine sand, a sand/clay mix and 100 percent kaolinite produced significant discrepancies in estimates of the intrinsic permeability as well as dissimilar permeant behavior. While a clear deviation from Darcy's law was observed for distilled water in the fine sand, fairly constant values of k were obtained using decane up to a gradient of 77. In the sand/clay mix, fairly uniform estimates of k were obtained using distilled water, while evidence of structural changes, possibly resulting in hydraulic channeling, was reflected in larger estimates of k with decane. Decane did not permeate the water saturated kaolinite sample under a hydraulic gradient of 277. However, an increase in the gradient to 750-800 was sufficient to drive decane into the sample pores in half of the tests. While estimates of k were subsequently determined, extrapolation to lower gradients is not warranted because of the high interfacial energy which needed to be overcome before flow commenced.

8. Site specific soil samples subjected to appropriate hydraulic conditions must be utilized in order to correctly evaluate the migration characteristics of hazardous wastes. Decane exhibited a variety of flow behavior in the wide range of soil types and under the wide range of hydraulic gradients utilized in this study.

9. No advantage can be realized by employing a centrifuge to physically model the percolation of leachate through an unsaturated soil profile where soil suction is high. Soil moisture suction gradients dominate water movement in the unsaturated soil, and are often 10 to 1000 times greater than the gradient due to gravity.

10. A centrifugal technique was developed for determining the relationship of the unsaturated hydraulic conductivity to the moisture content of a soil sample. An apparatus was designed to monitor the decrease in soil moisture suction with time as a saturated sample drains under the influence of increased acceleration levels. Computer simulation results indicated that significant reductions in testing time and a greater range of soil moisture content can be achieved by conducting the test in a centrifuge.

CHAPTER VIII
RECOMMENDATIONS

Several recommendations for further research in related areas arose during the course of this investigation.

1. The migration of hazardous wastes away from source areas will depend on the soil moisture characteristics of the unsaturated soil matrix; as such, techniques for determining the moisture retention and unsaturated hydraulic conductivity of soils using water and appropriate nonaqueous permeants should be incorporated into testing programs along with saturated tests. The centrifugal technique developed for determining unsaturated hydraulic conductivity can be utilized for a variety of soils. In addition, the centrifugal technique for determining soil moisture retention curves offers potential advantages over conventional bench methods.

2. Centrifugal models appear to have an advantage over bench models in that prototype effective stresses can be accurately reproduced due to the increasing acceleration levels with sample depth. Further research is needed to assess the importance of this phenomenon to permeability measurements.

3. Centrifugal techniques may be developed for other conventional laboratory procedures which could result in savings in time and/or costs. The major criterion is that the phenomena of interest are dominated by gravitational forces.

REFERENCES

Acar, Y. B., A. Hamidon, S. E. Field, and L. Scott, The effect of organic fluids on hydraulic conductivity of compacted kaolinite, in Hydraulic Barriers in Soil and Rock, pp. 171-187, Special Technical Publication 874, edited by A. I. Johnson et al., American Society for Testing and Materials, Philadelphia, Penn., 1985.

Adamson, A. W., Physical Chemistry of Surfaces, 4th ed., John Wiley and Sons, New York, 1982.

Ahuja, L. R., R. E. Green, S.-K. Chong, and D. R. Nielsen, A simplified functions approach for determining soil hydraulic conductivities and water characteristics in situ, Water Resources Research, 16, 947-953, 1980.

Alemi, M. H., D. R. Nielsen, and J. W. Biggar, Determining the hydraulic conductivity of soil cores by centrifugation, Soil Science Society of America Journal, 40, 212-219, 1976.

American Society for Testing and Materials, Standard test method for permeability of granular soils (constant head), in Annual Book of ASTM Standards, Part 19, pp. 368-374, American Society for Testing and Materials, Philadelphia, Penn., 1974.

American Society for Testing and Materials, Standard test method for centrifuge moisture equivalent of soils, in Annual Book of ASTM Standards, Part 19, pp. 130-133, American Society for Testing and Materials, Philadelphia, Penn., 1981.

Anderson-Nichols, Remedial Action Modeling, Volumes 1-4, Anderson-Nichols and Co., Palo Alto, Calif., 1984.

Arulanandan, K., P. Y. Thompson, N. J. Meegoda, B. L. Kutter, and R. B. Krone, Centrifuge modeling of advection and dispersion processes during pollutant travel in soil, University of California, Davis, unpublished, 1984.

Ashworth, R., written correspondence, Tyndall Air Force Base, Fla., 1985.

Bear, J., Dynamics of Porous Media, American Elsevier, New York, 1972.

Bear, J., Hydraulics of Groundwater, McGraw-Hill, Inc., New York, 1979.

Bloomquist, D. G., and F. C. Townsend, Centrifugal modeling of phosphatic clay consolidation, in Sedimentation/Consolidation Models; Predictions and Validation, pp. 565-580, edited by R. N. Yong and F. C. Townsend, American Society of Civil Engineers, New York, 1984.

Boersma, L., Field measurements of hydraulic conductivity above a water table, in Methods of Soil Analysis, part 1, pp. 234-252, edited by C. A. Black et al., American Society of Agronomy, Madison, Wisc., 1965a.

Boersma, L., Field measurements of hydraulic conductivity below a water table, in Methods of Soil Analysis, part 1, pp. 222-233, edited by C. A. Black et al., American Society of Agronomy, Madison, Wisc., 1965b.

Borden, R. C., M. D. Lee, J. T. Wilson, C. H. Ward, and P. B. Bedient, Modeling the migration and biodegradation of hydrocarbons derived from a wood-creosoting process water, in Petroleum Hydrocarbons and Organic Chemicals in Groundwater--Prevention, Detection and Restoration - A Conference and Exposition, pp. 130-143, National Water Well Association, Worthington, Ohio, 1984.

Bouma J., R. F. Paetzold, and R. B. Grossman, Measuring Hydraulic Conductivity for Use in Soil Survey, Soil Survey Investigations, Report No. 38., U. S. Dept. of Agriculture, Washington, D. C., 1982.

Boynton, S. S., and D. E. Daniel, Hydraulic conductivity tests on compacted clay, Journal of Geotechnical Engineering Division, American Society of Civil Engineers, 3, 465-478, 1985.

Briggs, L. J., and J. W. McLane, The moisture equivalents of soils, Bulletin 45, Bureau of Soils, U. S. Dept. of Agriculture, Washington, D. C., 1907.

Brooks, R. H., and A. T. Corey, Hydraulic properties of porous media, Hydrology Paper 3, Colorado State University, Fort Collins, Colo., 1964.

Brown, K. W., J. C. Thomas, and J. W. Green, Permeability of compacted soils to solvents mixtures and petroleum products, in Land Disposal of Hazardous Wastes, pp. 124-137, U. S. Environmental Protection Agency, EPA-600/9-84-007, Cincinnati, Ohio, 1984.

Cargill, K. W., Mathematical model of the consolidation / desiccation processes in dredged material, U. S. Army Engineer Waterways Experiment Station, Technical Report D-85-4, Vicksburg, Miss., 1985.

Cargill, K. W., and H. Y. Ko, Centrifugal modeling of transient water flow, Journal of Geotechnical Engineering, American Society of Civil Engineers, 109, 536-555, 1983.

Chemical Rubber Company, Handbook of Chemistry and Physics, 58th ed., Chemical Rubber Company Press, Inc., Cleveland, Ohio, 1978.

Childs, E., Collis-George, N., The permeability of porous materials, Proc. Roy. Soc. (London) A, 201, 392-405, 1950.

Chong, S., R. E. Green, and L. R. Ahuja, Simple in-situ determination of hydraulic conductivity by power function descriptions of drainage, Water Resources Research, 17, 1109-1114, 1981.

Christiansen, J. F., written discussion of Fixed-wall versus flexible-wall permeameters, in Hydraulic Barriers in Soil and Rock, pp. 124-126, Special Technical Publication 874, edited by A. I. Johnson et al., American Society for Testing and Materials, Philadelphia, Penn., 1985.

Corey, A. T., Mechanics of Heterogenous Fluids in Porous Media, Water Resources Publications, Fort Collins, Colo., 1977.

Croce, P., Evaluation of Consolidation Theory by Centrifugal Model Tests, M. S. thesis, University of Colorado, Boulder, 1982.

Croce, P., V. Pane, D. Znidarcic, H. Ko, H. W. Olsen, and R. L. Schiffman, Evaluation of consolidation theory by centrifuge modeling, in Proceedings on Applications of Centrifuge Modeling to Geotechnical Design, University of Manchester, United Kingdom, 1984.

Dane, J. H., Comparison of field and laboratory determined hydraulic conductivity values, Soil Science Society of America Journal, 44, 228-231, 1980.

Dane, J. H., D. K. Cassel, J. M. Davidson, W. L. Pollaus, and V. L. Quisenberry, Physical characteristics of soils of the southern region - Troup and Lakeland series, Southern Cooperative Series Bulletin 262, Auburn University, Auburn, Ala., 1983.

Dane, J. H., and S. Hruska, In-situ determination of soil hydraulic properties during draining, Soil Science Society of America Journal, 47, 619-624, 1983.

Daniel, D. E., D. C. Anderson, and S. S. Boynton, Fixed-wall versus flexible-wall permeameters, in Hydraulic Barriers in Soil and Rock, Special Technical Publication 874, pp. 107-123, edited by A. I. Johnson et al., American Society for Testing and Materials, Philadelphia, Penn., 1985.

Darcy, H., 1856, Determination of the laws of the flow of water through sand, in Physical Hydrogeology, edited by R. A. Freeze and W. Back, Hutchinson Ross Publishing, Stroudsburg, Penn., 1972.

Davidson, J. M., P. S. C. Rao, and P. Nkedi-Kizza, Physical processes influencing water and solute transport in soils, Florida Agricultural Experiment Station, J Series, No. 4322, Gainesville, Fla., 1983.

Day, S. R., and D. E. Daniel, Hydraulic conductivity of two prototype clay liners, Journal of Geotechnical Engineering Division, American Society of Civil Engineers, 3, 957-970, 1985.

Dunn, R. J., Hydraulic Conductivity of Soils in Relation to the Subsurface Movement of Hazardous Wastes, Ph.D. dissertation, University of California, Berkeley, 1983.

Edil, T. B., and A. E. Erickson, Procedure and equipment factors affecting permeability testing of a bentonite-sand liner material, in Hydraulic Barriers in Soil and Rock, Special Technical Publication 874, pp. 155-170, edited by A. I. Johnson et al., American Society for Testing and Materials, Philadelphia, Penn., 1985.

Fox, R. W., and A. T. McDonald, Introduction to Fluid Mechanics, 2nd. ed., John Wiley and Sons, New York, 1978.

Giles, R. V., Fluid Mechanics and Hydraulics, 2nd. ed., McGraw-Hill, New York, 1962.

Gordon, B. B., and M. Forrest, Permeability of soils using contaminated permeant, in Permeability and Groundwater Contaminant Transport, Special Technical Publication 746, pp. 101-120, edited by T. F. Zimmie and C. O. Riggs, American Society for Testing and Materials, Philadelphia, Penn., 1981.

Green, R. E., L. R. Ahuja, and S. K. Chong, Unsaturated hydraulic conductivity, soil water diffusivity and sorptivity: Field methods, American Society of Agronomy, Madison, Wisc., in press, 1983.

Hamilton, J., Olsen, R., Daniel, D., Measurement of the hydraulic conductivity of partially saturated soils, Permeabilty and Groundwater Contaminant Transport, pp. 182-196, Special Technical Publication 746, American Society for Testing and Materials, 1981.

Heaney, J. P., Five year research and development plan, hazardous waste transport, draft final report to U. S. Air Force, Water Resources Research Center, University of Florida, Gainesville, 1984.

Hillel, D., Introduction to Soil Physics, Academic Press, New York, 1982.

Jackson, R., On the calculation of hydraulic conductivity, Soil Science Society American Proceedings, 36, 380-382, 1972.

Johnson, A. I., R. C. Prill, and D. A. Monis, Specific yield-column drainage and centrifuge moisture content, Water Supply Paper 1662-A, U. S. Geological Survey, Washington, D. C., 1963.

Johnson, W., Study predicts permeability of clay liners, in Hazardous Materials and Waste Management, Lehigh University, Bethlehem, Penn., 1984.

Jones, A. J., and R. J. Wagenet, In situ estimation of hydraulic conductivity using simplified methods, Water Resources Research, 20, 1620-1626, 1984.

Kirkham, D., and W. L. Powers, Advanced Soil Physics, Wiley-Interscience, New York, 1972.

Klute, A., The determination of the hydraulic conductivity and diffusivity of unsaturated soils, Soil Science, vol. 113, no. 4, 264-276, 1972.

Klute, A., Laboratory measurements of hydraulic conductivity of unsaturated soil, in Methods of Soil Analysis, part 1, pp. 253-261, edited by C. A. Black et al., American Society of Agronomy, Madison, Wisc., 1965a.

Klute, A., Water diffusivity, in Methods of Soil Analysis, part 1, pp. 262-272, edited by C. A. Black et al., American Society of Agronomy, Madison, Wisc., 1965b.

Libardi, P. L., K. Reichardt, D. R. Nielson, and J. W. Biggar, Simple field methods for estimating soil hydraulic conductivity, Soil Science Society of America Journal, 44, 3-7, 1980.

Mikasa, M., and N. Takada, Selfweight consolidation of very soft clay by centrifuge, in Sedimentation/Consolidation Models; Predictions and Validation, pp. 121-140, edited by R. N. Yong and F. C. Townsend, American Society of Civil Engineers, New York, 1984.

Mitchell, J. K., Fundamentals of Soil Behavior, John Wiley and Sons, New York, 1976.

Mualem, Y., A new model for predicting the hydraulic conductivity of unsaturated porous media, Water Resources Research, vol. 12, no. 3, 513-522, 1976.

Olsen, H. W., Darcy's law in saturated kaolinite, Water Resources Research, 2, 287-295, 1966.

Olson, R. E., and D. E. Daniel, Measurement of the hydraulic conductivity of fine-grained soils, in Permeability and Groundwater Contaminant Transport, Special Technical Publication 746, pp. 18-64, edited by T. F. Zimmie and C. O. Riggs, American Society for Testing and Materials, Philadelphia, Penn., 1981.

Rao, P. S. C., and R. E. Jessup, Sorption and movement of pesticides and other toxic organic substances in soils, in Chemical Mobility and Reactivity in Soils, American Society of Agronomy, Madison, Wisc., 1983.

Reichmuth, D. R., Subsurface gasoline migration perpendicular to ground water gradients: a case study, in Petroleum Hydrocarbons and Organic Chemicals in Groundwater--Prevention, Detection and Restoration - A Conference and Exposition, pp. 43-52, National Water Well Association, Worthington, Ohio, 1984.

Schwille, F., Migration of organic fluids immiscible with water in the unsaturated zone, in Pollutants in Porous Media, edited by B. Yaron et al., Springer-Verlag, New York, 1984.

Soilmoisture Equipment Corp., Product Bulletin - A16, Santa Barbara, Calif., 1978.

Strauss, H. J., and M. Kaufman, Handbook for Chemical Technicians, McGraw-Hill Book Company, New York, 1976.

University of California, American Literature on Geotechnical Centrifuge Modeling, in Proceedings of the Symposium on Recent Advances in Geotechnical Centrifuge Modeling, University of California, Davis, 1984.

Uppot, J. O., A Study of the Permeability of Clays Subjected to Organic and Inorganic Permeants, Ph.D. dissertation, University of Missouri-Rolla, 1984.

U. S. Army Engineer Waterways Experiment Station, Laboratory Soils Testing, Engineering Manual 1110-2-1906, Vicksburg, Miss., 1970.

U. S. Geological Survey, Soil water, in National Handbook of Recommended Methods for Water-Data Acquisition, Reston, Va., 1982.

van Genuchten, M., A closed-form equation for predicting the hydraulic conductivity of unsaturated soils, Soil Science Society of America Journal, 44, 892-898, 1980.

Znidarcic, D., Laboratory Determination of Consolidation Properties of Cohesive Soils, Ph.D. dissertation, University of Colorado, Boulder, 1982.

(The reverse of this page is blank)

APPENDIX
DERIVATION OF VARIABLE HEAD PERMEABILITY EQUATIONS

Bench Tests

Energy equation: $H_1 = H_0 - H_f$ (A-1)

Bernoulli equation: $(P/pg + z + V^2/2g)_1 = (P/pg + z + V^2/2g)_2$ (A-2)

Continuity equation: $dV/dt = qA$ (A-3)

Darcy's Law: $q = -K\, dH/dz$ (A-4)

$$H_1 = P_1/pg + z_1 + V_1^2/2g - H_{f1} \quad \text{(A-5)}$$

Rewriting the Bernoulli equation between the influent reservoir (subscript M) and the top of the soil sample

$$P_1 = P_M + pg(z_M - z_1) + (pV_M^2 - pV_1^2)/2 \quad \text{(A-6)}$$

From continuity, $V_M = V_1$ (A-7)

The elevation of the fluid surface in the influent reservoir is determined from the initial elevation and the rise in the surface during the test

$$z_M = z_{M0} - h_M \quad \text{(A-8)}$$

Substituting equations A-6, A-7 and A-8 into A-5 yields the expression for the hydraulic potential at the top of the soil sample

$$H_1 = P_M/pg + z_{M0} - h_M + V_1^2/2g - H_{f1} \quad \text{(A-9)}$$

The hydraulic potential at the lower soil boundary can be determined in a similar manner as

$$H_2 = P_L/pg + z_{L0} + h_L + V_2^2/2g + H_{f2} \quad \text{(A-10)}$$

h_L is related to h_M due to continuity; $h_L = h_M\,(a_M/a_L) = b\, h_M$ (A-11)

For steady flow, $V_1 = V_2$; however, in the variable head permeability test, the flow rate is not constant. Fortuitously, the

velocity term in the energy equation is of minor importance for flow through a soil specimen. Negligible error is introduced by assuming that $V_1 = V_2$ during the permeability test. The difference in potential across the sample is

$$dH = H_2 - H_1 \tag{A-12}$$

$$dH = (P_L - P_M) + (z_{LO} - z_{MO}) + (1+b)\, h_M + (H_{f1} + H_{f2}) \tag{A-13}$$

Define $dP_0 = P_L - P_M$, $dz_0 = z_{LO} - z_{MO}$ and $H_f = H_{f1} + H_{f2}$

and substitute into equation A-13 yields

$$dH = dP_0 + dz_0 + (1+b)h_M + H_f \tag{A-14}$$

The differential $dz = L$ (A-15)

Substituting equations A-14 and A-15 into Darcy's Law (A-4) yields

$$q = -K/L\ [dP_0 + dz_0 + (1+b)h_M + H_f] \tag{A-16}$$

From continuity, $dV/dt = qA$ (A-17)

Evaluating the left hand side,

$$dV/dt = d(a_M h_M)/dt = a_M\, dh_M/dt \tag{A-18}$$

Substituting equations A-17 and A-18 into A-16 yields

$$a_M\, dh_M/dt = -KA/L\ [dP_0 + dz_0 + (1+b)h_M + H_f] \tag{A-19}$$

Dividing through by a_M results in the differential equation

$$dh_M/dt = -KA/a_M L\ [dP_0 + dz_0 + (1+b)h_M + H_f] \tag{A-20}$$

which can be rewritten as

$$dh_M/dt = C_1 + C_2 h_M \tag{A-21}$$

where $C_1 = -KA/a_M L\ (dP_0 + dz_0 + H_f)$ (A-22)

$$C_2 = -(1+b)\ KA/a_M L \tag{A-23}$$

This equation is a first order differential equation which was solved by the use of an integrating factor, $-\exp(C_2 t)$, yielding

$$h_M e^{-(C_2 t)} = -C_1/C_2\, e^{-(C_2 t)} + C_0 \tag{A-24}$$

C_0 was evaluated at time $t = 0$, when $h_M = 0$, yielding

$$C_0 = C_1/C_2 \qquad \text{(A-25)}$$

Solving for K yields

$$K = \frac{a_M L}{(1+b)At} \ln\left[1 + \frac{(1+b)h_R}{dP_0 + dz_0 + H_f}\right] \qquad \text{(A-26)}$$

Or, in a more familiar form,

$$K = \frac{a_M L}{(1+b)At} \ln\left[\frac{h_i}{h_f}\right] \qquad \text{(A-27)}$$

where $h_i = dP_0 + dz_0 + H_f$ (A-28)

$$h_f = dP_0 + dz_0 + (1+b)h_R \qquad \text{(A-29)}$$

When the diameters of the permeant burettes are the same, $a_L = a_M$ and $b = 1$, yielding

$$K = \frac{a L}{2At} \ln\left[\frac{h_i}{h_f}\right] \qquad \text{(A-30)}$$

Centrifuge Tests

Energy equation: $H_1 = H_0 - H_f$ (A-31)

Bernoulli equation for flow in a centrifuge:

$$(P/p + V^2/2 - w^2r^2/2)_1 = (P/p + V^2/2 - w^2r^2/2)_2 \qquad \text{(A-32)}$$

Continuity equation: $dV/dt = qA$ (A-33)

Darcy's Law: $q = -K\, dH/dr$ (A-34)

The hydraulic potential at the top of the soil sample (subscript 1) is

$$H_1 = P_1/p + V_1^2/2 - w^2r_1^2/2 - H_{f1} \qquad \text{(A-35)}$$

Rewriting the centrifuge form of the Bernoulli equation between the surface of the influent reservoir (subscript M) and the top of the soil

$$P_1 = P_M + pw^2(r_1^2 - r_M^2)/2 + (V_M^2 - V_1^2)/2 \qquad \text{(A-36)}$$

From continuity, $V_M = V_1$ (A-37)

The elevation of the influent reservoir is related to the initial surface elevation and the rise in the fluid surface, h_M, by

$$r_M = r_{MO} + h_M \quad \text{(A-38)}$$

Inserting equations A-37 and A-38 into A-36 yields

$$P_1 = P_M + pw^2[r_1^2 - (r_{MO} + h_M)^2]/2 \quad \text{(A-39)}$$

Carrying out the algebra,

$$P_1 = P_M + pw^2[r_1^2 - (r_{MO}^2 + 2r_{MO}h_M + h_M^2)]/2 \quad \text{(A-40)}$$

$$P_1 = P_M + pw^2(r_1^2 - r_{MO}^2 - 2r_{MO}h_M - h_M^2)/2 \quad \text{(A-41)}$$

Inserting equation A-41 into A-35 yields the expression for the total hydraulic potential at the top of the soil sample

$$H_1 = [P_M + pw^2(r_1^2 - r_{MO}^2 - 2r_{MO}h_M - h_M^2)/2]/p + V_1^2/2 - w^2r_1^2/2 - H_{f1} \quad \text{(A-42)}$$

Simplifying

$$H_1 = [P_M + pw^2(- r_{MO}^2 - 2r_{MO}h_M - h_M^2)/2]/p + V_1^2/2 - H_{f1} \quad \text{(A-43)}$$

A similar analysis was carried out for the hydraulic potential at the lower boundary of the soil sample, incorporating terms of opposite sign for the rise in the effluent reservoir surface and the energy losses

$$H_2 = [P_L + pw^2(- r_{LO}^2 + 2r_{LO}h_L - h_L^2)/2]/p + V_2^2/2 + H_{f2} \quad \text{(A-44)}$$

The difference across the sample is given by

$$dH = H_2 - H_1 \quad \text{(A-45)}$$

$h_L = h_M = h$ since the diameters of the two reservoirs are identical.

As in the bench test equation derivation, the difference between V_1 and V_2 is assumed to be 0.0.

Define $dP_0 = (P_L - P_M)/p$ and $H_f = H_{f1} + H_{f2}$

$$dH = dP_0 + H_f + w^2(- r_{LO}^2 + 2r_{LO}h - h^2)/2 - w^2(- r_{MO}^2 - 2r_{MO}h - h^2)/2 \quad \text{(A-46)}$$

Grouping common terms yields

$$dH = dP_0 + H_f + w^2(r_{MO}^2 - r_{LO}^2)/2 + w^2h\,(r_{LO} + r_{MO}) \quad \text{(A-47)}$$

$$dr = L \quad \text{(A-48)}$$

Substituting equations A-47 and A-48 into Darcy's law,

$$q = -K/L\ [dP_0 + H_f + w^2(r_{M0}^2 - r_{L0}^2)/2 + w^2 h\ (r_{L0} + r_{M0})] \qquad (A\text{-}49)$$

From continuity, $dV/dt = qA$ (A-50)

Evaluating the left hand side yields

$$dV/dt = d(ah)/dt = a\ dh/dt \qquad (A\text{-}51)$$

Substituting equations A-49 and A-51 into Equation A-50 yields

$$a\ dh/dt = -KA/L\ [dP_0 + H_f + w^2(r_{M0}^2 - r_{L0}^2)/2 + w^2 h\ (r_{L0} + r_{M0})] \qquad (A\text{-}52)$$

Dividing by a results in the differential equation

$$dh/dt = -KA/aL\ [dP_0 + H_f + w^2(r_{M0}^2 - r_{L0}^2)/2 + w^2 h\ (r_{L0} + r_{M0})] \qquad (A\text{-}53)$$

$$dh/dt = C_1 + C_2 h \qquad (A\text{-}54)$$

where $$C_1 = -KA/aL\ [dP_0 + H_f + w^2(r_{M0}^2 - r_{L0}^2)/2] \qquad (A\text{-}55)$$

$$C_2 = -KA/aL\ [w^2(r_{L0} + r_{M0})] \qquad (A\text{-}56)$$

This equation is a first order differential equation which was solved by the use of the integrating factor, $\exp(C_2 t)$

$$h\, e^{-(C_2 t)} = -C_1/C_2\, e^{-(C_2 t)} + C_0 \qquad (A\text{-}57)$$

C_0 is evaluated at time $t = 0$, when $h = 0$, yielding

$$C_0 = C_1/C_2 \qquad (A\text{-}58)$$

Solving for K yields

$$K = \frac{-aL}{At[w^2(r_{L0} + r_{M0})]} \ln\left[\frac{w^2(r_{L0} + r_{M0})h}{dP_0 + w^2(r_{M0} - r_{L0}) + H_f} + 1\right] \qquad (A\text{-}59)$$

Carrying the negative sign to the logarithm and inverting the argument yields

$$K = \frac{aL}{Ath_0} \ln\left(\frac{h_1}{h_2}\right) \qquad (A\text{-}60)$$

where $$h_0 = w^2(r_{L0} + r_{M0}) \qquad (A\text{-}61)$$

$$h_1 = dP_0 + w^2(r_{M0}^2 - r_{L0}^2) + H_f \qquad (A\text{-}62)$$

$$h_2 = h_1 + h_0 h \qquad (A\text{-}63)$$

(The reverse of this page is blank.)